Universidad Autónoma de Madrid
Facultad de Ciencias
Departamento de Física Teórica

Phenomenological viability of supersymmetric and superstring models with three Higgs families

Tesis Doctoral realizada por
NICOLÁS ESCUDERO PRIETO

Trabajo dirigido por el
Dr. Carlos Muñoz López,
Profesor Titular del Departamento de Física Teórica

Madrid, enero de 2008

A mi madre,
al recuerdo de mi padre.

Contents

Introducción

Determinar el origen del mecanismo de generación de masas y comprender la ruptura de la simetría electrodébil serán, sin duda, uno de los mayores logros para la Física de Partículas de este siglo. Durante las últimas décadas de investigación en este campo, la propuesta del Modelo Estándar (SM) [1] y su verificación experimental hasta un enorme grado de precisión sugieren fuertemente que la última pieza restante del rompecabezas, el bosón de Higgs [2], será pronto descubierta. En el marco del Modelo Estándar, la hipótesis de un único doblete de Higgs es suficiente para romper de forma satisfactoria la simetría $SU(2)$ electrodébil, dando masa a los bosones gauge. Además, con la incorporación adicional de interacciones de Yukawa, también proporciona un mecanismo adecuado para generar las masas de quarks y leptones. El descubrimiento del bosón de Higgs se ha convertido en una de las motivaciones principales para la construcción del próximo Gran Colisionador de Hadrones (LHC) en el CERN, que será capaz de explorar energías a la escala del TeV. Hasta el momento, las medidas de precisión del sector electrodébil realizadas favorecen un Higgs ligero del SM con masa no muy superior al límite de exclusión de 114.6 GeV [3].

A pesar del gran éxito del Modelo Estándar, parece evidente que ha de ser considerado como un modelo que necesita ser extendido para explicar la Física a energías mayores. La razón de ir más allá es, sencillamente, porque el Modelo Estándar resulta insuficiente para resolver muchas preguntas de gran importancia, como el origen del número de generaciones de materia, la fuerte jerarquía de masas presente en quarks y leptones (es decir, la jerarquía de los acoplos de Yukawa) o las correcciones cuadráticas a la masa del Higgs, que de forma natural tienden a situarla a una alta escala de energía. Además de estas cuestiones, otros problemas relevantes a nivel fundamental, como son la incorporación de la gravedad en la teoría o la unificación de las fuerzas, siguen siendo un misterio en el marco Estándar.

Un apartado especialmente intrigante es el del número de generaciones de quarks y leptones. Desde un punto de vista fenomenológico y experimental, tenemos fuertes motivos para aceptar que existen sólo tres copias de quarks up y down, así como de leptones cargados y neutrinos activos. No obstante, desde un punto de vista teórico, existen pocas pistas sobre el origen de esta multiplicidad. La condición de cancelación de anomalías requiere un número idéntico de

familias, pero no añade ninguna información a su número total. Sobre la posibilidad de poseer una replicación en el sector de Higgs, vale la pena mencionar que el número de partículas de Higgs que toman parte en la ruptura electrodébil no está predicha ni restringida por la teoría, y que el único motivo de considerar sólo un Higgs en el Modelo Estándar obedece principalmente a un criterio de mínimo en el contenido de materia.

El más firme candidato a remediar algunas de las limitaciones del SM es probablemente la Supersimetría (SUSY) [4]. En las teorías supersimétricas, la inclusión de un mismo número de grados de libertad fermiónicos y bosónicos garantiza la ausencia de divergencias cuadráticas en la masa del Higgs, gracias a la cancelación de diagramas divergentes. Dicha cancelación proporciona una jerarquía estable entre la escala electrodébil y la escala de Planck. Adicionalmente, la versión local de la supersimetría, conocida como Supergravedad (SUGRA) [5], lleva a una unificación parcial con la gravedad. No obstante, el hecho de que las partículas supersimétricas aún no hayan sido observadas nos sugiere que dicha simetría ha de estar rota a una energía característica mayor que la escala electrodébil.

Hasta la fecha, la teoría de cuerdas [6] es la única teoría capaz de unificar todas las interacciones de una forma consistente y renormalizable, proporcionando un marco propicio para una gravedad cuántica, y siendo capaz de unificar la fuerza gravitatoria con las interacciones fuertes y electrodébiles. Todo ello hace de la teoría de cuerdas un candidato prometedor a convertirse en la "teoría del todo". Históricamente, la teoría de cuerdas fue desarrollada como una posible teoría de las interacciones fuertes [7]. En esta formulación, los diferentes hadrones correspondían a los modos de oscilación de la cuerda. Esta propuesta dio una visión unificadora (aunque no exenta de ciertos problemas) en la que la cuerda era postulada para explicar los distintas partículas observadas. Algo más tarde, cuando la Cromodinámica Cuántica (QCD) fue desarrollada, la teoría de cuerdas cayó en el olvido. Pero pasados algunos años, resultó ser adecuada para cumplir un ambicioso propósito: la construcción de una teoría final con el potencial de dar una descripción completa de todas las fuerzas de la naturaleza y explicar tanto la física de partículas como la cosmología, empleando la cuerda como único objeto fundamental cuyas vibraciones generan todo el espectro de partículas (incluyendo una partícula sin masa de spin dos que puede asociarse con el gravitón).

Uno de los principios básicos de la teoría de cuerdas es considerar las partículas como objetos extendidos en lugar de puntuales, a diferencia de lo que sucede en teoría cuántica de campos. Cuando la cuerda evoluciona en el tiempo, barre una superficie bidimensional en el espacio-tiempo, conocida como la *worldsheet* u "hoja de mundo", que representa la contrapartida de una "línea de mundo" para una partícula puntual. En teoría cuántica de campos analizada como teoría de perturbaciones, las contribuciones a las amplitudes se asocian a diagramas de Feynman, que representan las posibles configuraciones de las líneas de mundo. Del mismo modo, las expansiones perturbativas en teoría de cuerdas implican hojas de mundo de diferentes topologías.

La existencia de interacciones en teoría de cuerdas puede ser comprendida como la consecuencia de la topología de la hoja de mundo en vez de una singularidad local de la línea de mundo. Esta diferencia con las teorías en las que las partículas se estudian como puntos tiene la importante consecuencia de que, dado que las interacciones de la cuerda no poseen singularidades de corta distancia, las amplitudes en teoría de cuerdas no presentan divergencias ultravioleta, haciendo que la escala de la cuerda actúe como "cutoff".

Probablemente, una de las consecuencias más sorprendentes de la teoría de cuerdas es que sólo es consistente para un número específico de dimensiones espacio-temporales. En la formulación bosónica de la teoría, carente de supersimetría y donde únicamente hay bosones presentes en el espectro, esta dimensión es veintiséis [8]. En la formulación de supercuerda, que contiene además fermiones y supersimetría, el número de dimensiones espacio-temporales compatible con la cancelación de anomalías es diez [9]. En consecuencia, para poder relacionar la teoría de cuerdas con el mundo de cuatro dimensiones, la hipótesis más directa es pensar que las dimensiones extra están enrolladas en una variedad interna, con un tamaño suficientemente pequeño como para haber escapado a la detección. Esta idea fue originalmente propuesta por Kaluza y Klein en los años veinte [10, 11] y hoy en día se conoce con el nombre de *compactificación*.

La primera revolución de las supercuerdas comenzó en 1984, cuando se produjo un paso fundamental en la búsqueda de teorías de dimensiones superiores. Trabajando en el formalismo de la supercuerda y considerando un marco supersimétrico de $N = 1$, Green y Schwarz observaron que en escenarios de diez dimensiones no se producían anomalías si el grupo gauge era $SO(32)$ o $E_8 \times E_8$ [12]. Básicamente, estos extensos grupos gauge eran necesarios para cancelar cualquier anomalía proveniente del gravitino en diez dimensiones. Un año más tarde, la propuesta del formalismo de la cuerda heterótica [13] supuso una solución a este problema, ya que contenía la realización de estos grupos gauge como los modos de *winding* o arrollamiento de los modos de oscilación de las cuerdas cerradas. La cuerda heterótica está construida utilizando el formalismo de veintiséis dimensiones de la cuerda bosónica para los modos *left-mover* y el formalismo de la supercuerda en diez dimensiones para para los modos *right-mover*. Esta no equivalencia de dimensiones fuerza a las dieciséis dimensiones bosónicas restantes a ser compactificadas en un toro que, para dar una teoría consistente, debe corresponder exactamente al álgebra de Lie de $SO(32)$ o de $E_8 \times E_8$.

Históricamente, la cuerda heterótica $E_8 \times E_8$ ha sido estudiada con una mayor profundidad que la $SO(32)$. Esto se debe principalmente a la relación del grupo $E_8 \times E_8$ con los grupos de unificación más prometedores, como $SO(10)$ o $SU(5)$. Desde este punto de vista, resulta notable que la representación adjunta de $E_8 \times E_8$ contenga la representacion espinorial de $SO(10)$. Pero lo mismo no sucede en el grupo $SO(32)$. Éste es el motivo fundamental de que la cuerda heterótica $E_8 \times E_8$ haya sido el marco preferente en el que buscar un modelo estándar de cuerdas.

Otro ingrediente crucial para alcanzar un modelo realista en teorías de diez dimensiones es el poder obtener fermiones quirales tras la compactificación, ya que experimentalmente sabemos que las interacciones débiles no tratan de la misma forma las componentes "left" y las "right". En el formalismo del Modelo Estándar, esto es equivalente a decir que el grupo $SU(2)$ del grupo $SU(2) \times U(1)$ electrodébil no actúa trivialmente para las componentes quirales "left-handed". Bajo la hipótesis más simple, que resulta de compactificar seis de las diez dimensiones en un toro T_6, la supersimetría $N = 1$ se convierte en una supersimetría $N = 4$ en cuatro dimensiones. Sin embargo, sabemos que las teorías supersimétricas con $N \geq 2$ son automáticamente no quirales [6], por lo que si empleamos la supersimetría para solucionar el problema de jerarquía gauge, la única posibilidad desde el punto de vista fenomenológico es emplear una teoría $N = 1$ en cuatro dimensiones. Por todo ello, el primer criterio de compactificación de una teoría de cuerdas diez-dimensional es requerir SUSY $N = 1$ y, como consecuencia, la existencia de fermiones quirales en la teoría efectiva de cuatro dimensiones.

La solución a este problema vino de estudiar cuál debía ser el espacio más apropiado en el que compactificar la cuerda heterótica. Para responder a esta pregunta, debemos comenzar por reducir las diez dimensiones a un espacio de Minkowski de cuatro dimensiones por un espacio interno compacto de seis dimensiones. Candelas *et al.* [14] demostraron que la condición para conservar una supersimetría $N = 1$ era requerir que el espacio interno poseyera holonomía $SU(3)$, es decir, que debía existir un espinor covariantemente constante en la variedad interna seis-dimensional. Los espacios con holonomía $SU(3)$ fueron conjeturados y demostrados respectivamente por Calabi [15] y Yau [16]. La compactificación de la cuerda heterótica en una variedad Calabi-Yau rompe 3/4 de la supersimetría original $N = 4$ obtenida por compactificación toroidal. Los modelos Calabi-Yau parecían ser en un primer momento la clave de la fenomenología de cuerdas, pero muy pronto se mostraron como una herramienta complicada con la que construir modelos.

Para reducir la supersimetría $N = 4$ hasta $N = 1$, Dixon, Harvey, Vafa y Witten [17] introdujeron un sencillo espacio de compactificación conocido como *orbifold*. El orbifold añade grupos discretos sobre la compactificación toroidal, introduciendo puntos fijos en el espacio interno. La existencia de dichos puntos impide que el orbifold sea una auténtica variedad, ya que producen singularidades cónicas en las que el orbifold deja de ser isomorfo a un espacio plano R^6. No obstante, esas singularidades pueden ser eliminadas cortando los puntos fijos y pegando la frontera con superficies de disco con el mismo número de Euler. Por lo tanto, un orbifold ha de ser considerado como un límite singular de una variedad Calabi-Yau y, de hecho, para un observador a baja energía, el orbifold resulta un espacio tan bueno como un Calabi-Yau. Otra importante propiedad de la compactificación en un orbifold es la simplicidad en su formulación (casi equivalente a la compactificación en un toro), que nos permite calcular fácilmente sus propiedades fenomenológicas más interesantes, como su espectro de partículas a baja energía,

el potencial de Kähler o la intensidad en sus acoplos de Yukawa. Toda esta información resulta indispensable para conectar cualquier teoría de cuerdas con el Modelo Estándar y sus señales experimentales.

Con el objetivo de encontrar construcciones de cuerdas con el Modelo Estándar como límite de baja energía, a finales de los años ochenta se hizo un gran esfuerzo para encontrar modelos de orbifolds con grupos gauge $SU(3) \times SU(2) \times U(1)_Y$ y un contenido de materia realista. Se demostró que el uso de modelos de orbifolds Z_3 con líneas de Wilson [17, 18] (integrales de línea cerradas a lo largo de la dirección tangente al campo gauge) podían llevar de forma natural a espectros de baja energía con tres generaciones de partículas estándar junto con una cierta cantidad de materia exótica, así como un grupo gauge $SU(3) \times SU(2) \times U(1)^{\mathrm{n}} \times G_{\mathrm{oculto}}$ [19, 20]. Posteriormente, se realizó el cálculo de las cargas $U(1)$ de dichos modelos, junto con el estudio de sus mecanismos de cancelación de anomalías [21], dado que normalmente existía un $U(1)$ anómalo tras la compactificación [22]. Ello llevó a comprobar que la construcción de ciertas combinaciones lineales de los $U(1)$ no anómalos podían ser identificadas con la hipercarga de las partículas del Modelo Estándar, aunque se verificó que el sector oculto estaba en general mezclado con el sector observable a través de las cargas $U(1)$. Afortunadamente, también se encontró que la presencia de un término D de Fayet-Iliopoulos (FI) [22] como consecuencia del $U(1)$ anómalo podía proporcionar una ruptura adicional de los $U(1)$, junto con la separación del sector oculto previamente mezclado [21, 23, 24]. Esto sucede ya que, para conservar la supersimetría a altas energías, algunos escalares con cargas $U(1)$ adquieren valores esperados de vacío (VEVs) para cancelar el término D. De esta forma, fue posible construir en modelos supersimétricos donde el grupo gauge original se rompía hasta un $SU(3)\times SU(2)\times U(1)_Y$ estándar con tres generaciones de materia [24, 25]. Además, como un efecto extra de la ruptura FI, mucha de la materia exótica se desacopla del espectro de baja energía, proporcionando el espectro del Modelo Estándar Supersimétrico Mínimo (MSSM) junto con algunas partículas extra (tripletes de $SU(3)$, dobletes de $SU(2)$ y singletes de $SU(3) \times SU(2)$).

El empleo de compactificaciones de orbifolds propociona también la capacidad de calcular explícitamente todos los acoplos de Yukawa de la teoría, con una interpretación puramente geométrica [26–35]. Se puede demostrar que la intensidad de las interacciones de Yukawa pueden ser consideradas como un efecto de distancia entre las partículas situadas en los puntos fijos del espacio del orbifold. Estas distancias diferentes se traducen en una supresión exponencial de los acoplos de Yukawa relacionada con los *moduli* del orbifold, ofreciendo una interesante explicación del patrón experimental de las masas y mezclas de quarks y leptones, ya que en el contexto del Modelo Estándar permanecen como parámetros iniciales fijados a mano. La forma en que los modelos de orbifolds proporcionan una solución a este problema los hace muy atractivos, no sólo desde un punto de vista teórico sino también a nivel práctico, dado que todos los acoplos pueden ser calculados y contrastados con el experimento de forma sistemática.

En cuanto a la fenomenología de los escenarios de orbifolds, la característica genérica común a todos los modelos es la existencia de materia extra a baja energía. Concretamente, una de las propiedades más peculiares de algunos modelos Z_3 es la triple replicación de toda la materia, incluyendo el sector de Higgs. Obviamente, cuando se incluye más de un doblete de Higgs en el espectro, se ha de esperar una fenomenología mucho más extensa [36–43]. Nótese, por ejemplo, que la presencia de seis dobletes de Higgs en el MSSM implicaría la existencia de veintiún bosones físicos de Higgs, once de los cuales son neutros y diez cargados. Por otra parte, es bien conocido que cuando un tipo de fermiones recibe sus masas a través de más de un doblete de Higgs, se pueden producir corrientes neutras con cambio de sabor (FCNCs) a nivel árbol potencialmente peligrosas [44, 45]. Esto sucede porque las transformaciones que diagonalizan las matrices de masa no diagonalizan, en principio, las interacciones de Yukawa. Ésta sería precisamente la situacion en los modelos de orbifold previamente comentados, ya que habría tres generaciones de Higgses dando masa a cada fermión. En general, el límite más restrictivo a los procesos con cambio de sabor viene de la pequeña diferencia de masas existente entre los kaones K_L y K_S [46, 47], pero dependiendo de la textura de Yukawa específica dada, este efecto puede también ser importante en otros sistemas de mesones neutros o incluso en el sector leptónico. Existen dos aproximaciones a la hora de resolver este problema. En uno de ellos se asume que los Higgses adicionales son suficientemente masivos como para no contradecir los datos experimentales [46–50]. En la otra aproximación, la existencia de ciertas simetrías entre los acoplos de Yukawa elimina completamente las FCNCs [44]. El ejemplo más sencillo de esta posibilidad sería cuando los acoplos de los Higgses extra y los fermiones están prohibidos. Otra posibilidad de eliminar el cambio de sabor es que las matrices de Yukawa sean proporcionales.

Una posible forma de resolver este problema en escenarios de orbifolds es evitar la presencia de los Higgses extra del espectro haciéndolos lo suficientemente masivos como para desacoplarse, a causa de algún tipo de ruptura asimétrica [51] por medio de términos no renormalizables. Sin embargo, no debemos olvidar que un escenario con múltiples Higgses está en principio siempre permitido por la teoría, con la restricción de que los límites experimentales sobre FCNCs permanezcan bajo control. En este sentido, resulta muy interesante analizar la capacidad de los modelos multi-doblete para respetar las cotas experimentales, así como estudiar su fenomenología asociada.

En consecuencia, y a modo de resumen, la motivación principal de este trabajo viene de la idea de estudiar los escenarios supersimétricos con tres familias de Higgses, aplicando los resultados obtenidos a modelos de orbifolds Z_3 provenientes de la teoría de cuerdas. Aunque en nuestro análisis estudiamos modelos de orbifolds, se podría generalizar fácilmente a otros modelos de cuerdas con propiedades similares, utilizando la misma estrategia. Como veremos a través de los distintos capítulos, la multiplicidad de familias de Higgs posee numerosas consecuencias fenomenológicas. El requisito más importante de los escenarios de orbifolds estudiados será el

poder proporcionar masas realistas a los quarks y a los leptones, reproduciendo sus patrones de mezcla y respetando al mismo tiempo las cotas en los procesos con cambio de sabor.

Este trabajo se organiza del siguiente modo. En el Capítulo 1 repasaremos las propiedades más importantes relacionadas con el formalismo de la cuerda heterótica y los rudimentos de la compactificación en orbifolds, explicando las diferentes técnicas necesarias para conseguir escenarios con grupos gauge estándar y tres generaciones de materia, mediante el *embedding* de los grados de libertad gauge y el empleo de líneas de Wilson. Expondremos también el problema de la cancelación de anomalías en estos escenarios y su solución mediante el término D de Fayet-Iliopoulos. Veremos que dicha cancelación posee fuertes implicaciones físicas, como la reducción del grupo gauge o la obtención de un espectro realista de partículas.

En el Capítulo 2 analizamos detalladamente las características principales de un modelo genérico supersimétrico con tres familias en el sector de Higgs. Presentaremos las expresiones de las condiciones de mínimo del potencial y de las matrices de masa, dando una estimación del *fine tuning* esperado en el modelo. Estudiaremos los efectos de un modelo de múltiples Higgses en las interacciones del sector quark con FCNC, gracias a la ayuda de un modelo de juguete basado en interacciones de tipo Fritzsch, discutiendo qué tipo de sector de Higgs es compatible con los experimentos. Haremos el mismo análisis para diferentes sistemas de mesones neutros.

En el Capítulo 3 presentamos la estructura de Yukawa y las matrices de masa de un escenario de orbifold Z_3 genérico, teniendo en cuenta las implicaciones de la ruptura FI. Analizaremos la viabilidad de dichos escenarios para proporcionar masas y mezclas realistas en el sector de los quarks, sin contradecir los límites experimentales en los procesos con cambio de sabor.

En el Capítulo 4 realizaremos un estudio análogo para el sector leptónico. Mostraremos que los orbifolds Z_3 son también capaces de generar masas para los leptones cargados en acuerdo con los experimentos, respetando las cotas en los procesos con violación del sabor leptónico. Extenderemos el análisis al sector de los neutrinos, encontrando que las compactificaciones de orbifolds ofrecen varias posibilidades interesantes para generar mecanismos efectivos de tipo *seesaw*, dando lugar a neutrinos realistas.

Los Capítulos 2, 3 y 4 están basados en los resultados publicados en [52], [53] y [54], resprectivamente.

Introduction

The determination of the origin of mass generation and the complete understanding of the electroweak symmetry breaking should doubtlessly be a major goal for high-energy physics in this century. During the last decades of research on this field, the proposal of the Standard Model (SM) [1] of particle physics and its experimental verification to an extremely high degree of precision strongly suggest that the last piece of the puzzle, the Higgs boson [2], will soon be detected. In the Standard Model, the assumption of just one Higgs $SU(2)$ doublet is enough to account for the succesful breaking of the electroweak symmetry and the mass generation for the gauge bosons. Moreover, with the additional inclusion of Yukawa interactions, it also provides a nice mechanism for giving masses to quarks and leptons. The discovery of the Higgs boson is one of the main motivations for the construction of the upcoming Large Hadron Collider (LHC) at CERN, which will be able to explore energies at the TeV scale. Until now, the electroweak precision measurements favour a relatively light SM Higgs boson not too far above the direct exclusion limit of 114.6 GeV [3].

Despite the great success of the SM, it is clear that it should be regarded as a model that needs to be extended in order to describe physics at higher energies. The reason for going beyond is simply because the SM is unable to solve many important questions, such as the origin of matter generations, the strong mass hierarchy between quarks and leptons (that is the hierarchy in the Yukawa couplings) or the quadratic quantum corrections to the Higgs mass, which naturally tend to push it to a high energy. Some other more fundamental questions, as for instance the inclusion of gravity or the unification of forces, remain yet as a mistery within the SM framework.

Another particularly puzzling topic is that of the number of quark and lepton generations. From a phenomenological and experimental point of view, we have strong reasons to accept that there are indeed only three copies of up- and down-type quarks, as well of charged leptons and active neutrinos. However, on the theoretical side, there is little hint to the origin of this three-fold replication. The cancellation of anomalies requires identical number of quark and lepton families, but adds no information to the total number. Regarding the possibility of having family replication inside the Higgs sector, it is worth noting that the number of Higgs particles taking

part in the electroweak symmetry breaking is neither predicted nor restricted by the theory, and the main reason for considering just one boson within the Standard Model obbeys a criterium of minimal matter content.

The firmest candidate to remedy some of the shortcomings of the Standard Model is perhaps supersymmetry (SUSY) [4]. In supersymmetric theories, the inclusion of equal number of bosonic and fermionic degrees of freedom ensures the absence of Higgs quadratic corrections via the cancellation of divergent diagrams. Such cancellation provides a stable hierarchy between the electroweak and the Planck scale. Furthermore, the local version of supersymmetry, supergravity (SUGRA) [5], leads to a partial unification of the Standard Model with gravity. However, the fact that SUSY has not yet been discovered suggests that this symmetry should be broken at a characteristic energy above the electroweak scale.

Until now, string theory [6] is the only theory capable of unifying all interactions in a fully consistent and renormalisable way, providing a satisfactory framework for quantum gravity. It also appears able to unify gravity with the strong and the electroweak interactions, which makes string theory a promising candidate to be a "theory of everything". Historically, relativistic string theory was developed as a possible theory of strong interactions [7]. In this formulation, hadrons corresponded to the oscillation modes of the string. This proposal gave a very unified picture (although with some problems) in which the string was postulated to explain the different particles observed. But when quantum chromodynamics (QCD) was developed, the string theory approach went out of favour. However, after some years, it turned out to be well suited for an ambitious purpose: the construction of a final theory with the potential to provide a complete description of all forces of nature and the full understanding of particle physics and cosmology, by employing the string as the fundamental object whose vibrations generate the whole particle spectrum (including a massless spin-2 particle which can be associated with the graviton).

One of the basic ideas that motivate string theory is to consider elementary particles as extended objects rather than pointlike, unlike the case of quantum field theory. As a string evolves in time, it sweeps out a two-dimensional surface in space-time, which is called the *worldsheet* of the string. This is the string counterpart of the worldline for a point particle. In quantum field theory, analysed in perturbation theory, contributions to amplitudes are associated to Feynman diagrams, which depict possible configurations of worldlines. Similarly, perturbation expansions in string theory involve string worldsheets of various topologies.

The existence of interactions in string theory can be understood as a consequence of worldsheet topology rather than of a local singularity on the worldline. This difference from the point-particle theories has the crucial implication that, since string interactions are not associated with short-distance singularities, string theory amplitudes have no ultraviolet divergences, with the string scale acting as a cutoff.

Probably one of the most striking consequences of string theory is that is only consistent for a specific number of space-time dimensions. In the bosonic formulation of the theory, where only bosons and no supersymmetry are included into the theory, this dimension is twenty six [8]. For the superstring formulation of string theory, which contains fermions and supersymmetry in its formulation, the number of space-time dimensions compatible with anomaly cancellation is ten [9]. To make contact between string theory and the four-dimensional world, the most straightforward possibility is that the extra-dimensions are compactified on an internal manifold, whose size is sufficiently small to have scaped detection. This idea was firstly proposed by Kaluza and Klein in the 1920s [10, 11] and nowadays it is referred to as *compactification*.

The first superstring revolution began in 1984, when a breakthough was made in the search for higher-dimensional theories. Working with the superstring formalism, and considering a $N = 1$ supersymmetric framework, Green and Schwarz observed that in ten-dimensional formulations no anomaly appears if the gauge group is $SO(32)$ or $E_8 \times E_8$ [12]. Basically, these large gauge groups are required to cancel any anomaly arising from the ten-dimensional gravitino. One year later, the proposal of the heterotic string formulation [13] became the answer to this problem, since it contained the realisation of these large groups as the oscillation modes of the closed strings and winding modes. The heterotic string is constructed by employing the formalism of the 26-dimensional bosonic string for the left-mover modes and the formalism of the 10-dimensional superstring for the right-mover modes. The mismatch in space-time coordinates forces the 16 extra bosonic dimensions to be compactified on a torus that, in order to give a consistent theory, must correspond exactly either to the $SO(32)$ or the $E_8 \times E_8$ Lie algebras.

Historically, the $E_8 \times E_8$ has been discussed in much more detail than the $SO(32)$ heterotic string. This is mainly due to the relation of $E_8 \times E_8$ with the most studied unification groups, such as $SO(10)$ and $SU(5)$. Under this point of view, it is remarkable that the adjoint representation of $E_8 \times E_8$ contains the spinor representation of $SO(10)$, but this no longer true for the $SO(32)$. This has been the main motivation for studing the $E_8 \times E_8$ formulation as the usual framework for finding a heterotic-string standard model.

Another crucial ingredient to succesfully reach a realistic model in ten-dimensional field theories is to obtain chiral fermions after compactification, since we experimentally know that the weak interactions do not treat left and right chiral components in the same way. In the Standard Model formulation, this is equivalent to saying that the $SU(2)$ of the electroweak $SU(2) \times U(1)$ is realised non-trivially by the left chiral components. Under the most simple assumption, which is to compactify six of the ten dimensions on a flat torus T_6, the ten-dimensional $N = 1$ supersymmetry becomes $N = 4$ supersymmetry in four dimensions. But theoretically we know that supersymmetries with $N \geq 2$ are automatically non-chiral [6], so if one introduces a supersymmetry as way to understand the gauge hierarchy problem, the only allowable one from a phenomenological point of view is $N = 1$ supersymmetry in four dimensions. Therefore, the

first criterium when compactifying the ten-dimensional string theory is to keep $N = 1$ SUSY, allowing the existence of chiral fermions in the four-dimensional effective theory.

The solution to this problem came from studying which could be the most appropriate space into which compactify the higher-dimensional heterotic string. In order to answer that question, one should start from reducing ten dimensions to a flat four-dimensional Minkowski space times a compact 6D internal space. Candelas *et al.* [14] showed that the condition for the $N = 1$ SUSY is to require that the internal space possesses $SU(3)$ holonomy, i.e. that to preserve just one of the supersymmetries there should exist a covariantly constant spinor on the internal six-dimensional manifold. The spaces with $SU(3)$ holonomy were respectively conjectured and proved by Calabi [15] and Yau [16]. Calabi-Yau compacifications of ten-dimensional heterotic string theories break 3/4 of the original $N = 4$ obtained through the toroidal compactification. Calabi-Yau models seemed to be the key to string phenomenology, but they soon turned out to be tools rather difficult to work with.

For reducing the $N = 4$ SUSY down to $N = 1$, a simpler method known as orbifold compactification was introduced by Dixon, Harvey, Vafa and Witten [17]. The orbifold method uses discrete groups on top of torus compactification, introducing fixed points inside the internal space. The existence of such points prevents the orbifold from being a good manifold, since they introduce conical singularities in which the orbifold fails to be isomorphic to a flat R^6. However, these singularities can be eliminated by cutting out the fixed points and gluing the boundaries with good disk-like surfaces with the same final Euler number. Therefore, an orbifold can be considered a singular limit of a good manifold such as a Calabi-Yau. In this sense, to a low-energy observer, the orbifold is as good as a Calabi-Yau space. Another important property of orbifold compactification is the simplicity in its formulation (almost equivalent to flat toroidal compactification), which allows us to easily calculate the most interesting phenomenological properties, such as the low-energy particle spectrum, the Kähler potential and the intensity of the Yukawa couplings. All this information becomes crucial to connect any string theory to the Standard Model physics accesible to the experiment.

In order to find a Standard-like string constructions, in the late eighties a huge effort was made to find orbifold models with a $SU(3) \times SU(2) \times U(1)_Y$ gauge group and a realistic matter content. Is was shown that Z_3 orbifold models with Wilson lines [17, 18] (closed line integrals along the direction tangent to a gauge field) could naturally lead to low-energy spectra with three generations of Standard-Model particles plus some exotic matter and a gauge group $SU(3) \times SU(2) \times U(1)^{\mathrm{n}} \times G_{\mathrm{hidden}}$ [19, 20]. The next step was the calculation of the $U(1)$ charges and the study of the mechanism for anomaly cancelation in these models [21], since an anomalous $U(1)$ is usually present after compactification [22]. This allowed the construction of linear combinations of the non-anomalous $U(1)$'s which could be identified with the physical hypercharge for the particles of the Standard Model, although it was found that the hidden sector is,

in general, mixed with the observable one through the extra $U(1)$ charges. Fortunately, it was also noted that the Fayet-Iliopoulos (FI) D-term [22], which appears because of the presence of the anomalous $U(1)$, can give rise to the breaking of the extra $U(1)$'s and, as a consequence, to the hiding of the previously-mixed hidden sector [21, 23, 24]. This is because, in order to preserve supersymmetry at high energies, some scalars with $U(1)$ quantum numbres acquire large vacuum expectation values (VEVs). In this way it was possible to construct supersymmetric models where the original gauge group was broken down to the standard $SU(3) \times SU(2) \times U(1)_Y$ with three generations of matter [24, 25]. Moreover, as an extra effect of the FI breaking, most of the exotic matter decoupled from the low-energy theory, leading to the particle spectrum of the Minimal Supersymmetric Standard Model (MSSM) plus some remaining extra states ($SU(3)$ triplets, $SU(2)$ doublets and $SU(3) \times SU(2)$ singlets).

The use of orbifold compactifications provides also the ability to explicitly calculate all the Yukawa couplings of the theory, with a purely geometrical interpretation [26–35]. It can be shown that the intensity of the Yukawa interactions can be considered as a distance effect between the particles stacked at the fixed points in the internal orbifold space. These different distances translate into an exponential supression of the Yukawa couplings related to the orbifold moduli, thus offering a nice explanation to the peculiar experimental pattern of quark and lepton masses and mixing angles, which are unpredicted in the Standard Model, remaining as initial parameters put by hand. The way in which orbifold models give a solution to this problem makes them very attractive not only from a theoretical point of view but also at the practical level, since all the couplings in orbifold scenarios can be computed and compared to the experiment in a systematic way.

Regarding the phenomenology of these orbifold scenarios, the main characteristic common to all models is the presence of extra matter at low energies. In particular, one of the most peculiar properties of some Z_3 models with two Wilson lines is the three-fold replication of all matter, including the Higgs sector. Obviously, when more than one Higgs family is present, one should expect a much richer phenomenology [36–43]. Note, for instance, that the presence of six Higgs doublets implies the existence of twenty one physical Higgs bosons, eleven of them are neutral and ten charged. On the other hand, it is well known that potentially dangerous flavour-changing neutral currents (FCNCs) may appear when fermions of a given charge receive their mass through couplings with several Higgs doublets [44, 45]. This is because the transformations diagonalising the fermion mass matrices do not, in principle, diagonalize the Yukawa interactions. This situation would be present in these orbifold models since there are three generations of supersymmetric Higgses giving mass to each fermion. In general, the most stringent limit on flavour-changing processes comes from the small value of the $K_L - K_S$ mass difference [46, 47], but depending on the Yukawa texture given this effect can also be important in other neutral meson systems or even in the leptonic sector, where tree-level lepton flavour-violating (LFV)

processes might occur. There are two approaches in order to solve this problem. In one of them one assumes that the extra Higgses are sufficiently massive making neutral currents small enough not to contradict the experimental data [46–50]. In the other approach the Yukawa couplings have some symmetries eliminating FCNCs completely [44]. The simplest example of the latter is when the couplings between the extra Higgses and quarks of a given charge are forbidden. If the three Yukawa-coupling matrices are present, still one can avoid FCNCs if the matrices are proportional.

One possible approach to solve the FCNC problem in orbifold scenarios is simply to avoid the presence of the extra-Higgses in the spectrum by making them massive enough to decouple from the low-energy spectrum due to some asymmetric breaking [51] through non-renormalisable terms. However, a multi-Higgs doublet scenario is in principle always allowed by the theory, provided that the bounds on FCNCs remain under control. In this sense, it is very interesting to analyse the ability of these multi-doublet models to fulfill the experimental restrictions and study their associated phenomenology.

Summing up, the main motivation for this work comes from the idea of studying supersymmetric models with three Higgs families, applying the results obtained to string Z_3 orbifold scenarios. Although we have analysed orbifold models, the same strategy could be applied to other string models with similar properties. As we shall see through the different chapters, the multiplicity of Higgs families involves many phenomenological consequences. The most important requirement for the orbifold scenarios considered will be to provide realistic masses for quarks and leptons, reproducing their mixing patterns, while avoiding conflict with the experimental bounds on FCNC processes.

This work is organised as follows. In Chapter 1 we review the most important properties concerning the heterotic string formulation and the rudiments of orbifold compactification, explaining the different techniques necessary to achive scenarios with standard-like gauge groups and three generations of matter, through the embedding of the gauge degrees of freedom and the employment of Wilson lines. We will also expose the problem of anomaly cancellation and how the existence of the Fayet-Iliopoulos D-term can overcome this difficulty leading to strong physical implications, reducing the gauge group and providing a very realistic particle spectrum.

In Chapter 2 we thoroughly analyse the main features of a general SUSY model with three families in the Higgs sector. We will present the expresions of the minima equations for the potential and the mass matrices, giving an estimate of the fine-tuning expected within the model. We will study the effects of multiple-Higgs models on the FCNC tree-level interactions for the quark sector, with the help of a toy model based on Fritzsch-like Yukawa quark-Higgs interactions, discussing how compatibility with current experimental data constrains the Higgs sector. We will perform the same analysis for different systems of neutral mesons.

In Chapter 3 we present the structure of Yukawa couplings and mass matrices for a general Z_3 orbifold scenario, taking into account the implications of the FI breaking. We will study the viability of these Z_3 scenarios in providing realistic masses and mixings for the quark sector without contradicting the experimental data on FCNC processes.

In Capter 4 we perform an analogous analysis for the leptonic sector. We will show that Z_3 orbifolds are also able to generate masses for the charged leptons in agreement with the experiment, respecting the bounds on lepton-flavour violating processes. We will extend the analysis to the neutrino sector, finding that orbifold compactifications offer several interesting possibilities for the generation of effective seesaw-like mechanisms.

Chapters 2, 3 and 4 are based on the results published in [52], [53] and [54], respectively.

Chapter 1

Overview of orbifold compactifications of the Heterotic String

As mentioned in the Introduction, a simple way to obtain a four-dimensional effective theory from the Heterotic String consists in compactifying on an orbifold [17]. The orbifold is a six dimensional space obtained by identifying points on the torus that are mapped into one another by certain symmetries of the lattice of the torus, referred to as the point group. This approach retains the advantage of toroidal compactification that the linear string equations of motion are still unmodified. At the same time, we shall see that it is possible for orbifold compactification to produce a four dimensional theory with N=1 supersymmetry, rather than the undesired N=4 supersymmetry of toroidal compactifications. The basic idea is as follows: one starts from a six-dimensional torus which has some discrete symmetry group that does not act freely. If one mods out this torus by the symmetry, the resulting space, called orbifold, has some singular points, corresponding to the fixed points. Orbifolds are flat everywhere, except at these singular points where the curvature has a delta singularity. These models are exactly solvable as one can describe the string on the torus and take into account the action of the symmetry group by twisting the closed string boundary conditions. It is for this reason that we are able to calculate all of the parameters and functions of the emergent theory: the gauge group and the matter content; the Yukawa couplings and the Kähler potential (which determine the quark and lepton mass matrices and mixing angles); the gauge kinetic function, including string loop corrections, which determine the unification scale of the gauge coupling constants. There are, of course, other methods of string compactification including Calabi-Yau manifolds [14, 55], fermionic constructions [56], N=2 superconformal field theories [57] or intersecting D-

branes [58]. Orbifold compactifications are connected to some of these models. Nevertheless, most of the alternatives has not been as worked out as the orbifold theories.

Through this chapter, we will review the most interesting properties of heterotic-string orbifold compactifications, focusing on the construction of Z_3 models and their ability to obtain low-energy spectra very close to the Standard Model. We will also address the problem of obtaining models with the correct $SU(3) \times SU(2) \times U(1)_Y$ gauge group and the rudiments of symmetry breaking through the use of gauge orbifold embedding and Wilson lines. Finally, we will study the way in which orbifold models may solve the problem of anomaly cancellation and the preservation of supersymmetry at low energies.

1.1 The heterotic string. Mode expansions and quantisation

The construction of the ten-dimensional heterotic string has been fully described in the literature (see, for example, [6]). In the heterotic formulation [13], a non-abelian gauge group may be obtained by using the right movers of a type II superstring and the left movers of a bosonic string. In this chapter we shall see how, following this approach, 16 of the left mover dimensions X^μ can be compactified on a torus, giving rise to some gauge fields in the Kaluza-Klein manner [59]. There are also additional gauge fields of a stringy origin whose existence depends on the possibility of having winding numbers for the string on the torus. In this way, the extra 16 left-mover dimensions provide the gauge group of the resulting 10-dimensional theory. For the heterotic string, it is found that the possible gauge groups consistent with gauge and gravitational anomaly cancellation are $SO(32)$ or $E_8 \times E_8$ [12]. The latter possibility has led to phenomenologically promising models since one of the E_8's can contain E_6 which in turn contains $SO(10)$, with useful subgroups as $SU(5) \times U(1)$ or $SO(6) \times SO(4)$, while the other E_8 can be treated as a hidden sector group. We will therefore focus in the heterotic string with $E_8 \times E_8$ gauge group.

For the right movers, the mode expansions for the heterotic string are the same as those of the closed superstring. For the bosonic degrees of freedom one has

$$X_R^\mu(\tau - \sigma) = \frac{1}{2}x^\mu + \frac{1}{2}p^\mu(\tau - \sigma) + \frac{i}{2}\sum_{n\neq 0}\frac{\alpha_n^\mu}{n}e^{-2in(\tau-\sigma)}\,. \tag{1.1}$$

In the above, τ and σ are the worldsheet coordinates, while x^μ and p^μ denote the location and momentum of the string center of mass and α_n^μ are the mode coefficients of the expansion.

The fermionic degrees of freedom are given by

$$\Psi_R^\mu(\tau - \sigma) = \sum_{n\in\mathbb{Z}} d_n^\mu e^{-2in(\tau-\sigma)} \qquad \text{R sector}\,, \tag{1.2}$$

and

$$\Psi^{\mu}_{R}(\tau-\sigma)=\sum_{r\in\mathbb{Z}+1/2} b^{\mu}_{r}e^{-2ir(\tau-\sigma)} \qquad \text{NS sector}\,, \tag{1.3}$$

where in each case $\mu=0,1,...,9$. "R" and "NS" respectively denote Ramond and Neveu-Schwarz sectors corresponding to periodic and antiperiodic boundary conditions.

For the left movers, it is convenient to introduce a notation that distinguishes the first ten degrees of freedom, which we denote by X^{μ}_{L}, $\mu=0,1,...,9$, from the last 16 degrees of freedom. We denote these 16 'internal' degrees of freedom by X^{I}_{L}, I=1,...,16. For the first ten degrees of freedom the mode expansion is analogous to that of the closed-bosonic-string left movers

$$X^{\mu}_{L}(\tau+\sigma)=\frac{1}{2}x^{\mu}+\frac{1}{2}p^{\mu}(\tau+\sigma)+\frac{i}{2}\sum_{n\neq 0}\frac{\tilde{\alpha}^{\mu}_{n}}{n}e^{-2in(\tau+\sigma)}\,, \tag{1.4}$$

where again $\mu=0,1,...,9$.

For the 16 internal degrees of freedom we write

$$X^{I}_{L}(\tau+\sigma)=\frac{1}{2}x^{I}+\frac{1}{2}p^{I}(\tau+\sigma)+\frac{i}{2}\sum_{n\neq 0}\frac{\tilde{\alpha}^{I}_{n}}{n}e^{-2in(\tau+\sigma)}\,, \tag{1.5}$$

where $I=1,...,16$.

The quantisation for $\mu=0,1,...,9$ is the following:

$$[x^{\mu},p^{\nu}]=-\,i\,\eta^{\mu\nu}\,, \tag{1.6}$$

$$[\alpha^{\mu}_{m},\alpha^{\nu}_{n}]=[\tilde{\alpha}^{\mu}_{m},\tilde{\alpha}^{\nu}_{n}]=-m\,\delta_{m+n,0}\,\eta^{\mu\nu}\,, \tag{1.7}$$

$$\{d^{\mu}_{m},d^{\nu}_{n}\}=-\,\delta_{m+n,0}\,\eta^{\mu\nu} \qquad \text{R sector}\,, \tag{1.8}$$

$$\{b^{\mu}_{r},b^{\nu}_{s}\}=-\,\delta_{r+s,0}\,\eta^{\mu\nu} \qquad \text{NS sector}\,, \tag{1.9}$$

where in each case $\mu,\nu=0,...,9$. $\eta^{\mu\nu}$ is the Minkowski space-time metric diag$(1,-1,-1,-1)$. For the case of X^{I}_{L}, $I=0,...,16$, the commutation rules are

$$[x^{I}_{L},p^{J}_{L}]=-\,\frac{i}{2}\,\eta^{IJ}=-\frac{i}{2}\,\delta^{IJ}\,, \tag{1.10}$$

$$[\tilde{\alpha}^{I}_{m},\tilde{\alpha}^{J}_{n}]=-\,m\,\delta_{m+n,0}\,\eta^{IJ}=-m\,\delta_{m+n,0}\,\delta^{IJ}\,. \tag{1.11}$$

1.2 Compactification of the heterotic string on a torus

A ten dimensional theory may be constructed by compactifying the 16 left-mover internal dimensions of the heterotic string, with a gauge group arising from the compactification. As done in the quantisation, it is necessary to impose boundary conditions on X^{I}_{L} $(I=1,...,16)$, with

both left and right movers, and then to eliminate the right movers. As mentioned before, sixteen of the left-mover dimensions X^μ can be compactified on a torus, a possibility that we now wish to address.

A 16-dimensional torus may be defined by introducing a lattice Λ with basis vectors e_a^I $(a = 1, ..., 16)$, chosen to have length $\sqrt{2}$. One must then establish the identification

$$x^I \equiv x^I + \sqrt{2}\pi \sum_{a=1}^{16} n_a R_a e_a^I \,, \tag{1.12}$$

where the R_a are radii and the n_a are arbitrary integers. There are then extra ways of satisfying the closed string boundary conditions by winding the string round the torus so that

$$X^I(\tau, \sigma + \pi) = X^I(\tau, \sigma) + \sqrt{2}\pi \sum_{a=1}^{16} n_a R_a e_a^I = X^I(\tau, \sigma) + 2\pi L^I \,, \tag{1.13}$$

where

$$L^I = \frac{1}{\sqrt{2}} \sum_{a=1}^{16} n_a R_a e_a^I \,. \tag{1.14}$$

In the above, L^I are the winding numbers. Then, the mode expansions are given by

$$X^I(\tau, \sigma) = x^I + p^I \tau + 2L^I \sigma + \frac{i}{2} \sum_{n \neq 0} \frac{1}{n} (\alpha_n^I e^{-2in(\tau - \sigma)} + \tilde{\alpha}_n^I e^{-2in(\tau + \sigma)}) \,. \tag{1.15}$$

As before, we decompose into right and left movers

$$X^I = X_R^I + X_L^I \,, \tag{1.16}$$

where

$$X_R^I(\tau - \sigma) = x_R^I + p_R^I(\tau - \sigma) + \frac{i}{2} \sum_{n \neq 0} \frac{1}{n} (\alpha_n^I e^{-2in(\tau - \sigma)}) \,, \tag{1.17}$$

$$X_L^I(\tau + \sigma) = x_L^I + p_L^I(\tau + \sigma) + \frac{i}{2} \sum_{n \neq 0} \frac{1}{n} (\tilde{\alpha}_n^I e^{-2in(\tau + \sigma)}) \,, \tag{1.18}$$

with

$$p_{R,L}^I = \frac{1}{2}(p^I \mp 2L^I) \,. \tag{1.19}$$

We now wish to eliminate the right movers, which in particular means that we should take $p_R^I = 0$, with the consequence that $p_L^I = 2L^I$. Moreover, we should take $x_R^I = 0$, which translates into

$$x_L^I \equiv x_L^I + \sqrt{2}\pi \sum_{a=1}^{16} n_a R_a e_a^I \,. \tag{1.20}$$

The commutation relation of Eq. (1.10) implies that it is $2p_L^I$ rather than p_L^I that generates translations of x_L^I. This implies that we should require $\exp(2i\sum_{I=1}^{16} p_L^I x_L^I)$ to be single valued when x_L is replaced by the equivalent coordinates of Eq. (1.20). Let us now consider the lattice Λ^*, dual to Λ, with basis vectors denoted by e_a^{*I}. If Λ^* is defined by

$$\sum_{I=1}^{16} e_a^I e_b^{*I} = \delta_{ab}\,, \tag{1.21}$$

then p_L must be given by

$$p_L = \frac{1}{\sqrt{2}} \sum_{a=1}^{16} \frac{m_a}{R_a} e_a^{*I}\,, \tag{1.22}$$

where m_a are arbitrary integers. In the light-cone gauge, the expresion of the ten-dimensional mass-squared operator for the physical states is given by

$$M^2 = M_L^2 + M_R^2\,. \tag{1.23}$$

For the superstring right-movers, with D=10,

$$\frac{1}{4} M_R^2 = N\,, \tag{1.24}$$

where

$$N = \sum_{n=1}^{\infty} (\alpha_{-n}^i \alpha_n^i + n\, d_{-n}^i d_n^i) \qquad \text{R sector}\,, \tag{1.25}$$

$$N = \sum_{n=1}^{\infty} \alpha_{-n}^i \alpha_n^i + \sum_{r=1/2}^{\infty} r\, b_{-r}^i b_r^i - \frac{1}{2} \qquad \text{NS sector}\,. \tag{1.26}$$

For the bosonic string left movers with 16 dimensions compactified on a torus, the mass-squared operator takes the form

$$\frac{1}{4} M_L^2 = \frac{1}{2} \sum_{I=1}^{16} (p_L^I)^2 + \tilde{N} - 1\,, \tag{1.27}$$

with

$$\tilde{N} = \sum_{n=1}^{\infty} (\tilde{\alpha}_{-n}^i \tilde{\alpha}_{in} + \alpha_{-n}^I \alpha_{In})\,. \tag{1.28}$$

In the above, a sum over i from 1 to 8, and over I from 1 to 16 should be understood. Also, massless states require that

$$M_R^2 = M_L^2 = 0\,. \tag{1.29}$$

For massless vector bosons, the form appropriate to the NS sector has to be employed. There are 16 massless vectors $\tilde{V}_I^i, I = 1, ..., 16$, of Kaluza-Klein type:

$$\tilde{V}_I^i = b_{-1/2}^i |0\rangle_R\, \tilde{\alpha}_{-1}^I |0\rangle_L \qquad\qquad I = 1, ..., 16\,, \tag{1.30}$$

which thus provide a $U^{16}(1)$ gauge group. This gauge group can be enhanced for special choices of the lattice Λ and the radii R_a. Let us use the notation $|p_L^I\rangle$ to denote a state obtained from the left-mover ground state by taking the momentum p_L^I in the compactified dimensions. In this case, the extra gauge fields arising are

$$W^i(p_L^I) = b^i_{-1/2}|0\rangle_R \, |p_L^I\rangle \,, \tag{1.31}$$

with p_L obeying

$$\sum_I (p_L^I)^2 = 2 \,. \tag{1.32}$$

This ensures that M_L^2 is zero. The internal momenta for which the above equation is satisfied depend on the lattice Λ, its dual Λ^*, and the choice of the radii R_a. There are very few choices of the lattice Λ consistent with an acceptable string theory. Demanding modular invariance [13], in order to ensure absence of anomalies and finiteness of loop contributions to scattering amplitudes, we get a restriction on the radii of the torus, namely

$$R_a = \frac{1}{\sqrt{2}} \qquad\qquad a = 1, ..., 16 \,. \tag{1.33}$$

The lattice Λ is restricted to be an even self-dual lattice, for which $\Lambda = \Lambda^*$, and

$$g_{ab} \equiv \sum_{I=1}^{16} e_a^I e_b^I = \text{even integer.} \tag{1.34}$$

One may check [13] that there are only two such lattices in 16 dimensions, Λ_{16} and $\Lambda_8 \times \Lambda_8$. The first one contains the root lattice of $SO(32)$ as a sublattice, leading to an $SO(32)$ gauge group. The second possibility, in which we will focus, is the direct product of two E_8 root lattices. The momenta p_L^I are on the root lattice of $E_8 \times E_8$, and the momenta of length two are the weight vectors of the adjoint representation of an $E_8 \times E_8$ gauge group, which arises from the toroidal compactification of the left-mover internal degrees of freedom of the heterotic string. Other massless states may be constructed by using the superstring right movers $b^i_{-1/2}|0\rangle_R$ $(i = 1, ..., 8)$ for the NS sector, or $|0\rangle_R$ for the R sector, together with the bosonic string left movers $\tilde{\alpha}^j_{-1}|0\rangle_L$ $(j = 1, ..., 8)$. In this way, we obtain in the NS sector the massless states

$$b^i_{-1/2}|0\rangle_R \, \tilde{\alpha}^j_{-1}|0\rangle_L \qquad\qquad i, j = 1, ..., 8 \,, \tag{1.35}$$

which decompose into a traceless symmetric ten-dimensional graviton, a dilaton, and an anti-symmetric tensor. In the R sector we have the states

$$|0\rangle_R \, \tilde{\alpha}^j_{-1}|0\rangle_L \qquad\qquad j = 1, ..., 8 \,. \tag{1.36}$$

The decomposition of the product of the spinor right-mover and the vector left-mover provides a ten-dimensional gravitino together with an eight-component ten-dimensional spinor. In this

way, the complete multiplet for ten-dimensional N=1 supergravity [60] is generated. The theory contains no tachyons, because the only right-mover state with negative M_R^2 is the NS sector ground state $|0\rangle_R$ with $M_L^2 = -2$, and the only left-mover state with negative M_L^2 is the bosonic string ground state $|0\rangle_L$with $M_L^2 = -4$, so we cannot satisfy $M_R^2 = M_L^2$.

1.2.1 Toroidal compactifications to four dimensions

The simplest way of producing a four-dimensional theory from the ten-dimensional heterotic string is by compactifying six of the remaining spatial dimensions on a torus, as we did before. This ensures that the linear string wave equations of motion are unaffected, since the torus differs from flat space only in the imposition of spatial periodicity. Working in the light-cone gauge, there are eight transverse bosonic degrees of freedom denoted by $X^i(\tau,\sigma)$ where $i = 1, 2$ labels the two four-dimensional space-time coordinates, and $X^k(\tau,\sigma)$ where $k = 3, ..., 8$ labels the remaining six spatial degrees of freedom. X^i and X^k may be split into right and left moving components in the usual manner. In addition, there are eight right-moving fermionic degrees of freedom $\Psi_R^{i(k)}(\tau-\sigma)$, and the 16 internal left-moving bosonic degrees of freedom $X_L^I(\tau+\sigma)$ with $I = 1, ..., 16$ which generate the $E_8 \times E_8$ gauge group. The toroidal compactification of the six spatial coordinates $X^k(\tau,\sigma)$ does not affect the mode expansions of $X^i(\tau,\sigma)$, $\Psi_R^{i(k)}(\tau-\sigma)$ or $X_L^I(\tau+\sigma)$. On the other hand, the mode expansions for the bosonic degrees of freedom X_R^k and X_L^k need to be amended to take account of the compactification. Following the steps taken in the previous section, we use a lattice defining the six-dimensional torus, with basis vectors e_t^k $(k, t = 3, ..., 8)$, so that for $X^k(\tau,\sigma)$ we have extra ways of satisfying the closed string boundary conditions

$$X^k(\tau,\sigma+\pi) = X^k(\tau,\sigma) + 2\pi L^k\,, \tag{1.37}$$

where the numbers L^k are given by

$$L^k = \frac{1}{\sqrt{2}}\sum_{t=3}^{8} n_t R_t e_t^k\,. \tag{1.38}$$

Therefore, we can write

$$X_R^k(\tau-\sigma) = x_R^k + p_R^k(\tau-\sigma) + \frac{i}{2}\sum_{n\neq 0}\frac{1}{n}(\alpha_n^k e^{-2in(\tau-\sigma)})\,, \tag{1.39}$$

$$X_k^I(\tau+\sigma) = x_L^k + p_L^k(\tau+\sigma) + \frac{i}{2}\sum_{n\neq 0}\frac{1}{n}(\tilde{\alpha}_n^k e^{-2in(\tau+\sigma)})\,, \tag{1.40}$$

with

$$p_{R,L}^k = \frac{1}{2}(p^k \mp 2L^k)\,. \tag{1.41}$$

Unlike before, we do not wish to eliminate the right movers. We must require $\exp(i\sum_{k=3}^{8} p^k x^k)$ to be single valued when x^k is replaced by

$$x^k \equiv x^k + \sqrt{2}\pi \sum_{t=3}^{8} n_t R_t e_t^k \,. \tag{1.42}$$

If the lattice with basis vectors e_t^k has a dual lattice with basis e_t^{*k} where

$$\sum_{t=3}^{8} e_t^k e_u^{*k} = \delta_{tu} \,, \tag{1.43}$$

then p^k must be given by

$$p^k = \sqrt{2}\sum_{t=3}^{8} \frac{m_t}{R_t} e_t^{*k} \,, \tag{1.44}$$

where m_t are arbitrary integers.

The four-dimensional mass-squared operator for the physical states is given by

$$M^2 = M_R^2 + M_L^2 \,, \tag{1.45}$$

with $M_R^2 = M_L^2$. For the superstring right movers,

$$\frac{1}{4}M_R^2 = N + \sum_{t=3}^{8} (p_R^k)^2 \,, \tag{1.46}$$

while for the bosonic left movers one has

$$\frac{1}{4}M_L^2 = \tilde{N} + \frac{1}{2}\sum_{I=1}^{16} (p_L^I)^2 + \frac{1}{2}\sum_{t=3}^{8} (p_L^k)^2 \,, \tag{1.47}$$

with N and $\tilde{N}$ analogous to what was defined in Eqs.(1.25,1.26) and Eq.(1.28). Massless states only arise when momenta and winding numbers on the compact manifold are zero. In fact, the particles we observe in nature must all derive from massless string states, since otherwise their masses would be of the order of the string scale ($\sim 10^{17}$ GeV). In the case of four-dimensional gravity, the graviton is the NS sector state given by

$$b_{-1/2}^i |0\rangle_R \, \tilde{\alpha}_{-1}^j |0\rangle_L \qquad\qquad i,j = 1,2 \,. \tag{1.48}$$

We also have four gravitini

$$|0\rangle_R \, \tilde{\alpha}_{-1}^j |0\rangle_L \qquad\qquad j = 1,2 \,, \tag{1.49}$$

where $|0\rangle_R$ is the Ramond ground state, which transforms as an eight-component $SO(8)$ chiral spinor. This spinor may be decomposed into representations of $SO(2) \times SO(6) \subset SO(8)$, the

$SO(2)$ corresponding to the two transverse space-time coordinates, and the $SO(6)$ to the six compactified spatial coordinates. Then

$$\mathbf{8_L} = (+1/2)\mathbf{4} + (-1/2)\bar{\mathbf{4}}\,, \tag{1.50}$$

so there are four space-time spinor particles of each chirality, as required for four gravitini. Evidently, the toroidal compactification of x^k inevitably leads to N=4 space-time supersymmetry, and hence to a non-chiral gauge symmetry (theories based on $N \geq 2$ supersymmetry are always non-chiral [6]). This means that the toroidal compactification of the extra six spatial dimensions is not appropriate. In the following section we shall see how orbifolds can solve this problem.

1.3 Space groups, point groups and orbifolds

In toroidal compactifications of the ten-dimensional heterotic string, the six left and right movers, X_R^k, X_L^k $(k = 3, ..., 8)$ are compactified on the torus T^6 generated by a lattice Γ, while the 16 left movers X_L^I are compactified on the self-dual torus $T^{E_8 \times E_8}$, generated by the root lattice vectors of the group $E_8 \times E_8$. In an orthonormal basis, the root lattice vectors take the form

$$(n_1, n_2, ..., n_8) \qquad \text{or} \qquad (n_1 + 1/2, n_2 + 1/2, ..., n_8 + 1/2)\,, \tag{1.51}$$

with n_i integer numbers and

$$\sum_{i=1}^{8} n_i = 0 \mod 2\,. \tag{1.52}$$

The torus is defined by identifying points of the underlying space which differ by a lattice vector $\boldsymbol{l} \in \Gamma$, that is

$$\boldsymbol{x} \equiv \boldsymbol{x} + \boldsymbol{l}. \tag{1.53}$$

It could be equivalently viewed as the euclidean space R^6 divided by the action of the discrete translation group Γ ,

$$T^6 = R^6/\Gamma\,. \tag{1.54}$$

We can generalise this definition of the torus by enlarging the translation group to include some discrete rotations. This generalised group is called the *space group* S, and consists of elements made of pairs of rotations θ and translations $\boldsymbol{l}$, denoted by $g = (\theta, \boldsymbol{l})$. Then, the action of the group elements on a vector $\boldsymbol{x}$ is given by

$$g\boldsymbol{x} = \theta\boldsymbol{x} + \boldsymbol{l}\,. \tag{1.55}$$

To be well defined on the torus, θ must be an automorphism of the lattice, i.e. $\theta\boldsymbol{l} \in \Gamma$ and preserve the scalar products defined by

$$\theta e_t \cdot \theta e_u = e_t \cdot e_u\,. \tag{1.56}$$

The isometry group is called the *point group* P. This gives us two equivalent wayss of describing an orbifold [17]. We can either start with euclidean space and divide by the space group, or consider the corresponding torus and divide by the point group. That is

$$\Omega = R^6/S = T^6/P\,. \tag{1.57}$$

Evidently, the six-dimensional orbifold may be obtained by identifying points of the underlying space R^6 which are related by the action of the space group

$$\boldsymbol{x} \equiv \theta\boldsymbol{x} + \boldsymbol{l}\,. \tag{1.58}$$

The solution of the string equations propagating on an orbifold are almost the same as for a toroidal compactification, since the orbifold is flat almost everywhere. The exceptions are the points of the torus which are fixed by the point group. At these *fixed points* the orbifold fails to be a manifold. Some lines emanating from them are identified with each other, so that a conical singularity occurs and the orbifold is not locally isomorphic to R^6. The fixed points satisfy the relation

$$\boldsymbol{x}_f = \theta\boldsymbol{x}_f + \boldsymbol{l}\,. \tag{1.59}$$

Therefore, the internal degrees of freedom $X^k_{L,R}, \Psi^k_R$ satisfy free field equations of motion as in a flat background but with boundary conditions dictated by the orbifold geometry. If we take into account the action of S, we find that we have more ways of satisfying the closed string boundary conditions. Regarding this effect, the spectrum in an orbifold may be divided into different sectors, that we call *untwisted* and *twisted*. In the untwisted sector the boundary conditions are of the form

$$\boldsymbol{X}(\tau, \sigma + \pi) = \boldsymbol{x}(\tau, \sigma) + \boldsymbol{l}, \tag{1.60}$$

while in the twisted sector the boundary conditions are given by

$$\boldsymbol{X}(\tau, \sigma + \pi) = \theta\boldsymbol{x}(\tau, \sigma) + \boldsymbol{l}\,. \tag{1.61}$$

Twisted sectors correspond to strings that are closed up to the action of the space group. Moreover, in order for a twisted state to be invariant under P, the position of the string center of mass must correspond to a fixed point of θ. Then, roughly speaking, twisted sectors are labelled by the element θ and the corresponding fixed point.

Elements of P act on the internal bosonic coordinates as $SO(6)$ rotations. Possible choices of P are further restricted by the phenomenological requirement of obtaining a N=1 supersymmetric spectrum (which is phenomenologically interesting due to the solution to the hierarchy problem that it presents). To get N=1 supersymmetry, P must be a subgroup of $SU(3)$ [14]. This may be seen by recalling that $SO(6)$ is isomorphic to $SU(4)$, so if $P \subset SU(3)$, there is a covariantly constant spinor on the six-dimensional orbifold, and it is this extra symmetry that

generates the required supersymmetry. In this work we shall restrict our attention to the cases in which the point group P is abelian (however, even if P is abelian, the space group S is in general non-abelian). Then it must belong to the Cartan subalgebra of $SO(6)$ associated with $X^k\,(k=3,...,8)$. We denote the generators of this subalgebra by M_{34}, M_{56}, M_{78}. Then, in the complex basis defined by

$$Z^1 = (1/\sqrt{2})(X^3 + iX^4)\,, \qquad Z^2 = (1/\sqrt{2})(X^5 + iX^6)\,, \qquad Z^3 = (1/\sqrt{2})(X^7 + iX^8)\,, \quad (1.62)$$

the point group element θ acts diagonally and may be written

$$\theta = \exp[2\pi i(v_1 M_{34} + v_2 M_{56} + v_3 M_{78})]\,, \tag{1.63}$$

with $0 \leq |v_i| < 1$ $(i = 1,2,3)$. A theory free of tachyons and the conditions for modular invariance impose

$$\pm v_1 \pm v_2 \pm v_3 = 0\,. \tag{1.64}$$

This restriction also guarantees that $P \subset SU(3)$. It can be showed [17] that the requirement that θ acts cristallographically on Γ, together with the condition of Eq. (1.64), lead to the conclusion that the point group P must either be Z^N with $N = 3,4,6,7,8,12$ or $Z_N \times Z_M$ with N a multiple of M and $N = 2,3,4,6$. Products of more Z_N's are not contained in $SU(3)$. A Z_N group is generated by a twist θ with $\theta^N = 1$, i.e. $P = \{\theta^n, n = 0,...,N-1\}$. In all cases it is possible to find a lattice where P acts cristallographicaly, and in many cases there are several lattices for a given P. In Table 1.1 we give the complete list of point group generators for Z_N.

So far we have discussed the action of S on the space-time degrees of freedom. We could also allow the space group S to act on the gauge degrees of freedom. This is called the *embedding* of S in the gauge group [17]. Choosing the action of (θ, Γ) on the gauge degrees of freedom implies associating a gauge transformation with a translation on the torus, for which the action of Γ can be simply represented as translations by shift vectors. Thus, we can extend the definition of an orbifold to

$$\Omega = T^6/P \times T^{E_8 \times E_8}/G\,, \tag{1.65}$$

where G is the embedding of S in the gauge group. Often, the massless spectrum and gauge group of the orbifold are independent of the choice of the lattice, and are determined only by P. For each point group there correspond many inequivalent space groups, depending on which lattice we pick and how the shift vectors have been chosen. However, when the full space group S, not just P, is embedded in the $E_8 \times E_8$ group, then the orbifold properties do depend upon the lattice Γ.

Point group	(v_1, v_2, v_3)	Point group	(v_1, v_2, v_3)
Z_3	$(\frac{1}{3}(1,1,-2))$	Z_4	$(\frac{1}{4}(1,1,-2))$
$Z_6 - I$	$(\frac{1}{6}(1,1,-2))$	$Z_6 - II$	$(\frac{1}{6}(1,2,-3))$
Z_7	$(\frac{1}{7}(1,2,-3))$	$Z_8 - I$	$(\frac{1}{8}(1,2,-3))$
$Z_8 - II$	$(\frac{1}{8}(1,3,-4))$	$Z_{12} - I$	$(\frac{1}{12}(1,4,-5))$
$Z_{12} - II$	$(\frac{1}{12}(1,5,-6))$		

Table 1.1: Complete list of point group generators for Z_N [61].

Before concluding this section, we will explicitly see how orbifold models are able to remove the unwanted gaugino and gravitino states of N=4 supersymmetry. We have just explained that the definition of an orbifold requires the specification a discrete group G comprising the space group S and its embedding in the gauge degrees of freedom. Thus, to each element $g \in G$ there corresponds an operator $\bar{g}$ which implements the action of g on the Hilbert space. Since the orbifold is defined by moding out the action of G, it follows that physical states must be invariant under G, i.e. they are eigenvectors of $\bar{g}$ with unit eigenvalues. If we consider the four gravitino states of the previous section,

$$|0\rangle_R \, \tilde{\alpha}^j_{-1} |0\rangle_L \qquad\qquad j = 1, 2\,. \tag{1.66}$$

Since $j = 1, 2$ correspond to the transverse space-time coordinates which are unaffected by the point group transformations, it is clear that g acts trivially on the left moving piece of the state. The right moving piece is the Ramond sector ground state, which is an $SO(8)$ chiral spinor. The explicit decomposition of Eq. (1.50) under $SO(2) \times SO(6)$, is given by

$$\mathbf{8_R} = (1/2,\, 1/2,\, 1/2,\, 1/2), (1/2,\, \underline{1/2,\, -1/2,\, -1/2}) + (-1/2,\, -1/2,\, -1/2,\, -1/2), (-1/2,\, \underline{-1/2,\, 1/2,\, 1/2}) \tag{1.67}$$

where the underlining denotes the inclusion of all permutations, and the individual entries are the eigenvalues of $M^{12}, M^{34}, M^{56}, M^{78}$ respectively. The point group generator θ is given by Eq. (1.61), and we see that acting on the first four states its eigenvalues are

$$\bar{\theta} = e^{\pi i(v_1+v_2+v_3)},\, e^{\pi i(v_1-v_2-v_3)},\, e^{\pi i(-v_1+v_2-v_3)},\, e^{\pi i(-v_1-v_2+v_3)}\,. \tag{1.68}$$

In the above, the second four states having complex conjugate eigenvalues. The condition of $v_1 \pm v_2 \pm v_3 = 0$ ensures that at least one of the states has $\bar{\theta}$=1. If we assume that

$$v_1 + v_2 + v_3 = 0\,, \tag{1.69}$$

then the eigenvalues of the above four states are

$$\bar{\theta} = 1,\, e^{2\pi i v_1},\, e^{2\pi i v_2},\, e^{2\pi i v_3}\,. \tag{1.70}$$

So, provided that v_1, v_2, v_3 are all non-zero, the last three states all have $\bar{\theta} \neq 1$. It follows that they are not invariant under the action of the space group. Thus, three of the four gravitini are deleted, as required if we want to obtain an N=1 space-time supersymmetric theory. On the other hand, if one of the v_i is zero, only two of the gravitini are removed and we obtain N=2 supersymmetry.

1.4 Construction of the space group of Z_3

In this section we shall see an explicit example of an orbifold model, namely the Z_3. This will be very useful to apply the orbifold elements previously discussed, and also to illustrate the forthcoming sections, in which we will try to build phenomenologically interesting models. In fact, the Z_3 will reveal itself as our best tool to construct models very similar to the Standard Model. We work with the complex coordinates Z^α of Eq. (1.62), with $\alpha = 1, 2, 3$. The lattice for the underlying torus is defined by making the identifications

$$Z^\alpha \equiv Z^\alpha + 1\,, \tag{1.71}$$

$$Z^\alpha \equiv Z^\alpha + e^{2\pi i/3}\,. \tag{1.72}$$

Thus, we can assemble Z^1, Z^2, Z^3 into a vector $\boldsymbol{Z}$,

$$\boldsymbol{Z} = \boldsymbol{Z} + \sum_{\rho=1}^{3} (m_\rho \boldsymbol{e}_\rho + n_\rho \boldsymbol{f}_\rho)\,, \tag{1.73}$$

where the basis vectors $\boldsymbol{e}_\rho$ and $\boldsymbol{f}_\rho$ for the lattice are defined by

$$\boldsymbol{e}_1 = (100)\,, \qquad \boldsymbol{e}_2 = (010)\,, \qquad \boldsymbol{e}_3 = (001)\,, \tag{1.74}$$

with

$$\boldsymbol{f}_\rho = e^{2\pi i/3} \boldsymbol{e}_\rho \qquad\qquad \rho = 1, 2, 3\,, \tag{1.75}$$

and where m_ρ, n_ρ are integers. The point group for the Z_3 orbifold is the discrete group generated by the element

$$\theta = \mathrm{diag}(e^{2\pi i/3}, e^{2\pi i/3}, e^{2\pi i/3})\,, \tag{1.76}$$

acting on $\boldsymbol{Z}$. The complex coordinates provide a basis for the three dimensional representation of the $SU(3)$ subgroup of the $SO(6)$ rotation group for the real coordinates X^k $(k = 3, ..., 8)$ and θ is a finite element of the latter $SU(3)$. The action of θ on the basis vectors is given by

$$\theta \boldsymbol{e}_\rho = \boldsymbol{f}_\rho \,, \tag{1.77}$$

$$\theta^2 \boldsymbol{e}_\rho = \theta \boldsymbol{f}_\rho = -\boldsymbol{e}_\rho - \boldsymbol{f}_\rho \,, \tag{1.78}$$

$$\theta^3 \boldsymbol{e}_\rho = \boldsymbol{e}_\rho \,. \tag{1.79}$$

Thus, the discrete group generated by θ is a symmetry of the torus. Now we want to identify the fixed points of the orbifold, such that

$$(\theta, \boldsymbol{l})\boldsymbol{Z} = \theta \boldsymbol{Z} + \boldsymbol{l} = \boldsymbol{Z} \,, \tag{1.80}$$

where $\boldsymbol{l}$ is of the form

$$\boldsymbol{l} = \sum_{\rho=1}^{3} (m_\rho \boldsymbol{e}_\rho + n_\rho \boldsymbol{f}_\rho) \,. \tag{1.81}$$

One may check that the fixed points may be written in the form

$$\boldsymbol{Z} = \frac{e^{i\pi/6}}{\sqrt{3}} (m_1 + n_1, m_2 + n_2, m_3 + n_3) - (n_1, n_2, n_3) \,. \tag{1.82}$$

Thus, there are 27 inequivalent fixed points

$$\boldsymbol{Z} = \frac{e^{i\pi/6}}{\sqrt{3}} (p_1, p_2, p_3) \,, \tag{1.83}$$

with $p_\rho = 0, \pm 1$ for $\rho = 1, 2, 3$, with all other fixed points differing from these by a lattice vector, and thus occupying the same points on the torus. The fixed points satisfy the condition $(\theta, \boldsymbol{l})\boldsymbol{Z} = \boldsymbol{Z}$ with

$$\boldsymbol{l} = \sum_{\rho=1}^{3} p_\rho \boldsymbol{e}_\rho + (I - \theta)\boldsymbol{k}, \tag{1.84}$$

for any lattice vector $\boldsymbol{k}$, since $\boldsymbol{Z} - \boldsymbol{k}$ is equivalent to $\boldsymbol{Z}$ on the torus.

1.5 Point group embedding in the gauge group

As previously mentioned, the space group S may be embedded in the gauge degrees of freedom, and in general (as we shall later see) this embedding is compulsory. This is made by mapping the element $(\theta, \boldsymbol{l})$ of S on to $(\Theta, \boldsymbol{V})$ where Θ is an automorphism of the $E_8 \times E_8$ lattice and $\boldsymbol{V}$ is a shift on the lattice. In this section we will focus on the (compulsory) embedding of the point group elements $(\theta, \boldsymbol{0})$ in the gauge group. The optional embedding of the point group elements

(1,$\boldsymbol{l}$) by *Wilson lines*, is discussed in following sections. The embedding becomes easier by using the fermionic formulation [6] of the gauge degrees of freedom. In this formulation, the 16 bosonic left movers X^I are represented by 32 real fermionic left movers $(\lambda^A, \bar{\lambda}^A)$, with $A = 1, ..., 16$. The real fermionic movers $\lambda^A, \bar{\lambda}^A$ may separately have R or NS boundary conditions. These fermions transform as the $(\mathbf{16}, \mathbf{1}) + (\mathbf{1}, \mathbf{16})$ representation of the maximal subgroup $O(16) \times O(16) \subset E_8 \times E_8$. The simplest non-trivial embedding is achieved by picking an $O(6)$ subgroup of $O(16)$, in which the vector representation decomposes into a six-dimensional vector representation of $SO(6)$ plus ten $SO(6)$ singlets. Then we form three complex fermions from the real fermions, and then take the action of the point group on them to be precisely the same in the right moving fermions Ψ^α_R (where we have constructed complex Ψ^α in the same way as we did for Z^α), and the other ten fermions are untransformed. This is called the *standard embedding*. The second set of fermions $\bar{\lambda}$ remains untransformed. This embedding amounts to a shift in the $E_8 \times E_8$ lattice when we use the bosonic formulation. To see this we employ the relationship

$$\Psi^I(\tau + \sigma) = \exp(2iX^I_L) \tag{1.85}$$

between the bosonic toroidal coordinates and the complex fermions. Then, multiplying Ψ by a phase factor $\exp(2\pi i V)$ amounts to adding πV^I to the bosonic coordinates, X^I_L. Thus the embedding of $(\theta, 0)$ on the $E_8 \times E_8$ lattice is realised as $(1, \pi V^I)$, and the twisted sector boundary conditions for the X^I_L become

$$X^I_L(\tau + \sigma + \pi) = X^I_L(\tau + \sigma) + \pi V^I \,. \tag{1.86}$$

The mode expansion satisfying this is

$$X^I_L = x^I_L + (p^I_L + V^I)(\tau + \sigma) + \frac{i}{2} \sum \frac{1}{n} \tilde{\alpha}^I_n e^{-2in(\tau+\sigma)} \,. \tag{1.87}$$

Evidently, the net effect of the twist θ is to shift the momentum p^I_L by V^I. In the standard embedding, which we have so far discussed,

$$V^I = (v_1, v_2, v_3, 0^5)(0^8) \,, \tag{1.88}$$

where v_α, $(\alpha = 1, 2, 3)$ are the twists of the three complex compactified coordinates. We may also explore the possibility of more general non-standard embeddings. Then the only constraint on the shift V^I is that for a Z_N orbifold NV^I is on the $E_8 \times E_8$ root lattice,

$$NV^I \in E_8 \times E_8 \,. \tag{1.89}$$

The requirement that $\pm v_1 \pm v_2 \pm v_3 = 0$ ensures that the above constraint is always satisfied by the standard embedding.

We have already observed that orbifold models remove the unwanted supersymetries via the requirement of point group invariance. This point group invariance also reduces the gauge

symmetry when the point group is embedded in the gauge degrees of freedom, as it should in general be. Precisely what gauge symmetry survives depends upon the details of the particular orbifold. However, we can make a general statement when the standard embedding is adopted. The constraint $P \subset SU(3)$ ensures that the point group is embedded in an $SU(3)$ subgroup of one of the E_8 groups. Since

$$E_8 \supset E_6 \times SU(3)\,, \tag{1.90}$$

it is clear that the surviving gauge symmetry will always include $E_6 \times E_8$. Further, the rank of the gauge group is unaffected by the embedding, since the gauge bosons associated with the Cartan subalgebra are all invariant under the action of the point group. As we have seen, the point group embedding in the gauge group breaks one of the E_8 symmetries to a smaller group with the same rank, while leaving the other E_8 unbroken. This affords the prospect of achieving further symmetry breaking, by Wilson lines for example, leaving a realistic gauge group. For this reason the broken E_8 is called the *observable sector*, and the unbroken E_8 the *hidden sector*.

1.6 Space group embedding and Wilson lines

Further breaking of the of the gauge group can be achieved by embedding the complete space group S in the gauge group. This means that not only should the point group element be embedded as a shift on the $E_8 \times E_8'$ bosonic degrees of freedom, but also the various basis vectors of the torus lattice underlying the orbifold should be embedded as such shifts. This mechanism requires the existence in the theory of non-zero quantities U of the form

$$U \sim \exp \oint A_k dx^k\,, \tag{1.91}$$

where $k = 3, ..., 8$. These integrals, referred to as Wilson lines [18], are defined over some closed loop not contractible to zero on the underlying torus of the orbifold. The A_k are components of some 10-dimensional gauge field with zero field strength. Wilson lines cannot be gauged to zero by an ordinary gauge transformation, but they can be gauged away by means of a non-single valued gauge transformation. In this alternative formulation of the theory the Wilson lines are not present. Instead, the fermionic degrees of freedom realising the gauge group in the fermionic formulation of the heterotic string acquire extra phases upon a circuit of the torus as a result of the non-singled valued gauge transformation that has been performed. Equivalently, in the bosonic formulation, the bosonic degrees of freedom acquire extra shifts upon a circuit of the torus. As a consequence, the boundary conditions for the twisted sector are modified. As we shall see, the introduction of Wilson lines produces the gauge symmetry breaking and also modifies the matter content, so that three-generation models can be obtained.

Consider a twisted sector with boundary conditions twisted by the space group element $(\theta, \boldsymbol{l})$, where θ is the point group element and $\boldsymbol{l}$ is a lattice vector,

$$\boldsymbol{l} = \sum \boldsymbol{r}_\rho \boldsymbol{e}_\rho \,, \tag{1.92}$$

where $\boldsymbol{e}_\rho$ are integral coefficients and $\boldsymbol{r}_\rho$ are basis vectors of the six torus lattice. In the bosonic formulation, if the embedding of θ in the gauge group is represented by a shift πV^I on the boundary conditions, the embedding of $\boldsymbol{e}_\rho$ will be represented by a shift πa^I_ρ, while the momenta are shifted from the $E_8 \times E_8'$ momenta p^I_L by $V^I + r_\rho a^I_\rho$. Then, the spectrum of massless states is now different for different fixed points, due to the influence of the Wilson lines a^I_ρ. In addition, we must demand space group invariance in the untwisted sector . The extra invariance due to the embedding of $\boldsymbol{l}$ must reflect the fact that πa^I_ρ is a shift on the coordinates x^I and that $\exp(2\pi i p^I_L a^I_\rho)$ should be 1, or equivalently

$$p^I_L a^I_\rho = \text{integer} \,. \tag{1.93}$$

To ensure that we have an embedding, we must check that we obtain a homomorphism. Thus, for two space group elements $(\theta_1, \boldsymbol{l}_1)$ and $(\theta_2, \boldsymbol{l}_2)$,

$$(\theta_1, \boldsymbol{l}_1)(\theta_2, \boldsymbol{l}_2) = (\theta_1\theta_2, \boldsymbol{l}_1 + \theta_1 \boldsymbol{l}_2) \,, \tag{1.94}$$

while for a Z_N point group generated by θ,

$$(\theta, \boldsymbol{l})^N = (I, 0) \,. \tag{1.95}$$

Consequently, it is necessary to have

$$N(V^I + a^I_\rho) \in E_8 \times E_8' \,, \tag{1.96}$$

which in turn implies that

$$NV^I \qquad \text{on an } E_8 \times E_8' \text{ lattice} \,, \tag{1.97}$$

$$Na^I_\rho \qquad \text{on an } E_8 \times E_8' \text{ lattice} \,. \tag{1.98}$$

Moreover, the fundamental modular invariance property of a consistent theory [61] requires, for the Z_N orbifold, that

$$N\left(n^2 \sum_{\alpha=1}^{3} (v^\alpha)^2 - \sum_{I=1}^{16} (nV^I + r_\rho a^I_\rho)^2 \right) = 0 \ \text{mod}\ 2 \,, \tag{1.99}$$

for the θ^n twisted sector, with $n = 0, ..., N-1$ and $r_\rho = 0, ..., N-1$. In particular, embeddings of the point group in the gauge group consistent with modular invariance are required to satisfy the relation

$$N\left(\sum_{I=1}^{16} (V^I)^2 - \sum_{\alpha=1}^{3} (v^\alpha)^2 \right) \equiv N(V^2 - v^2) = 0 \ \text{mod}\ 2 \,. \tag{1.100}$$

This constraint is not satisfied by the trivial embedding $V = 0$. It is in this sense that we say that the point group embedding is compulsory in this class of models.

1.7 Explicit models with Wilson lines

Regarding the construction of explicit models, it turns out that a wide class of four dimensional models can be built with the desired N=1 supersymmetry. From each of the possible Z_N's, we can select several lattices where they can act. For each of them, we can make different embeddings of the point group in the gauge group. For each embedding we can have several independent Wilson lines; the amount of models grows geometrically. For instance, in the Z_3 orbifold there are four different independent embeddings. Adding one Wilson line, the total number of possible models is $\mathcal{O}(10^3)$. Adding a second and third Wilson line increases the number to an estimate number of 10^9 different models [20, 51]. Wilson lines also allow to explicitly differentiate lattices with the same point group, which would lead to equivalent models if they are not present. To this list we have to add all models constructed by non-abelian embeddings and by left-right asymmetric twists, and also the ones with a $Z_N \times Z_M$ twist. A general classification of all these models is extremely difficult. Rather than doing this, it is better to look for interesting models from the phenomenological point of view. This can be done if we have some idea of what can be expected from a particular construction. We have seen that the introduction of Wilson lines breaks the gauge group and modifies the matter content. We can use these properties to find models, focusing on Z_N orbifolds. If we use the number of generations (three) as a guide, the best candidate is the Z_3 orbifold, because there is an overall factor of three coming from the right-moving part of the untwisted sector matter. This is due to the fact that the three complex coordinates are twisted by the same angle, and that the degeneracy factor in the twisted sectors is either one or a multiple of three.

As seen before, massless states in the untwisted sector are given by the $E_8 \times E_8$ roots $[(p_L^I)^2 = 2]$ projected onto those which are Wilson-line singlets, i.e.

$$p_L^I a_\rho^I \in \mathbb{Z}\,. \tag{1.101}$$

These roots are split into three groups, according to how they transform under $e^{2\pi i \boldsymbol{p}\cdot\boldsymbol{v}}$. The invariant states

$$p_L^I v^I \in \mathbb{Z}\,, \tag{1.102}$$

combine with the right movers $b^i_{-1/2}|0\rangle_R$ $(i = 1, ..., 8)$, which are invariant under the point group P, to make the gauge boson multiplet. The roots with

$$p_L^I v^I = \frac{2}{3} \mod 1\,, \tag{1.103}$$

lead to invariant states after combining the right moving states $b^\alpha_{-1/2}|0\rangle_R$ $(\alpha = 1, 2, 3)$, which transform as $e^{-2\pi i/3}$ under P. They generate three copies of matter fields transforming under some representation of the gauge group.

$3v$	$(2,1,1,1,1,0,0,0)(2,0,0,0,0,0,0,0)$
$3a_1$	$(2,1,1,0,0,1,1,0)(0,1,1,1,1,0,0,0)$
$3a_2$	$(0,0,2,0,0,0,0,0)(-1,0,0,1,2,1,1,0)$
Gauge group	$[SU(3)\times SU(2)\times U(1)^5]$ $\times[SU(2)^2\times U(1)^6]$
Matter content	$3[(3,2)+2(3^*,1)+(1,2)+(1,1)]$ $+12(1,2)$+hidden matter+singlets

Table 1.2: A model with 3 families of $SU(3)\times SU(2)\times U(1)^n$ [20].

1.7.1 Three-generation Z_3 models with $SU(3)\times SU(2)\times U(1)^n$ gauge group

As we have mentioned, there are around 10^3 models for Z_3 with one Wilson line. If we focus only on models with three generations, we will find the gauge groups $SU(5)\times SU(2)^2\times U(1)^2$, $SO(10)\times SU(2)\times U(1)^2$, $SU(7)\times U(1)^2$, $SU(6)\times SU(3)\times U(1)$, and $E_6\times U(1)^2$ [20, 51]. Thus all the most interesting grand unifying groups can be obtained with three generations of quarks and leptons. For these kind of models, the smallest subgroup one can obtain from an E_8 is $SU(3)^3\times U(1)^2$. In order to get even smaller groups such as $SU(3)\times SU(2)\times U(1)^5$, we would have to add more Wilson lines.

The addition of one or two extra Wilson lines will give rise to an enormous number of models (as large as 10^5-10^9) for the Z_3 [20]. As before, we can reduce this number by imposing further phenomenological constraints, such as a realistic gauge group or the requirement of three particle generations. At the end of the day, one will be left with a three-generation gauge group $SU(3)\times SU(2)\times U(1)^n$. Within the Z_3 orbifold with two Wilson lines, for instance, one can construct in principle a number of order 50000 of three-generation models with $SU(3)\times SU(2)\times U(1)^n$. However, it can be shown that most of them turn out to be equivalent [62]. Let us recall that this mechanism for obtaing realistic groups does not reduce the rank of the group and we cannot avoid the extra $U(1)$'s. Imposing the output for the gauge group, we want the invariant roots to be $\pm(1,-1,0,...,0)$ defining $SU(2)$, and $\pm(0,0,1,-1,0,...,0)$, $\pm(0,0,0,1,-1,0,...,0)$, $\pm(0,0,1,0,-1,0,...,0)$ defining $SU(3)$. This fixes the $SU(2)$ and $SU(3)$ regions in the eight-dimensional vectors. As an example, a possible choice for the shift and two Wilson lines that provides a model with three families and $SU(3)\times SU(2)\times U(1)^n$ gauge group is presented in Table 1.2.

In this class of models, one can easily find a linear combination of the unbroken $U(1)$'s which may be identified with the hypercharge. In order to lower the rank of the gauge group, one may look for singlet flat directions to break de extra $U(1)$'s, finding that there are indeed many possibilities to do so. On the other hand, all these models have an anomalous $U(1)$ and hence an associated Fayet-Iliopoulos D-term [22]. To cancel this term in the scalar potential generically some singlets in the model are dynamically forced to acquire a VEV and thus produce the reduction of the particle spectrum. As we see, all these effects involve strong phenomenological consequences which turn out to be extremely useful for model building.

We see that these models are very close to the Standard Model, but they still fail in providing complete phenomenological success. It is necessary to know the number n of the $U(1)$'s that couple to quarks and leptons, the possible effects of the anomalous $U(1)$ that usually appears in these constructions, and the role of $U(1)$'s mixing the hidden and the observable sector.

1.8 $U(1)$ charges and anomaly cancellation

In this section we will show how the $U(1)$ charges can be calculated, determining which of them are anomalous [21]. These $U(1)$'s are in such a way that can be cancelled by the Green-Schwarz mechanism [12]. The complete knowledge of the anomalies is essential for a phenomenological analysis of the different models. The existence of an anomalous $U(1)$ can produce further symmetry breaking that can be used to lower the rank down to $SU(3)\times SU(2)\times U(1)_Y$. As an illustrative example, let us consider the explicit three-generation $SU(3)\times SU(2)\times U(1)^n$ model analysed in [19, 21], with the following embedding and Wilson lines:

$$\begin{aligned} 3v^I &= (1,1,1,1,2,0,0,0)(2,0,0,0,0,0,0,0)\,,\\ 3a_1^I &= (0,0,0,0,0,0,0,2)(0,1,1,0,0,0,0,0)\,,\\ 3a_2^I &= (1,1,1,2,1,0,1,1)(1,1,0,0,0,0,0,0)\,. \end{aligned} \tag{1.104}$$

As we know, the gauge bosons are obtained by projecting the $E_8\times E_8$ roots ($p^2=2$) onto those which are Wilson line singlets, and satisfy $p^I v^I\in\mathbb{Z}$. They are

$$\begin{aligned} &(\underline{1,-1,0},0,0,0,0,0)\,,\\ &\pm(0,0,0,1,1,0,0,0)\,,\\ &(0,0,0,\underline{\pm,1,\pm1,0,0,0})'\,, \end{aligned} \tag{1.105}$$

where the prime denotes the E_8' part. These roots correspond to the gauge group

$$[SU(3)\times SU(2)\times U(1)^5]\times[SO(10)\times U(1)^3]'\,. \tag{1.106}$$

The last three entries of E_8 and the first three of E_8' correspond to six of the eight $U(1)$ charges. The rest of them lie on the directions orthogonal to the roots of $SU(3)$ and $SU(2)$. Explicitly, the $U(1)$'s are

$$\begin{aligned} U_1 &: (1,1,1,0,0,0,0,0), & U_2 &: (0,0,0,1,-1,0,0,0)\,, \\ U_3 &: (0,0,0,0,0,1,0,0), & U_4 &: (0,0,0,0,0,0,1,0)\,, \\ U_5 &: (0,0,0,0,0,0,0,1), & U_6 &: (1,0,0,0,0,0,0,0)'\,, \\ U_1 &: (0,1,0,0,0,0,0,0)', & U_8 &: (0,0,1,0,0,0,0,0)'\,. \end{aligned} \tag{1.107}$$

One can look for the matter fields of this model that belong to the untwisted and twisted sectors, by projecting the $E_8 \times E_8'$ roots along the directions of the $SU(3)$, $SU(2)$ and $SO(10)$ roots. Finally, one gets the $U(1)$ charges by projecting onto the directions of Eq. (1.107).

Regarding the anomalies of these models, it must be noted that modular invariance guarantees that the anomaly of the 10-dimensional heterotic string has a factor $tr(F^2) - tr(R^2)$, where F denotes the field strength of the gauge group and R is the Riemann tensor. This remaining anomaly can be canceled using the Green-Schwarz mechanism. As a consequence, one can expect the presence of anomalous $U(1)$'s in the four dimensional effective theory after compactification. The above mentioned factorisation implies that if there is an anomaly, there must be just one anomalous $U(1)$ (i.e. if there are n $U(1)$'s in a specific model, there will be one anomalous combination of them and $n-1$ non-anomalous ones). In the example previously considered, the anomalies may either involve three $SU(3)$ gauge bosons, one $U(1)$ and two $SU(N)$ or $SO(N)$ bosons, three $U(1)$ gauge bosons, or one $U(1)$ boson and two gravitons. One can verify that from the eight U_i defined in Eq. (1.107), five of them are non-anomalous: U_1, U_2, U_3, U_4 and U_5. From the other three it is possible to form an anomalous combination. This allows to factorise the anomaly [63] in the form

$$\partial^\mu J_\mu^x = \frac{g^2}{-32\pi^2} \sum_n Q_x (F\tilde{F} - R\tilde{R})\,. \tag{1.108}$$

where n runs over the states of the model and Q_x are the charges under the anomalous $U(1)$. This anomaly is canceled by the term $b(F\tilde{F} - R\tilde{R})$ (b is the physical massless degree of freedom of the four-dimensional, antisymmetric tensor $B_{\mu\nu}$) by assigning to b a non-trivial transformation law $b \to b + c\lambda$ under the anomalous $U(1)$ for an appropriate c (λ is the gauge transformation parameter). In fact this term is the remnant of the ten-dimensional Green-Schwarz after compactification. The transformation rule for b is that of a Goldstone boson. Thus, the gauge symmetry is broken and the b-field becomes a longitudinal mode of the massive anomalous gauge boson, which disappears from the low-energy theory. This is the first important consequence of the existence of anomalous $U(1)$'s after compactification. In the next section we will discuss even more important effects.

1.9 Fayet-Iliopoulos terms and $SU(3) \times SU(2) \times U(1)_Y$ models

As we have mentioned, some four-dimensional theories with $SU(3) \times SU(2) \times U(1)^n$ lead to an anomalous $U(1)$ factor. Therefore, at string one loop order a Fayet-Iliopoulos D-term is generated for this $U(1)$ [22]. This D-term can break supersymmetry by the Fayet-Iliopoulos mechanism. However, the supersymmetry can often be preserved by simultaneously allowing some scalar fields to acquire VEVs. In order to see whether this happens we have to consider the explicit form of the anomalous D-term,

$$D^{(a)} = -e^{-\phi}\Big[e^{-2\phi}c^{(a)} + \sum_i Q_i^{(a)}\eta_i^*\eta_i\Big]\,, \tag{1.109}$$

where η_i are the scalars fields with charges $Q_i^{(a)}$ under the anomalous $U(1)$, ϕ is the dilaton and the coefficient c^a is given by

$$c^{(a)} = \frac{2g}{192\pi^2}\sum_i Q_i^{(a)}\,. \tag{1.110}$$

Obviously, this quantity is vanishing if the model does not have any anomalous $U(1)$. In addition, we have to consider the non-anomalous D-terms,

$$D^j \sim \sum_i Q_i^{(j)}\eta_i^*\eta_i\,, \tag{1.111}$$

where $Q_i^{(j)}$ are the charges of the η_i fields under the non-anomalous $U(1)^{(j)}$ of the model. The presence of the FI D-term leads to supersymmetry breaking unless there is a choice of VEVs for some of the scalar fields, say χ_k, which cancels it

$$\sum_k Q_k^{(a)}|\langle\chi_k\rangle|^2 = -e^{2\phi}c^{(a)}\,, \tag{1.112}$$

as well as the non-anomalous D-terms,

$$\sum_k Q_k^{(j)}|\langle\chi_k\rangle|^2 = 0\,. \tag{1.113}$$

Furthermore, the set of VEVs must be such that

$$W = \partial W/\partial\eta_i = 0\,, \tag{1.114}$$

(where W is the superpotential of the theory) in order to avoid non-vanishing F-terms which would also break supersymmetry. If such a set of VEVs exists, the gauge group of the three models here analysed will be further broken, since there are no fields that carry charge under the anomalous $U(1)$ only.

Another important issue is to check whether there is any combination of the non-anomalous $U(1)$'s which gives the correct hypercharge to the states. Generically, this class of models

presents some ambiguity related to the assignments of the states L, H_1, H_2, e^c. But, even for a specific assignment it is in principle posible to find many $U(1)$ combinations for the hypercharge.

In order to see whether there is a vacuum state preserving the physical hypercharge Y, one has to look for the subset of singlet fields with vanishing Y-charges. If these fields may acquire VEVs satisfying the conditions of Eqs. (1.112) and (1.114), the desired vacuum exists. In fact, in this case it is possible to find vacuum states preserving an unbroken gauge group $SU(3) \times SU(2) \times U(1)_Y \times G'$.

This shows that the Fayet-Iliopoulos breaking induced by the presence of anomalous $U(1)$'s is an efficient method to get realistic models. Now we can analyse the spectrum of massless particles after the breaking. Many particles acquire a high mass due to the generation of effective mass terms. These come from operators of the type

$$(\chi \cdots \chi)\xi \qquad , \qquad (\chi \cdots \chi)\xi\xi \,, \tag{1.115}$$

where χ refers to any field acquiring a VEV and ξ any other field. There is also a considerable number of operators involving color triplets of the form

$$f_i \bar{D}_j D_k \,, \tag{1.116}$$

where f_i are singlets and $D_{j,k}$ are triplets. As an example, in the model presented in Ref. [21], one can see that the massless coloured fields are

$$Q, \qquad u^c, \qquad (d^c, \bar{D}_i, \bar{D}_j) \,, \tag{1.117}$$

where $(d^c, \bar{D}_i, \bar{D}_j)$ stands for a certain combination of the fields inside the parenthesis with the quantum numbers of the d^c field. The remarkable point is that all the extra colour triplets become naturally massive, thus disappearing from the low energy theory. On the contrary, Standard Model triplets and doublets (i.e. Q, u^c, d^c, L, H_1, H_2) remain massless. It is also very attractive that all the extra colour triplets, which could mediate fast proton decay, can acquire high masses. The effective mass terms for the singlets that come from cubic couplings are of the type

$$\chi_i f_j f_k \,. \tag{1.118}$$

These terms give masses to most of the singlets of the model. However, some massless singlet states still remain after the breaking process, and one of these singlets is e^c. The final massless particle spectrum is very close to the three-generation supersymmetric standard model, plus some exotic matter ($SU(2)$ doublets and $SU(3) \times SU(2)$ singlets). In particular, one of the main generic features of Z_3 models with two Wilson lines is the family replication in the Higgs sector, composed by six doublets (three up-type and three down-type). In other orbifold models similar to this, also extra $SU(3)$ triplets may appear. Needless to say, the presence of extra

matter could affect the renormalisation group predictions for $\sin\theta_W$ and M_{GUT}. Although the number of these extra particles is not huge, a realistic unification seems to be problematic. However, the presence of the three generations of Higgses, and extra colour triplets may allow unification to be achieved at the string scale [64].

1.10 Summary and outlook

In this chapter we have reviewed the main properties concerning orbifold compactifications. Through the different sections we have learned that the compactification of the heterotic string on a six-dimensional orbifold is an attractive method to obtain the emergent 4D effective theory, including the gauge group and matter content. We have seen that the employment of Z_3 orbifold scenarios with two Wilson lines become very instrumental in obtaining realistic scenarios very close to the Standard Model. These scenarios are generically characterised by:

- Realistic $SU(3) \times SU(2) \times U(1)^n \times G'$ gauge group.
- Supersymmetric standard-like matter content.
- Existence of FI D-term which triggers further symmetry breaking down to a Standard $SU(3) \times SU(2) \times U(1)_Y \times G'$ gauge group.
- Some exotic matter remaining at low energy.
- Three generations of SUSY Higgses typically present in the spectrum.

From the phenomenological perspective, the last point on the list is worth special consideration. Indeed, the presence of three Higgs families in the low-energy theory has many disctintive implications which modify the minimal assumption of just one pair of Higgs doublet. Probably one of the most important non-minimal contributions of any model with Higgs replication is the appearance of FCNC a the tree level due to a Higgs exchange between particles of different flavour. A general study of SUSY models with three Higgs families and their requirements to avoid conflict with the FCNC bounds will be developed in Chapter 2.

Another important point that has been also not mentioned on the list concerns the ability of orbifold scenarios to give masses to the SM particles. Needless to say, a fully realistic Standard-like scenario must also include a mechanism to generate Yukawa couplings in order to provide the observed masses and mixings for the low-energy spectrum. This subject will be fully analysed in Chapter 3 (for the case of quarks) and Chapter 4 (for charged leptons and neutrinos).

Chapter 2

FCNCs in supersymmetric models with three Higgs families

2.1 Introduction

Given the existence of three families of quarks and leptons, and since neither theory nor experiment impose any constraints on the number of Higgs families, one could wonder whether the same family replication takes place in the Higgs sector. In addition to being very aesthetic, this scenario is not unexpected from a theoretical point of view. As we have analysed in the previous chapter, in four-dimesional SUSY models arising from the orbifold compactification of the 10 dimensional $E_8 \times E_8'$ heterotic string, the low-energy theory thus obtained is associated with a subgroup of the gauge group E_6. Under E_6, fermions and Higgses are assigned to the same representation, and the requirement of three families of fermions imposes replication of the Higgs content [13]. In fact, many string constructions that contain three fermion families also include Higgs family replication, as is the case of Z_3 orbifold heterotic compactifications, which also exhibit these low-energy spectrum composed of three supersymmetric Higgs families [24, 51, 53, 64–66], and that of some D-brane models [58]. Other models that include a non-minimal Higgs content have also been extensively addressed in the literature [36–43, 46–50, 67–70]. The consequences of extending the Higgs sector are abundant, and have implications which range from the theoretical to the experimental level. For instance, and if the extra Higgses are light, the addition of these states in a minimal SUSY scenario will spoil the unification of gauge couplings around 10^{16} GeV. Nevertheless, in models from the heterotic string, the high energy scale is different ($\sim g_{\rm GUT} \times 10^{17}$ GeV [71]), and the new states can even be helpful regarding unification [64]. Since ours is a low-energy oriented analysis, we will not consider the (more speculative) high-energy implications of the extended Higgs sector. The most challenging

implication of an extended Higgs sector is perhaps the potential occurrence of tree-level flavour changing neutral currents, mediated by the exchange of neutral Higgs states[1]. In the SM and the MSSM, these effects are absent at the tree-level, since the coupling of the quark-quark-Higgs mass eigenstates is flavour conserving. This arises from having the Yukawa couplings proportional to the quark mass matrices, so that diagonalising the mass matrices also diagonalises the Yukawas. Since experimental data is in good agreement with the SM predictions, the potentially large contributions arising from the tree-level interactions must be suppressed in order to have a model which is experimentally viable. In general, the most stringent limit on the flavour-changing processes emerges from the small value of the $K_L - K_S$ mass difference [46, 47].

Avoiding the FCNCs induced by the tree-level exchange of neutral Higgs bosons can be achieved by several distinct approaches, each involving a different sector of the model.

(i) Discrete symmetries. Imposing a discrete symmetry on the model ensures that only one generation of Higgs couples to quark and leptons, and completely eliminates tree level FCNCs from the predictions of the model [44, 45]. Naturally, one attempts to motivate such an assumption via topological and/or geometrical arguments. For instance, in [39, 40], adding four extra Higgs doublets to the MSSM content, and assuming that the FCNCs thus induced are suppressed via some symmetry, then the extra generations (labelled "pseudo-Higgs bosons") do not acquire vacuum expectation values (VEVs), do not mix with the two MSSM-like doublets, nor couple to fermions. Still, the lightest of the new states is stable so that it becomes a candidate for dark matter.

(ii) Suppression of Yukawa couplings. In this case, FCNCs are not eliminated, but the Yukawa interaction responsible for the tree-level flavour violation is made small enough to render the new contributions negligible. Since the most stringent bounds are usually associated with tree level contributions to the neutral kaon mass difference (Δm_K), the Yukawa couplings of down and strange quarks are forced to be very small. For example, in [43], a $U(2)$ flavour symmetry was considered as the candidate symmetry to suppress FCNCs. Although this second possibility is more appealing in the sense that it does not require excluding part of the Higgs content from Higgs-matter interactions, its major shortcoming lies in the fact that in general one lacks a full theory of flavour, which would predict the Yukawa couplings[2], as would be the case of string theory.

(iii) Decoupling of extra Higgses. If one does not wish (or is not allowed) to impose a symmetry, or if the Yukawa couplings are not free parameters of the model, a third possibility lies in making the new Higgs states heavy enough, so that the contributions they mediate are very

[1] For other consequences such as flavour-violating Higgs and top decays, and the associated experimental signatures at the next generation of colliders, see, for example, [72–74] and references therein.

[2] Nevertheless, it is worth noticing that in the framework of the MSSM, there are several models where it is found that via flavour symmetries one can successfully explain the observed pattern of masses and mixings.

suppressed [46–50]. The new states are thus decoupled, and the effective low-energy theory is very similar to the usual MSSM/SM. This possibility is sometimes the only "degree of freedom" remaining, especially in highly predictive models, where the Yukawas arise from some high-energy formulation, as is the case of string models. Nevertheless, it is important to stress that the decoupling scenario is in general achieved by enforcing very large values for some of the Higgs soft-breaking masses. This may lead to a fine-tuning scenario in association with electroweak symmetry breaking. When the decoupling approach is taken together with the suppression of Yukawa couplings (ii), it is possible to obtain Higgs spectra which manage to comply with experiment without excessively heavy Higgses [43, 46, 47, 49, 50, 68, 69].

From the above discussion, it is clear that a correct evaluation of the FCNC problem associated to multi-Higgs doublet models is indeed instrumental. In what follows, we propose to analyse the most general scenario of the MSSM extended to include three families of Higgs doublets. We do not impose any symmetry on the model, allowing for the most general formulation of both the superpotential and the SUSY soft breaking Lagrangian. We provide a generic overview of the extended Higgs sector, and discuss the minimisation of the scalar potential. In this analysis, we also compute the most general expression for the contribution of tree-level neutral Higgs exchange to neutral meson mass difference. Contrary to previous analyses [46, 47, 49, 50], we include the contributions from all physical (rather than interaction) Higgs states, scalar and pseudoscalar. Moreover, we take into account the mixing in the Higgs sector. Finally, as an example of how to apply our general formulation, we consider an ansatz for the Yukawa couplings along the lines of previous analyses (namely the "simple Fritzsch scheme" [75–77]), and evaluate the specific contributions to the neutral mesons mass differences. Our findings turn out to be more severe than those of previous works.

In this chapter we analyse the extended Higgs sector, paying special attention to the minimisation of the Higgs potential and addressing potential fine-tuning issues. This will be extremely useful for the study of orbifold models in the following chapters. We also compute the tree level mass matrices and discuss the associated spectra, analysing Higgs-matter interactions, and deriving a model-independent computation of the tree-level contributions to the neutral meson mass differences. Assuming an illustrative example for the Yukawa couplings, we present a numerical study of the FCNC contributions, investigating how the Higgs spectrum must be constrained in order to have compatibility with experimental data.

2.2 Extended Higgs sector

We begin our analysis by addressing the Higgs sector of a SUSY model where three generations of $SU(2)$ doublet superfields are comprised. In each generation, one finds hypercharge $-1/2$ and

+1/2 fields, coupling to down- and up-quarks, respectively:

$$\widehat{H}_{1(3,5)} = \begin{pmatrix} \widehat{h}^0_{1(3,5)} \\ \widehat{h}^-_{1(3,5)} \end{pmatrix}, \qquad \widehat{H}_{2(4,6)} = \begin{pmatrix} \widehat{h}^+_{2(4,6)} \\ \widehat{h}^0_{2(4,6)} \end{pmatrix}. \tag{2.1}$$

2.2.1 Tree-level Higgs potential

The most general superpotential of a model with three families of Higgs doublets can be written as follows:

$$\begin{aligned} W = {} & \widehat{Q}\,(Y_1^d \widehat{H}_1 + Y_3^d \widehat{H}_3 + Y_5^d \widehat{H}_5)\widehat{D}^c + \widehat{L}\,(Y_1^e \widehat{H}_1 + Y_3^e \widehat{H}_3 + Y_5^e \widehat{H}_5)\widehat{E}^c \\ & + \widehat{Q}\,(Y_2^u \widehat{H}_2 + Y_4^u \widehat{H}_4 + Y_6^u \widehat{H}_6)\widehat{U}^c + \widehat{L}\,(Y_2^\nu \widehat{H}_2 + Y_4^\nu \widehat{H}_4 + Y_6^\nu \widehat{H}_6)\widehat{\nu}^c \\ & + \mu_{12}\widehat{H}_1\widehat{H}_2 + \mu_{14}\widehat{H}_1\widehat{H}_4 + \mu_{16}\widehat{H}_1\widehat{H}_6 + \mu_{32}\widehat{H}_3\widehat{H}_2 + \mu_{34}\widehat{H}_3\widehat{H}_4 \\ & + \mu_{36}\widehat{H}_3\widehat{H}_6 + \mu_{52}\widehat{H}_5\widehat{H}_2 + \mu_{54}\widehat{H}_5\widehat{H}_4 + \mu_{56}\widehat{H}_5\widehat{H}_6\,, \end{aligned} \tag{2.2}$$

where $\widehat{Q}$ and $\widehat{L}$ denote the quark and lepton $SU(2)_L$ doublet superfields, $\widehat{U}^c$ and $\widehat{D}^c$ are quark singlets, and $\widehat{E}^c$, $\widehat{\nu}^c$, the lepton singlet superfields. Y_i^q are the Yukawa matrices associated with each Higgs superfield. Regarding the μ-terms, these are now extended in order to include all possible bilinear Higgs terms. Calling upon some specific model that would be responsible for generating the latter terms, it would be possible to reduce the number of free parameters. It is also important to recall that one could also impose a (discrete) symmetry acting on the superpotential, whose effect would be the suppression of some of the couplings in W. However, in our discussion, we consider the most generic form for W, thus taking the several bilinear parameters in W as effective μ-terms.

From the above one can derive the F- and D-terms, writing the latter in doublet component for simplicity:

$$\begin{aligned} V_F &= \sum_{\substack{i,j=1,3,5 \\ l=2,4,6}} \mu^*_{il}\,\mu_{jl}\,H_i^\dagger\,H_j + \sum_{\substack{i=1,3,5 \\ k,l=2,4,6}} \mu^*_{il}\,\mu_{ik}\,H_k^\dagger\,H_l\,, \\ V_D &= \frac{g^2}{8}\sum_{a=1}^{3}\left[\sum_{i=1}^{6} H_i^\dagger\,\tau^a\,H_i\right]^2 + \frac{g'^2}{8}\left[\sum_{i=1}^{6}(-1)^i\,|H_i|^2\right]^2, \end{aligned} \tag{2.3}$$

where H_i are the scalar doublets belonging to the superfields of Eq. (2.1), g, g' denote the gauge coupling constants, and τ^a are the $SU(2)_L$ generators. The soft SUSY-breaking terms trivially generalise the minimal two-doublet case, including the usual soft-breaking masses and $B\mu$-like terms in the Higgs potential.

$$V_{\text{soft}} = \sum_{i,j=1,3,5}(m_d^2)_{ij}\,H_i^\dagger\,H_j + \sum_{k,l=2,4,6}(m_u^2)_{kl}\,H_k^\dagger\,H_l - \sum_{\substack{i=1,3,5 \\ l=2,4,6}}\left[(B\mu)_{il}\,H_i\,H_l + \text{H.c.}\right]. \tag{2.4}$$

2.2.2 Minimisation of the potential: the superpotential basis and the Higgs basis

After electroweak symmetry breaking, the neutral components of the six Higgs doublets develop the following VEVs,

$$\langle h^0_{1(3,5)} \rangle = w_{1(3,5)} \,, \qquad \langle h^0_{2(4,6)} \rangle = w_{2(4,6)} \,, \tag{2.5}$$

and as usual one can write

$$h^0_i \to w_i + \frac{1}{\sqrt{2}} \left(\sigma_i + i \varphi_i \right) \,. \tag{2.6}$$

In the above we assume that all the VEVs are real[3]. The next step is to minimise the scalar potential with respect to the VEVs. Although the problem appears to be a simple generalisation of the two-Higgs doublet model (MSSM), it will prove to be much more involved. It happens that in the presence of six non-vanishing VEVs, finding a solution to the minima equations is a rather cumbersome task. As an illustration, we present the equations obtained from minimising with respect to the down-type Higgs:

$$\sum_{i=1,3,5} \left[(m^2_d)_{ji} + \sum_{l=2,4,6} \mu^*_{jl} \, \mu_{il} \right] w_i - \sum_{l=2,4,6} (B\mu)_{jl} \, w_l + w_j \, \frac{1}{2} \, M_Z^2 \, \frac{v_d^2 - v_u^2}{v_d^2 + v_u^2} = 0 \,, \tag{2.7}$$

where $j = 1, 3, 5$ and we have defined

$$\begin{aligned} v_d \equiv & \sqrt{w_1^2 + w_3^2 + w_5^2} \,, \\ v_u \equiv & \sqrt{w_2^2 + w_4^2 + w_6^2} \,. \end{aligned} \tag{2.8}$$

In addition to Eq. (2.7), which only ensure that we are in the presence of an extremum, we have to further impose the conditions for a minimum with respect to the several variables. Therefore, and for the down-type Higgs fields, having positive second derivatives is equivalent to the following inequalities:

$$(m^2_d)_{jj} + \sum_{l=2,4,6} \mu^*_{jl} \, \mu_{jl} + \frac{1}{2} \, M_Z^2 \left(\frac{v_d^2 - v_u^2 + 2 \, w_j^2}{v_d^2 + v_u^2} \right) > 0 \,, \tag{2.9}$$

provided that at the minimum the determinant of the six-dimensional matrix is positive, or equivalently, $\det(\partial^2 V \,/\, \partial h^0_i \, \partial h^0_j) > 0$.

The equations for the remaining cases (minimising with respect to the up-type Higgs fields) can be obtained from Eqs. (2.7,2.9) by interchanging $\{1, 3, 5\} \leftrightarrow \{2, 4, 6\}$ and changing the

[3] We do not discuss the possibility of spontaneous CP violation in association with this class of multi-Higgs doublet models.

sign in the terms proportional to M_Z^2 as $M_Z^2(v_d^2 - v_u^2) \to -M_Z^2(v_d^2 - v_u^2)$ (cf. Eq. (2.7)) and $M_Z^2(v_d^2 - v_u^2 + 2w^2) \to -M_Z^2(v_d^2 - v_u^2 - 2w^2)$ (cf. Eq. (2.9)). The only choice of parameters that would render the solution of the minima equations straightforward is to call upon the diagonal soft breaking masses ($(m_d)_{ii}$ and $(m_u)_{kk}$) to be fixed by the minima equations. For $(m_d)_{11}^2$ the minimum equation would read

$$(m_d)_{11}^2 = \sum_{j=2,4,6} (B\mu)_{1j} \frac{w_j}{w_1} - (m_d^2)_{13} \frac{w_3}{w_1} - (m_d^2)_{15} \frac{w_5}{w_1} - \sum_{i=1,3,5} \Big(\sum_{l=2,4,6} \mu_{1l}^* \mu_{il} \frac{w_i}{w_1} \Big) - \frac{1}{2} M_Z^2 \frac{v_d^2 - v_u^2}{v_d^2 + v_u^2} \,. \tag{2.10}$$

Naturally, the equations can be solved for a distinct set of parameters, but then finding an analytical solution is in general not possible. Analytical relations are very useful when writing down the mass matrices for the several Higgs sectors, since one can directly replace the parameters. In fact, the major handicap when relying on the diagonal soft masses as the minimum parameters is that then one loses control of the leading contributions to the Higgs boson mass eigenvalues. This will be made clear in a forthcoming section. Another shortcoming is that, even though we can define a generalised expression for $\tan\beta$ as $\tan\beta = \sqrt{w_2^2 + w_4^2 + w_6^2} \,/\, \sqrt{w_1^2 + w_3^2 + w_5^2}$, writing the minimisation equations as a function of $\sin\beta$, $\cos\beta$ (in an MSSM-like fashion), is impossible.

So far we have been working in the basis that naturally emerges from both the superpotential and soft-breaking Lagrangian formulation. To simplify the discussion, we will henceforth label this natural basis as the superpotential basis. However, this need not be the unique approach when addressing the minimisation of the potential.

As it has been shown, one can work in a basis where only two of the new six neutral fields have non-vanishing VEVs, the so-called Higgs basis [38, 48]. For the down-type Higgses, the new fields, ϕ_i, are related to the original ones by means of the following unitary transformation, P_d:

$$\phi_1^0 \equiv \frac{1}{\sqrt{w_1^2 + w_3^2 + w_5^2}} \left(w_1 \, h_1^0 + w_3 \, h_3^0 + w_5 \, h_5^0 \right) , \tag{2.11}$$

$$\phi_3^0 \equiv \frac{1}{\sqrt{w_1^2 + w_3^2 + w_5^2}} \left[\sqrt{w_3^2 + w_5^2} \, h_1^0 - \frac{w_1}{\sqrt{w_3^2 + w_5^2}} (w_3 \, h_3^0 + w_5 \, h_5^0) \right] , \tag{2.12}$$

$$\phi_5^0 \equiv \frac{1}{\sqrt{w_3^2 + w_5^2}} \left(w_5 \, h_3^0 - w_3 \, h_5^0 \right) . \tag{2.13}$$

An analogous transformation, P_u, can be derived for the up-quark-coupling Higgses ($h_{2,4,6}^0$), with the adequate replacements ($\{1,3,5\} \to \{2,4,6\}$). For simplicity, let us introduce the following global parametrisation for the transformations P_d and P_u:

$$\phi_i = P_{ij} h_j \,, \tag{2.14}$$

where P_{ij} is a 6×6 matrix whose entries are defined from P_d and P_u as

$$P_{ij} = \begin{cases} (P_d)_{\frac{i+1}{2}\,\frac{j+1}{2}} & i,j = 1,3,5 \\ (P_u)_{\frac{i}{2}\,\frac{j}{2}} & i,j = 2,4,6 \\ 0 & \text{elsewhere}\,. \end{cases} \tag{2.15}$$

From the above, it is clear that in the new basis only two of the fields do have a VEV

$$\langle \phi_1^0 \rangle = v_d\,, \qquad \langle \phi_2^0 \rangle = v_u\,, \tag{2.16}$$

with $v_{d,u}$ defined in Eq. (2.8), which in turn must satisfy

$$v_u^2 + v_d^2 = 2\,M_Z^2/(g^2 + g'^2) \approx (174\ \text{GeV})^2\,, \tag{2.17}$$

where M_Z is the mass of the Z^0 boson. In this basis one has the additional advantage that, similar to what occurs in the MSSM case, one can clearly define $\tan\beta$:

$$\tan\beta = \frac{v_u}{v_d}\,. \tag{2.18}$$

We can now write

$$\begin{aligned} &\phi_{1,2}^0 \to v_{d,u} + \frac{1}{\sqrt{2}}\,(R_{1,2} + iI_{1,2})\ , \\ &\phi_i^0 \to \frac{1}{\sqrt{2}}\,(R_i + iI_i) \qquad i = 3-6\,. \end{aligned} \tag{2.19}$$

Thus, one can now understand the three Higgs family model as an MSSM-like model, extended by four additional doublets, which do not directly interfere with the mechanism of electroweak symmetry breaking. In the Higgs basis, the potential preserves its original structure with respect to the dependence on the field combination, but the parameters associated with the F- and soft breaking terms are now redefined as

$$\begin{aligned} V_F &= \sum_{\substack{a,b=1,3,5 \\ l=2,4,6}} \bar{\mu}_{ab}^{l}\,\phi_a^\dagger\,\phi_b + \sum_{\substack{i=1,3,5 \\ c,d=2,4,6}} \bar{\bar{\mu}}_{cd}^{i}\,\phi_c^\dagger\,\phi_d\,, \\ V_{\text{soft}} &= \sum_{a,b=1,3,5} (\bar{m}_d^2)_{ab}\,\phi_a^\dagger\,\phi_b + \sum_{c,d=2,4,6} (\bar{\bar{m}}_u^2)_{cd}\,\phi_c^\dagger\,\phi_d - \sum_{\substack{a=1,3,5 \\ c=2,4,6}} \left[(\overline{B\mu})_{ac}\,\phi_a\,\phi_c + \text{H.c.}\right]\,, \end{aligned} \tag{2.20}$$

where

$$\begin{aligned} &\bar{\mu}_{ab}^{l} = (P_d)_{ai}\,\mu_{il}^*\,\mu_{jl}\,(P_d^\dagger)_{jb}\,, && \bar{\bar{\mu}}_{cd}^{i} = (P_u)_{cl}\,\mu_{il}^*\,\mu_{ik}\,(P_u^\dagger)_{kd}\,, \\ &(\bar{m}_d^2)_{ab} = (P_d)_{ai}\,(m_d^2)_{ij}\,(P_d^\dagger)_{jb}\,, && (\bar{\bar{m}}_u^2)_{cd} = (P_u)_{ck}\,(m_u^2)_{kl}\,(P_u^\dagger)_{ld}\,, \\ &(\overline{B\mu})_{ac} = (P_d^\dagger)_{ia}\,(B\mu)_{il}\,(P_u^\dagger)_{lc}\,, && i,j,a,b = 1,3,5\,; \qquad k,l,c,d = 2,4,6\,. \end{aligned} \tag{2.21}$$

In the new basis, the problem of minimising the scalar potential is quite simplified, and one is able to derive the six minimisation conditions in a compact form. The conditions for the down-type sector read

$$\begin{aligned} m_{11}^2 &= b_{12}\,\tan\beta - \frac{M_Z^2}{2}\,\cos 2\beta\,, \\ m_{13}^2 &= b_{32}\,\tan\beta\,, \\ m_{15}^2 &= b_{52}\,\tan\beta\,, \end{aligned} \tag{2.22}$$

while those related to the up-type Higgses are given by

$$\begin{aligned} m_{22}^2 &= b_{12}\,\cot\beta + \frac{M_Z^2}{2}\,\cos 2\beta\,, \\ m_{24}^2 &= b_{14}\,\cot\beta\,, \\ m_{26}^2 &= b_{16}\,\cot\beta\,. \end{aligned} \tag{2.23}$$

In the above, and for simplicity, we have introduced the short-hand notation

$$\begin{aligned} m_{ij}^2 &= \begin{cases} \sum_{l=2,4,6}\,\bar{\mu}_{ij}^l + (\bar{m}_d^2)_{ij} & i,j=1,3,5 \\ \sum_{k=1,3,5}\,\bar{\bar{\mu}}_{ij}^k + (\bar{\bar{m}}_u^2)_{ij} & i,j=2,4,6\,, \end{cases} \\ b_{ij} &= (\overline{B\mu})_{ij}\,, \end{aligned} \tag{2.24}$$

where we stress that both parameters $\bar{\mu}_{ij}$, and $\bar{\bar{\mu}}_{ij}$, as well as b_{ij} have dimensions (mass^2). Throughout the chapter we will be often using the above short-hand notation, even though this implies that the rotated μ-terms and Higgs soft breaking masses loose their individual character, becoming merged into the quantities m_{ij}^2. As a final comment, let us notice that the minima equations (2.22,2.23) are, in structure, very similar to those of the MSSM, namely the first in each set of three. It is worth referring that the electroweak scale is only explicitly present in two equations (those derived with respect to $\phi_{1,2}^0$, the VEV-acquiring fields). Notice however, that this is a mere consequence of working in a different basis.

In addition to the minima conditions Eqs. (2.22,2.23), one can also derive other conditions, which are useful in constraining the allowed parameter space. As an example, and from direct comparison of the minima equations for m_{11}^2 and m_{22}^2, we find the following inequality:

$$m_{11}^2\,m_{22}^2 \;\leq\; b_{12}^2\,, \tag{2.25}$$

strongly resembling the analogous MSSM condition.

2.2.3 Numerical minimisation of the potential: illustrative examples

In what follows, our goal is to conduct a short analysis of the issues discussed in the previous subsections. The phenomenological analysis of the Higgs sector (masses and mixings) will be

carried in detail in Section 2.3, working in the Higgs basis. Nevertheless, we find it interesting to evaluate how the minimisation of the scalar potential constrains the soft breaking terms. To do so, we consider several numerical examples for the minimisation of the scalar potential for distinct VEV regimes. In addition, we also discuss whether or not a specific choice of soft breaking terms may translate into a fine-tuning problem. Although the minima conditions are cast in a much more compact and appealing way in the Higgs basis, since only two of them explicitly involve the electroweak scale, a possible fine tuning problem may be unapparent in this case. Therefore, for this specific discussion, we will stick to the original superpotential basis. In this case, and since we make no assumptions regarding the mechanism of SUSY breaking associated with this generic multi-Higgs doublet model, we take the input parameters

$$(m_d^2)_{ij}\,, \quad (m_u^2)_{ij}\,, \quad \mu_{ij}\,, \quad (B\mu)_{ij}\,, \tag{2.26}$$

to be free at the electroweak scale. Regarding the Higgs VEVs (w_i), we impose no constraint other than satisfying the electroweak breaking conditions for a given value of $\tan\beta$. In order to further simplify the approach, we will fix, in each separate analysis, the value of $\mu_{ij} = \mu$, and assume a common overall scale for the off-diagonal masses $(m_d)_{ij}$ and $(m_u)_{ij}$, and for $(B\mu)_{ij}$. More specifically, we take universal $B\mu$ terms, $(B\mu)_{ij} = B\mu = M_S^2$, where M_S is a "typical soft-SUSY breaking scale". For the off-diagonal masses $(m_d)_{ij}$ and $(m_u)_{ij}$, the common scale is taken to be $(m_d)_{ij} = (m_u)_{ij} = 0.1\, M_S$[4].

As discussed in the previous subsection, the parameters which are (trivially) fixed by the six minima equations are the diagonal Higgs soft-breaking masses, $(m_d^2)_{ii}$ and $(m_u^2)_{ii}$. Clearly, from Eq. (2.10), the minima values for $(m_q^2)_{ii}$, and in particular those of the down-type Higgs sector, will be very dependent of the values of the VEVs considered, most specifically on whether one chooses a degenerate or hierarchical regime. Therefore, each case has to be separately investigated, and in each situation, one must analyse the impact of the other free parameters, namely that of the overall scale chosen for the soft-breaking parameters.

In addition, one has to investigate whether or not the parameters taken lead to a potential fine tuning (FT) problem for the parameters. In doing so, our approach will be the following. For a specific scenario defined by the parameters in Eq. (2.26), together with w_i and $\tan\beta$, we compute the values of the diagonal soft breaking masses, as imposed from complying with the minima equations. We then impose a tiny perturbation on the solutions,

$$(m_q^2)_{ii} \;\to\; (m_q^2)'_{ii} \;=\; (1+\lambda^q)\,(m_q^2)_{ii}\,, \tag{2.27}$$

where λ is taken to be around a few percent. Finally, we compute the new value of M_Z derived from perturbing the correct (true minima) solution for $(m_q^2)_{ii}$, M'_Z. To evaluate the amount of

[4]Notice that for $i \neq j$, values of $(m_q)_{ij} \gtrsim M_S$ are not compatible with viable solutions. This is evident from the minimisation conditions of Eq. (2.10), using $(m_q)^2_{ij} > 0$. Furthermore, the limit $(m_q)_{ij} \to 0$ occurs in well motivated models [78].

FT, we follow [79, 80], and introduce the parameter Δp, defined as

$$\Delta p_i \, \frac{\delta p_i}{p_i} \, = \, \frac{\delta M_Z^2}{M_Z^2} \, , \tag{2.28}$$

identifying p_i with $(m_q^2)_{ii}$. A rough measure of the fine-tuning can be derived from $(\Delta p_i)^{-1}$, since the latter can be identified with the probability of a cancellation between terms of a given size to obtain a final result Δp_i times smaller.

In what follows we take, as illustrative examples, two distinct cases for the Higgs VEVs: degenerate and hierarchical w_i. We stress here that at this point we are only investigating the constraints on the soft breaking terms arising from the minima conditions. A study of the spectrum is far simplified when moving to Higgs basis, as will be done in the following Section.

• Degenerate VEVs: $w_1 = w_3 = w_5$, $w_2 = w_4 = w_6$

In this case, the minima equations become much simpler, since in each sector the VEVs factor out. Therefore, having fixed the free parameters as above described, the six original equations essentially reduce to two independent ones: one for the down-type Higgs (e.g. $(m_d)^2_{11}$) and another for the up-type sector (e.g. $(m_u)^2_{22}$).

In Fig. 2.1, we plot $(m_d)^2_{11}$ and $(m_u)^2_{22}$, as computed from the tree-level minima equations, as a function of the common soft breaking term scale, M_S, for $\mu_{ij} = \mu = 200$ GeV. In each case, we consider two distinct values for $\tan\beta$: 5 and 10. From Fig. 2.1, several properties of this model become apparent. First of all, it becomes clear that in this basis (the superpotential basis) finding minima can be a challenging task. Notice that although one can find solutions for the down-type sector associated with low M_S, in this range we are in the presence of maxima (rather than minima) for the up-type soft masses. The situation slightly worsens with increasing $\tan\beta$. Taking other (higher) values of μ would lead to the displacement of the vertical line further to the right of the parameter space parametrised by M_S. This behaviour can be confirmed by inspection of Eqs. (2.7,2.9,2.10).

Let us now evaluate how fine-tuned these solutions are. In Fig. 2.2 we investigate Δp for the up and down sectors, by studying in each case the effect of perturbing the minima solutions $(m^d_{11})^2$ and $(m^u_{22})^2$ by $\lambda^{d,u} = 1\%$ and $\lambda^{d,u} = 5\%$. We again consider $\mu = 200$ GeV, and take $\tan\beta = 10$.

From Eqs. (2.27,2.28) together with the minimisation conditions in Eq. (2.10), it is apparent that $\Delta p_i \propto \frac{(m_q^2)_{ii}}{M_Z^2}$. Moreover, it can be seen that for the down-type sector, the dominant term $(B\mu)$ is further enhanced by a factor of $\tan\beta$, so that a tiny fluctuation in $(m^d_{11})^2$ is not easily cancelled. In the up-type masses, the situation is reversed. The up-type version of Eq. (2.10) would exhibit a suppression of $B\mu$ by $\cot\beta$, so that here we find a more relaxed scenario.

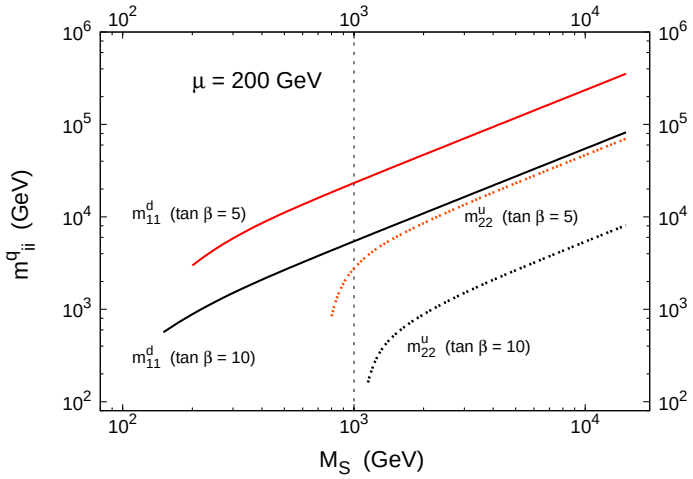

Figure 2.1: Minima solutions m^d_{11} and m^u_{22} as a function of the common SUSY breaking scale M_S for $\tan\beta$ =5, 10 and degenerate VEVs. To the left of the vertical dotted line, the solutions for m^q_{ii} are not true minima of the potential.

• Hierarchical VEVs: $w_5 = 10\, w_3 = 100\, w_1$, $w_6 = 10\, w_4 = 100\, w_2$

In this case, and when compared to the degenerate one, each soft mass exhibits a very distinct behaviour at the minima of the potential. We will thus analyse the solutions which in each case are associated with the lightest and heaviest VEV, $(m_d)^2_{11}$, $(m_u)^2_{22}$ and $(m_d)^2_{55}$, $(m_u)^2_{66}$. As before, in Fig. 2.3 we display the above masses as a function of M_S for $\mu = 200$ GeV, and $\tan\beta$ =10, similar to what was presented for degenerate VEVs in Fig. 2.1. As seen from Fig. 2.3, the range for the solutions is not strongly affected. Notice however that the minima values of $(m_u)^2_{22}$ and $(m_d)^2_{55}$ become degenerate for large values of M_S. Moreover, the soft mass associated with the largest VEV (m^u_{66}) presents, as expected, much smaller values than the others. This is a consequence of the suppression of w_j/w_6 on $B\mu$. Regarding the fine tuning, the situation is more involved. In Fig. 2.4 we plot Δp for the up and down sectors, considering only the effect of a $\lambda^{d,u} = \lambda = 1\%$ perturbation in $(m^u_{22})^2$, $(m^u_{44})^2$, $(m^d_{55})^2$ and $(m^u_{66})^2$. We take $\mu = 200$ GeV and $\tan\beta = 10$.

As seen from Fig. 2.4, the alterations emerge in both up- and down-type Higgs sectors. Regarding the down-type scalar (Δp_{55}) the fine tuning is typically larger now, and the effect is essentially due to the fact that it is now much more difficult to find cancellations among the several terms entering in the minimisation equations. In the up-type sector, we find a very similar situation to that of Fig. 2.2 for the second and third generations (associated with the larger VEVs). Conversely, and since it is now associated to a tiny VEV, the first generation

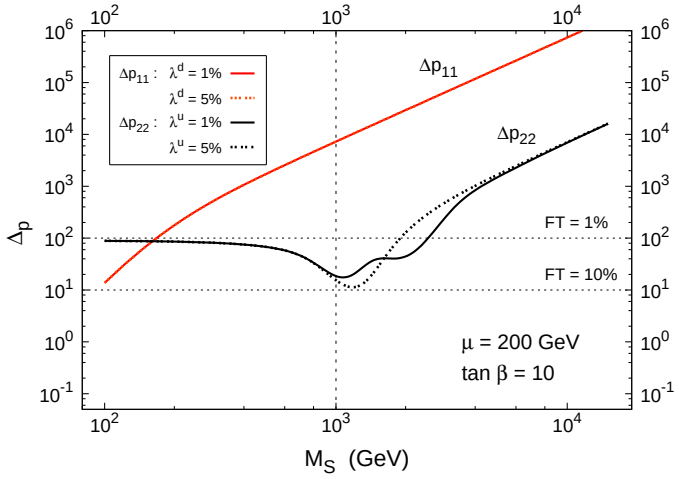

Figure 2.2: Δp as a function of the SUSY scale M_S for perturbations of 1% and 5% in $(m^d_{11})^2$ and $(m^u_{22})^2$. $\mu = 200$ GeV, and $\tan\beta = 10$ (the two lines for Δp_{11} appear over-set). To the left of the vertical dotted line, the solutions for m^q_{ii} are not true minima of the potential. Horizontal lines denote areas above which one roughly expects a FT stronger than 1% and 10%.

up-type diagonal soft mass is more unstable under perturbations, and its behaviour merges with that of $(m^d_{55})^2$ for larger values of M_S.

It has been shown in the MSSM that with a soft SUSY scale of a few hundred GeV the associated FT is around the level of 10% [80]. When compared to the MSSM, this extended model offers a more problematic FT scenario, as is manifest in Figs. 2.2 and 2.4. This can also be seen from the comparison of Eq. (2.10) with its MSSM counterpart. In addition to the single $(B\mu)_{12}$ and μ^2_{12} terms, one now encounters additional $(B\mu)_{1j}$ and $\mu_{1l}\mu_{il}$, as well as new soft breaking masses on the right hand-side of the above equation, which must cancel out to achieve the correct value of M_Z.

Finally, and even though in our analysis the VEVs were not fit by the minima equations, but taken as input parameters instead, let us consider the effect of imposing a small perturbation on the VEVs, while keeping the other parameters as defined either by input values and/or minima conditions. As for the previous case of perturbing the minima values of m^q_{ii}, we now impose that

$$w_i \;\to\; w'_i \;=\; (1+\rho^q)\, w_i \,. \tag{2.29}$$

In Fig. 2.5, we plot the effect on M_Z (parametrised by Δp) arising from taking $\rho^d = \rho^u = \rho = 1\,\%$ for the case of degenerate (left) and non-degenerate VEVs (right). Again we consider $\mu = 200$ GeV and $\tan\beta = 10$. It suffices to comment that the larger the VEVs, the more stable they are under perturbations, and this effect is particularly manifest for the non-degenerate VEV case.

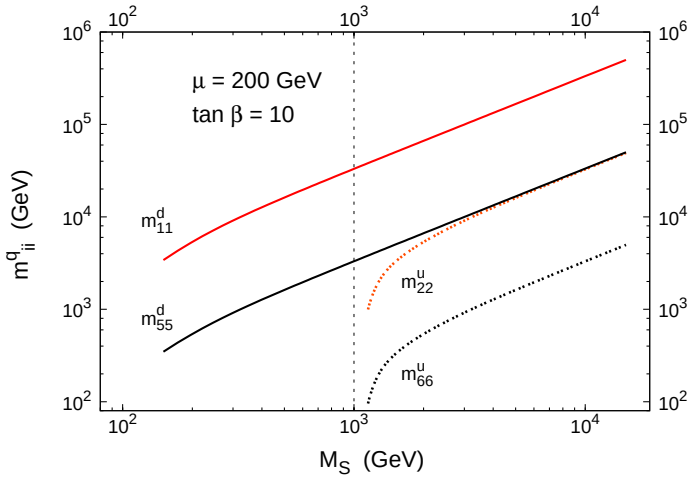

Figure 2.3: Minima solutions for non-degenerate VEVs as a function of the SUSY scale M_S, with $\mu = 200$ GeV, and $\tan\beta$ =10. To the left of the vertical dotted line, the solutions for m^q_{ii} are not true minima of the potential.

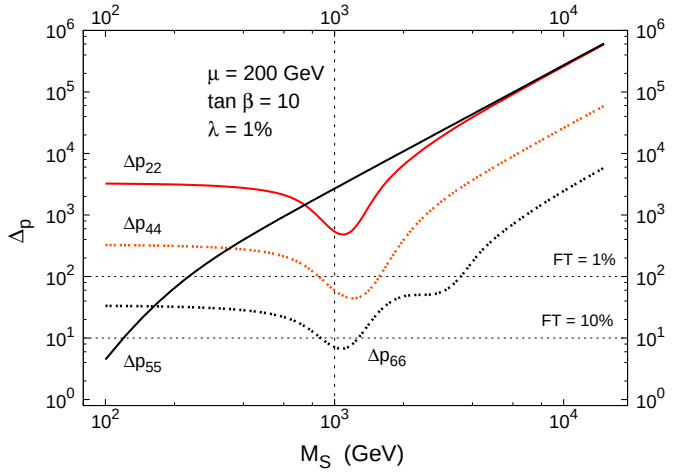

Figure 2.4: Δp as a function of the SUSY scale M_S for perturbations of 1% in the diagonal soft masses, for non-degenerate VEVS. We take μ =200 GeV and $\tan\beta$ =10. To the left of the vertical dotted line, the solutions for m^q_{ii} are not true minima of the potential. Horizontal lines denote areas above which one roughly expects a FT stronger than 1% and 10%.

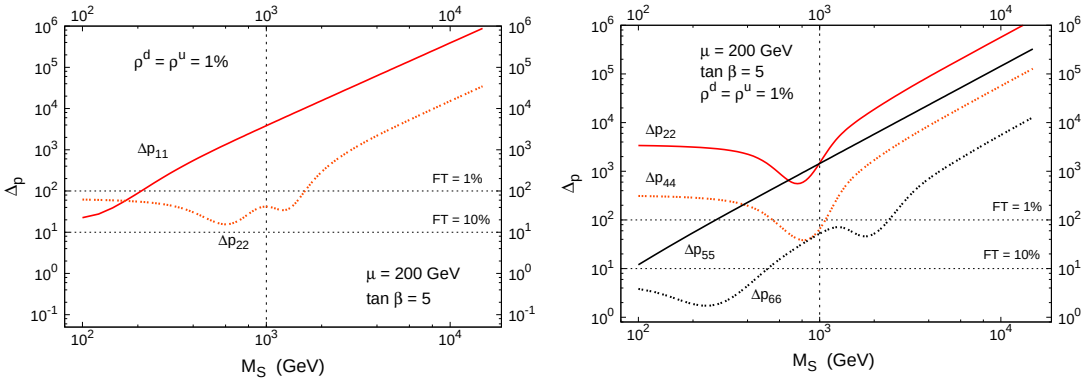

Figure 2.5: Δp as a function of the common SUSY scale M_S for perturbations of 1% in w_i, for μ =200 GeV and $\tan\beta = 10$. On the left we present the degenerate VEV case, on the right the non-degenerate case.

2.3 Tree-level Higgs mass matrices

We are now in conditions to investigate the Higgs spectrum, which will contain eleven neutral states, and ten charged physical particles. Let us begin with the derivation of the tree level mass matrices for the charged scalars.

2.3.1 Charged Higgses

In the basis defined by[5] $(\phi_1^-, \phi_2^{+*}, \phi_3^-, \phi_4^{+*}, \phi_5^-, \phi_6^{+*})$, the scalar potential for the charged components reads,

$$
\begin{aligned}
V^{\pm} = & \sum_{i=1,3,5} m_i^2 \, |\phi_i^-|^2 + \sum_{i=2,4,6} m_i^2 \, |\phi_i^+|^2 + \frac{g^2+g'^2}{8} \sum_{i=1}^{6} |H_i|^2 \, |H_i|^2 + \frac{g^2}{4} \sum_{\substack{i,j=1 \\ i\neq j}}^{6} |H_i^\dagger \, H_j|^2 \\
& - \frac{g^2+g'^2}{8} \sum_{\substack{i,j=1 \\ i+j=\text{odd}}}^{6} |H_i|^2 \, |H_j|^2 - \frac{g^2-g'^2}{8} \sum_{\substack{i,j=1 \\ i+j=\text{even} \\ i\neq j}}^{6} |H_i|^2 \, |H_j|^2 + (m_{13}^2 \, \phi_1^{-*} \, \phi_3^- \\
& + m_{15}^2 \, \phi_1^{-*} \, \phi_5^- + m_{35}^2 \, \phi_3^{-*} \, \phi_5^- + m_{24}^2 \, \phi_2^{+*} \, \phi_4^+ + m_{26}^2 \, \phi_2^{+*} \, \phi_6^+ + m_{46}^2 \, \phi_4^{+*} \, \phi_6^+ \\
& + \text{H.c.}) + (b_{12} \, \phi_1^- \, \phi_2^+ + b_{14} \, \phi_1^- \, \phi_4^+ + b_{16} \, \phi_1^- \, \phi_6^+ + b_{32} \, \phi_3^- \, \phi_2^+ + b_{34} \, \phi_3^- \, \phi_4^+ \\
& + b_{36} \, \phi_3^- \, \phi_6^+ + b_{52} \, \phi_5^- \, \phi_2^+ + b_{54} \, \phi_5^- \, \phi_4^+ + b_{56} \, \phi_5^- \, \phi_6^+ + \text{H.c.}) \, .
\end{aligned}
\tag{2.30}
$$

[5] The rotated basis of the charged fields is obtained via an identical transformation of Eq. (2.14).

At the minimum of the potential, the mass matrix for the charged states is:

$$\mathcal{M}^2_{\pm} = \begin{pmatrix} b_{12}\tan\beta + M_W^2\sin^2\beta & b_{12} + \frac{1}{2}M_W^2\sin 2\beta & b_{32}\tan\beta & b_{14} & b_{52}\tan\beta & b_{16} \\ b_{12} + \frac{1}{2}M_W^2\sin 2\beta & b_{12}\cot\beta + M_W^2\cos^2\beta & b_{32} & b_{14}\cot\beta & b_{52} & b_{16}\cot\beta \\ b_{32}\tan\beta & b_{32} & m_{33}^2 - T_W & b_{34} & m_{35}^2 & b_{36} \\ b_{14} & b_{14}\cot\beta & b_{34} & m_{44}^2 + T_W & b_{54} & m_{46}^2 \\ b_{52}\tan\beta & b_{52} & m_{35}^2 & b_{54} & m_{55}^2 - T_W & b_{56} \\ b_{16} & b_{16}\cot\beta & b_{36} & m_{46}^2 & b_{56} & m_{66}^2 + T_W \end{pmatrix}, \tag{2.31}$$

where M_W is the mass of the $W^{\pm}$ boson and $T_W = \frac{1}{2}M_W^2\cos(2\beta)(1-\tan^2\theta_W)$. One can easily identify the massless combinations that will give rise to the charged Goldstone bosons ($G^{\pm}$), "eaten away" as the $W^{\pm}$ acquire mass. The eigenstates will be henceforth denoted by $h_i^{\pm}$, with $i = 1$ corresponding to the unphysical massless state. The upper-left 4×4 sub-matrix of the one above displayed is similar in structure to that derived in [38], in the framework of a four-Higgs doublet model.

We stress here that the compact appearance of the matrix in Eq. (2.31) is a direct consequence of working in the Higgs basis. From direct inspection of the above matrix, one can impose that the diagonal blocks have semi-positive eigenvalues, thus deriving a zeroth order condition for avoiding tachyonic charged states. For example, for the $(\phi_3^- - \phi_4^+)$ sector, this would read:

$$m_{33}^2\, m_{44}^2 \gtrsim b_{34}^2\,, \tag{2.32}$$

while an identical argumentation within a sector (e.g.$(\phi_3^- - \phi_5^-)$ in the down-type Higgs) would in turn lead to

$$m_{33}^2\, m_{55}^2 \gtrsim m_{35}^4\,. \tag{2.33}$$

Albeit very useful, the above equations are only necessary (rather than sufficient) conditions to ensure the presence of true minima, so they should be interpreted as a means of orientation in the parameter space. Additionally, we notice that simple conditions as those above are only possible to derive in the Higgs basis.

2.3.2 Neutral Higgses

In our work, we are particularly interested in the neutral Higgs bosons. In order to find the neutral spectrum of the model, we decompose the complex fields as in Eq. (2.19), and derive the mass matrices associated with the real and imaginary components. CP conservation in the Higgs sector translates in the absence of terms mixing the R_i and I_i components, so that scalar and pseudoscalar states do not mix. For the scalar mass matrix we obtain

$$\mathcal{M}_R^2 = \frac{1}{2}\frac{\partial^2 V}{\partial R_i \partial R_j}\bigg|_{\min}$$

$$= \begin{pmatrix} b_{12}\tan\beta + M_Z^2\cos^2\beta & -b_{12} - \frac{M_Z^2}{2}\sin 2\beta & b_{32}\tan\beta & -b_{14} & b_{52}\tan\beta & -b_{16} \\ -b_{12} - \frac{M_Z^2}{2}\sin 2\beta & b_{12}\cot\beta + M_Z^2\sin^2\beta & -b_{32} & b_{14}\cot\beta & -b_{52} & b_{16}\cot\beta \\ b_{32}\tan\beta & -b_{32} & m_{33}^2 + \frac{M_Z^2}{2}\cos 2\beta & -b_{34} & m_{35}^2 & -b_{36} \\ -b_{14} & b_{14}\cot\beta & -b_{34} & m_{44}^2 - \frac{M_Z^2}{2}\cos 2\beta & -b_{54} & m_{46}^2 \\ b_{52}\tan\beta & -b_{52} & m_{35}^2 & -b_{54} & m_{55}^2 + \frac{M_Z^2}{2}\cos 2\beta & -b_{56} \\ -b_{16} & b_{16}\cot\beta & -b_{36} & m_{46}^2 & -b_{56} & m_{66}^2 - \frac{M_Z^2}{2}\cos 2\beta \end{pmatrix}. \tag{2.34}$$

It is straightforward to recognise the MSSM scalar Higgs mass matrix as the 2×2 upper left block of the previous 6×6 matrix. Likewise, the tree-level mass matrix for the pseudoscalar can be written as

$$\mathcal{M}_I^2 = \frac{1}{2}\frac{\partial^2 V}{\partial I_i \partial I_j}\bigg|_{\min}$$

$$= \begin{pmatrix} b_{12}\tan\beta & b_{12} & b_{32}\tan\beta & b_{14} & b_{52}\tan\beta & b_{16} \\ b_{12} & b_{12}\cot\beta & b_{32} & b_{14}\cot\beta & b_{52} & b_{16}\cot\beta \\ b_{32}\tan\beta & b_{32} & m_{33}^2 + \frac{M_Z^2}{2}\cos 2\beta & b_{34} & m_{35}^2 & b_{36} \\ b_{14} & b_{14}\cot\beta & b_{34} & m_{44}^2 - \frac{M_Z^2}{2}\cos 2\beta & b_{54} & m_{46}^2 \\ b_{52}\tan\beta & b_{52} & m_{35}^2 & b_{54} & m_{55}^2 + \frac{M_Z^2}{2}\cos 2\beta & b_{56} \\ b_{16} & b_{16}\cot\beta & b_{36} & m_{46}^2 & b_{56} & m_{66}^2 - \frac{M_Z^2}{2}\cos 2\beta \end{pmatrix}. \tag{2.35}$$

In the 2×2 submatrix defined by the $i,j = 1,2$ entries, it is easy to identify the combination associated with the massless Goldstone boson. As in the MSSM, the latter degree of freedom is "eaten" by the Z^0 boson, as it acquires a mass. After rotating away the massless state,

$$G^0 = \frac{1}{\sqrt{2}}(I_2\sin\beta - I_1\cos\beta)\,, \tag{2.36}$$

by means of the unitary transformation

$$\begin{pmatrix} I_1' \\ I_2' \end{pmatrix} = \begin{pmatrix} \cos\beta & -\sin\beta \\ \sin\beta & \cos\beta \end{pmatrix}\begin{pmatrix} I_1 \\ I_2 \end{pmatrix}, \tag{2.37}$$

the five remaining eigenstates are in general massive, and the new mass matrix reads

$$\mathcal{M}_I'^2 = \begin{pmatrix} \frac{2b_{12}}{\sin 2\beta} & b_{32}\sec\beta & b_{14}\csc\beta & b_{52}\sec\beta & b_{16}\csc\beta \\ b_{32}\sec\beta & m_{33}^2+\frac{m_Z^2}{2}\cos 2\beta & b_{34} & m_{35}^2 & b_{36} \\ b_{14}\csc\beta & b_{34} & m_{44}^2-\frac{m_Z^2}{2}\cos 2\beta & b_{54} & m_{46}^2 \\ b_{52}\sec\beta & m_{35}^2 & b_{54} & m_{55}^2+\frac{m_Z^2}{2}\cos 2\beta & b_{56} \\ b_{16}\csc\beta & b_{36} & m_{46}^2 & b_{56} & m_{66}^2-\frac{m_Z^2}{2}\cos 2\beta \end{pmatrix} . \tag{2.38}$$

When discussing the issue of minimising the scalar potential, we pointed out that each of the presented basis (Higgs and superpotential basis) had its own advantages/drawbacks. Here we are facing a very strong point in favour of the Higgs basis, namely the possibility of rotating away the pseudoscalar massless state via a transformation that only involves the first two states. Should we have been working in the superpotential basis, the transformation of Eq. (2.37) would be far more complex. Even though one could still define $\tan\beta$ as $\tan\beta = \sqrt{w_2^2+w_4^2+w_6^2}\,/\,\sqrt{w_1^2+w_3^2+w_5^2}$, the rotation parametrised by β would be extended to a 6×6 matrix, which would act upon the combination of $P^\dagger\,(I_1, I_2, \ldots I_6)^T$.

It is worth recalling that the above mass matrices (scalar and pseudoscalar) are not those associated with the original (interaction) eigenstates. The relation between the superpotential basis and the Higgs basis is trivially obtained from Eq. (2.14),

$$R_i = P_{ij}\sigma_j\,, \qquad I_i = P_{ij}\varphi_j\,, \qquad i,j = 1\ldots 6\,. \tag{2.39}$$

In the Higgs basis, the mass matrices can be easily diagonalised by

$$\begin{aligned} S_R\mathcal{M}_R^2 S_R^\dagger &= \Delta_R^2 = \mathrm{diag}(m_i^{s2})\,, \\ S_I\mathcal{M}_I^2 S_I^\dagger &= \Delta_I^2 = \mathrm{diag}(m_i^{p2})\,, \end{aligned} \tag{2.40}$$

where $\Delta_{R,I}^2$ are the diagonal scalar and pseudoscalar squared mass eigenvalues (notice that the $i=1$ term for the pseudoscalars corresponds to the unphysical massless would-be Goldstone boson). From the above it is straightforward to observe that the matrices that diagonalise the mass matrices in the original basis can be related to the latter as

$$S_{\sigma,\varphi} \;=\; S_{R,I}\,P\,. \tag{2.41}$$

2.3.3 Tree-level Higgs spectrum - a brief discussion

Although a thorough analysis of the Higgs parameter space lies beyond the scope of this work, it is important to comment on a few issues. The first regards radiative corrections, which play a key role in the MSSM and its extensions, especially in relation with the mass of the lightest scalar Higgs. Without radiative corrections, and as occurs in the MSSM, the mass of the lightest

scalar is bounded to be $m_{h_1^0} \lesssim M_Z$ [36]. In the framework of supersymmetric models with extended Higgs sectors, higher order contributions to the lightest Higgs mass have been already analysed [81], and the upper bound on $m_{h_1^0}$ does not differ significantly from the one derived in the MSSM. Since in this work our aim is not so much to study in depth the Higgs spectra, but rather investigate to which extent FCNCs push the lower bounds on the heavy Higgs masses, we simplify the analysis, and use the bare masses instead.

From the analysis of the tree-level mass matrices derived in this section, Eqs. (2.31), (2.34), (2.35), (2.38), and again working in the Higgs basis, a few interesting patterns can be extracted for the behaviour of the several mass eigenstates. Beginning with the lighter physical states ($i = 2$ for both charged and pseudoscalar states), the bare masses are very similar to what one has in the MSSM:

$$\begin{aligned} m_1^s &\lesssim |\cos 2\beta|\, M_Z\,, \\ (m_2^s)^2 &\approx (m_2^p)^2 + M_Z^2\,, \\ (m_2^p)^2 &\simeq 2\,\frac{b_{12}}{\sin 2\beta}\,, \\ (m_2^\pm)^2 &\approx (m_2^p)^2 + M_W^2\,. \end{aligned} \tag{2.42}$$

In the above, the approximations encode the fact that we have neglected the mixing between the several states (in each scalar, pseudoscalar and charged sector). Taking the mixing into account would lead to cumbersome expressions, involving all the states, which could only be numerically evaluated. For the remaining (heavier) states the physical masses are dominated to a large extent by the diagonal entries in the corresponding mass matrices, i.e., m^2_{33-66}. Although the general case is that the presence of the off-diagonal terms (m^2_{ij} and b_{ij}) does not substantially modify the mass spectrum, the situation can be distinct if either one of the latter quantities becomes close to the values of the diagonal entries, namely

$$m^2_{ij} \approx 0.9\; m^2_{ii}\,, \qquad \text{or} \qquad b_{ij} \approx 0.35\; m^2_{ii}\,. \tag{2.43}$$

If we are in the presence of the above regimes, then more mixing between the states is produced, and one is ultimately led to the appearance of tachyons. The presence of tachyons is also triggered by increasingly larger values of $\tan\beta$.

Even though we will not address experimental issues, we will adopt the following naïve bounds (mimicking the MSSM) for the bare masses of the lightest states [82]:

$$m_1^s \gtrsim 75\ \text{GeV}\,, \qquad m_2^p \gtrsim 91\ \text{GeV}\,, \qquad m_2^\pm \gtrsim 80\ \text{GeV}\,, \tag{2.44}$$

where the first bound translates in taking $\tan\beta > 3$.

2.4 Yukawa interaction Lagrangian

In agreement with the superpotential introduced in Section 2.2, the Lagrangian for the interaction of Higgs with up- and down-quarks can be written as

$$\mathcal{L}^0_{\text{Yukawa}} = -\sum_{i=1,3,5} h^0_i \, \bar{d}'_R \, Y^d_i \, d'_L - \sum_{i=2,4,6} h^0_i \, \bar{u}'_R \, Y^u_i \, u'_L + \text{H.c.}\,, \tag{2.45}$$

where $q_{L,R}$ ($Y^{u,d}_i$) are vectors (matrices) in flavour space, and the quarks appearing above are interaction (rather than mass) eigenstates, a prime being used to emphasise the latter. This Lagrangian gives rise to the quark mass matrices and to scalar and pseudoscalar Higgs-quark-quark interactions. The mass terms for the quarks read

$$\mathcal{L}_{\text{mass}} = -\bar{d}'_R \, M^d \, d'_L - \bar{u}'_R \, M^u \, u'_L + \text{H.c.}\,, \tag{2.46}$$

$$M^d = \sum_{i=1,3,5} w_i \, Y^d_i\,, \qquad M^u = \sum_{i=2,4,6} w_i \, Y^u_i\,. \tag{2.47}$$

The resulting up- and down-type quark mass matrices can be diagonalised as

$$V^q_R \, M^q \, V^{q\dagger}_L \;=\; \text{diag}(m^q_i)\,, \qquad q = u, d\,, \tag{2.48}$$

while the mass and interaction (primed) eigenstates are related by the following transformations

$$V^q_L \, q'_L = q_L \qquad V^q_R \, q'_R = q_R \qquad q = u, d\,. \tag{2.49}$$

The Cabibbo-Kobayashi-Maskawa (CKM) matrix is defined as

$$V_{\text{CKM}} = V^u_L \, V^{d\dagger}_L\,. \tag{2.50}$$

From the above equations it is manifest that in the quark sector, mass matrices and Yukawa couplings are in general misaligned, the only exception occurring for Yukawa couplings which are proportional. This misalignment translates into the impossibility of diagonalising both matrices simultaneously, and is the source of the existence of tree-level FCNCs, as we will briefly discuss.

Let us turn our attention to the Higgs-quark-quark interaction Lagrangian. In the unrotated basis, the latter reads

$$\begin{aligned}\mathcal{L}^0_{\text{Yukawa}} = &-\frac{1}{\sqrt{2}} \sum_{i=1,3,5} \Big[\sigma_i \, \bar{d}'_R \, Y^d_i \, d'_L + i\varphi_i \, \bar{d}'_R \, Y^d_i \, d'_L + \text{H.c.} \Big] \\ &-\frac{1}{\sqrt{2}} \sum_{i=2,4,6} \left[\sigma_i \, \bar{u}'_R \, Y^u_i \, u'_L + i\varphi_i \, \bar{u}'_R \, Y^u_i \, u'_L + \text{H.c.} \right]\,,\end{aligned} \tag{2.51}$$

while moving to the quark and Higgs mass eigenstate basis the couplings are

$$\begin{aligned}\mathcal{L}_{\text{Yukawa}} = &-\frac{1}{\sqrt{2}}\sum_{i=1,3,5}\Big[\,(\mathcal{V}_d)^{ij}_{ab}\;h^s_j\,\bar{d}^a_R\,d^b_L + i\,(\mathcal{W}_d)^{ij}_{ab}\;h^p_j\,\bar{d}^a_R\,d^b_L + \text{H.c.}\Big]\\ &-\frac{1}{\sqrt{2}}\sum_{i=2,4,6}\Big[(\mathcal{V}_u)^{ij}_{ab}\;h^s_j\,\bar{u}^a_R\,u^b_L + i\,(\mathcal{W}_u)^{ij}_{ab}\;h^p_j\,\bar{u}^a_R\,u^b_L + \text{H.c.}\Big]\,. \end{aligned} \tag{2.52}$$

In the above, a, b denote quark flavours, while $i, j = 1, \ldots, 6$ are Higgs indices, with s (p) denoting scalar (pseudoscalar) mass eigenstates. The latter are related to the original states as $h^s = S_\sigma \sigma$, $h^p = S_\varphi \varphi$, as from Eqs. (2.40,2.41). The scalar (pseudoscalar) couplings $\mathcal{V}$ ($\mathcal{W}$) are defined as

$$\begin{aligned}(\mathcal{V}_q)^{ij}_{ab} =& (S^\dagger_\sigma)_{ij}\;(V^q_R\,Y^q_i\,V^{q\dagger}_L)_{ab}\,,\\ (\mathcal{W}_q)^{ij}_{ab} =& (S^\dagger_\varphi)_{ij}\;(V^q_R\,Y^q_i\,V^{q\dagger}_L)_{ab}\,,\end{aligned} \tag{2.53}$$

with $i = 1, 3, 5$ $(2, 4, 6)$ for $q = d\,(u)$ and $j = 1, \ldots, 6$. The several rotation matrices appearing in the previous equation were defined in Eqs. (2.40,2.41,2.48). As a final remark, it is important to stress that the matrices $V_{L,R}$ which diagonalise the quark mass matrices do not, in general, diagonalise the corresponding Yukawa couplings. Hence, both scalar and pseudoscalar Higgs-quark-quark interactions may exhibit a strong non-diagonality in flavour space.

Finally, let us point out that in the Higgs basis R_1 and R_2 do not have flavour violating interactions. This is straightforward if one recalls that the Higgs basis mimics an MSSM-extended model. In the basis of the Higgs physical states, all six (five) scalars (pseudoscalars) mix, and all play a role in mediating the FCNC processes.

2.5 FCNCs at the tree-level

In this section, we compute the tree-level observables (such as neutral meson mass differences and CP violation in neutral meson mixing) induced by the exchange of neutral Higgs. These effects are absent in the SM, and play a determinant role in constraining the free parameters of the model. We discuss these effects for the case of the neutral kaons, as well as for the B_d, B_s and $D^0 - \bar{D}^0$ systems.

2.5.1 K-meson oscillations and contributions to Δm_K

We begin with the computation of the contributions of the several Higgs fields to the mass difference of the long- and short-lived neutral kaon states. In terms of effective Hamiltonians, the neutral kaon mass difference is defined as

$$\Delta m_K = m_{K_L} - m_{K_S} \simeq 2\left|\mathcal{M}^K_{12}\right| = 2\left|\langle\overline{K}^0\left|\mathcal{H}^{\Delta S=2}_{\text{eff}}\right|K^0\rangle\right|\,, \tag{2.54}$$

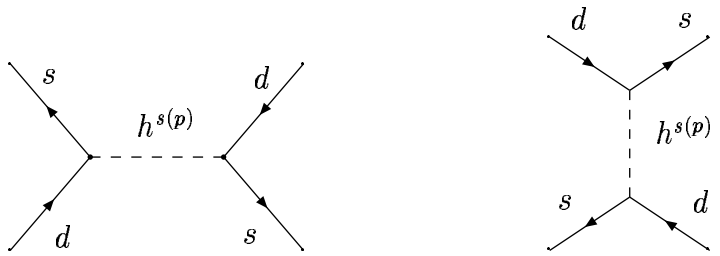

(a) (b)

Figure 2.6: Feynman diagrams contributing to Δm_K at tree-level.

where $\mathcal{H}_{\rm eff}^{\Delta S=2}$ is the effective Hamiltonian governing $\Delta S = 2$ transitions. The Hamiltonian can be decomposed as

$$\mathcal{H}_{\rm eff}^{\Delta S=2} = \mathcal{H}_{\rm tree} + \mathcal{H}_{\rm loop}\,. \tag{2.55}$$

In the above we have separated the contributions arising from tree-level diagrams from those associated with box and higher-loop diagrams. We will focus on the tree-level contributions to Δm_K induced by the exchange of scalar and pseudoscalar Higgs. From the interaction Lagrangians previously derived, it is now straightforward to compute the effective Hamiltonian for the diagrams in Fig. 2.6. One thus has $\mathcal{H}_{\rm eff} = \mathcal{H}_{\rm eff}^{\sigma} + \mathcal{H}_{\rm eff}^{\varphi}$, with

$$\mathcal{H}_{\rm eff}^{\sigma} = \sum_{j=1-6} \frac{1}{16(m_j^s)^2} \left\{ \bar{s} \sum_{i=1,3,5} \left[(\mathcal{V}_d^\dagger + \mathcal{V}_d)_{21}^{ij} + (\mathcal{V}_d^\dagger - \mathcal{V}_d)_{21}^{ij}\gamma_5 \right] d \right\}^2 + \text{H.c.}\,, \tag{2.56}$$

$$\mathcal{H}_{\rm eff}^{\varphi} = -\sum_{j=2-6} \frac{1}{16(m_j^p)^2} \left\{ \bar{s} \sum_{i=1,3,5} \left[(\mathcal{W}_d - \mathcal{W}_d^\dagger)_{21}^{ij} - (\mathcal{W}_d + \mathcal{W}_d^\dagger)_{21}^{ij}\gamma_5 \right] d \right\}^2 + \text{H.c.}\,, \tag{2.57}$$

where the scalar and pseudoscalar Higgs masses, $m^{s,p}$, have been defined in Eq. (2.40). Therefore, the contribution to the kaon mass difference associated with the exchange of a scalar Higgs boson (h^s) is given by

$$\begin{aligned} \mathcal{M}_{12}^K\big|^{\sigma} =& \frac{1}{8} \sum_{j=1-6} \frac{1}{(m_j^s)^2} \left\{ \left[\sum_{i=1,3,5} \left(\mathcal{V}_{d12}^{ij*} + \mathcal{V}_{d21}^{ij} \right) \right]^2 \langle \overline{K}^0 | (\bar{s}d)(\bar{s}d) | K^0 \rangle \right. \\ &\left. + \left[\sum_{i=1,3,5} \left(\mathcal{V}_{d12}^{ij*} - \mathcal{V}_{d21}^{ij} \right) \right]^2 \langle \overline{K}^0 | (\bar{s}\gamma_5 d)(\bar{s}\gamma_5 d) | K^0 \rangle \right\}, \end{aligned} \tag{2.58}$$

m_K	497.6 MeV	[82]	m_{D^0}	1.864 GeV	[82]
Δm_K	3.49×10^{-12} MeV	[82]	Δm_{D^0}	$< 46.07 \times 10^{-12}$ MeV	[82]
f_K	159 MeV	[83]	f_D	224 MeV	[84]
m_{B_d}	5.279 GeV	[82]	m_{B_s}	5.369 GeV	[82]
Δm_{B_d}	3.304×10^{-13} GeV	[82]	Δm_{B_s}	$> 94.8 \times 10^{-13}$ GeV	[82]
f_{B_d}	215 MeV	[85]	f_{B_s}	245 MeV	[85]

Table 2.1: Numerical values used throughout the computation with the corresponding references.

while the exchange of a pseudoscalar state (h^p) reads

$$\mathcal{M}_{12}^{K}|^{\varphi} = \frac{1}{8} \sum_{j=2-6} \frac{1}{(m_j^p)^2} \left\{ \left[\sum_{i=1,3,5} \left(\mathcal{W}_{d21}^{ij*} - \mathcal{W}_{d12}^{ij} \right) \right]^2 \langle \overline{K}^0 | (\bar{s}d)(\bar{s}d) | K^0 \rangle \right.$$
$$\left. + \left[\sum_{i=1,3,5} \left(\mathcal{W}_{d21}^{ij*} + \mathcal{W}_{d12}^{ij} \right) \right]^2 \langle \overline{K}^0 | (\bar{s}\gamma_5 d)(\bar{s}\gamma_5 d) | K^0 \rangle \right\} . \tag{2.59}$$

The theoretical prediction for the value of Δm_K thus obtained should be compared with the experimental value of $(\Delta m_K)_{\rm exp} = 3.49 \times 10^{-12}$ MeV. We stress here that in a SM/MSSM-like scenario, the $\mathcal{W}_d$, $\mathcal{V}_d$ matrices entering in Eqs. (2.58, 2.59) would be diagonal in flavour space, and thus no tree-level FCNC would occur. This is clear from Eqs. (2.53), since the flavour content of $\mathcal{W}$ and $\mathcal{V}$ is proportional to $(V_R^d Y_i^d V_L^{d\dagger})_{ab}$. In the SM and MSSM, the matrices that diagonalise the quark mass matrices $V_{L,R}$ also diagonalise the Yukawa couplings, so $(V_R^d Y_i^d V_L^{d\dagger})_{ab} \propto \delta_{ab}$. In multi-Higgs doublet models, where the underlying theory implies that the Yukawas are proportional among themselves (i.e. $Y_i^q \propto Y_j^q$), we also encounter a situation where no tree-level FCNCs emerge.

Given the purpose of the analysis, we have adopted a simple approach regarding the computation of the meson matrix elements, using the vacuum insertion approximation with non-renormalised operators. Following Ref. [83], we have

$$\langle \overline{K}^0 | (\bar{s}d)(\bar{s}d) | K^0 \rangle = \left[\frac{1}{12} - \frac{1}{12} \left(\frac{m_K}{m_s + m_d} \right)^2 \right] m_K f_K^2 ,$$
$$\langle \overline{K}^0 | (\bar{s}\gamma_5 d)(\bar{s}\gamma_5 d) | K^0 \rangle = \left[-\frac{1}{12} + \frac{11}{12} \left(\frac{m_K}{m_s + m_d} \right)^2 \right] m_K f_K^2 , \tag{2.60}$$

where m_K is the kaon mass, and f_K the kaon decay constant. In Table 2.1, we present several relevant input parameters for the computation of meson observables.

Before concluding the analysis of the neutral kaon sector, let us mention that in a scenario where one has flavour violating neutral Higgs couplings, and given the most generic possibility

of having a complex CKM matrix, it is natural to expect the occurrence of indirect CP violation at the tree-level. Although we will not pursue this issue in the following numerical analysis, let us just stress that the contributions to ε_K (which parametrises indirect CP violation in the kaon sector) are given by

$$\varepsilon_K = -\frac{e^{i\pi/4}}{\sqrt{2}} \frac{\mathrm{Im}\left[\mathcal{M}_{12}^K \lambda_u^2\right]}{|\lambda_u|^2 \, \Delta m_K} \,, \tag{2.61}$$

where λ_u is defined from CKM elements as $\lambda_u = V_{us}^* V_{ud}$, with $\mathcal{M}_{12}^K$ as computed in Eqs. (2.58,2.59) (under the assumption of complex Yukawa couplings). This new tree-level contribution would have to be compatible with the SM loop contribution and the experimental bound $\varepsilon_K = (2.284 \pm 0.014) \times 10^{-3}$ [82].

2.5.2 Other neutral meson systems: B_d, B_s and D^0

Computing the mass differences of neutral B and D mesons introduces no new elements into the analysis. The approach is entirely identical to that of the kaon system, the only difference lying in replacing the K^0 $(\bar{s}d)$ constituent quarks of Fig. 2.6 by $(\bar{u}c)$, $(\bar{b}d)$ and $(\bar{b}s)$, for D^0, B_d and B_s, respectively. In each case the effective Hamiltonian for scalar and pseudoscalar Higgs exchange reads as in Eqs. (2.56, 2.57), providing that the following replacements are done[6]:

B_d: $\mathcal{V}$ and $\mathcal{W}$ indices (21) $\rightarrow$ (31).

B_s: $\mathcal{V}$ and $\mathcal{W}$ indices (21) $\rightarrow$ (32).

D: $\mathcal{V}$ and $\mathcal{W}$ computed for the up-sector (see Eq. (2.53)); $\mathcal{V}$ and $\mathcal{W}$ indices (21) $\rightarrow$ (12); sum over interaction eigenstates $i = 1, 3, 5 \rightarrow i = 2, 4, 6$.

In each case, the hadronic matrix elements should be also recomputed, and the predictions for each of the above processes should be confronted with the experimental data summarised in Table 2.1. Before concluding this section, let us briefly comment on the several observables mentioned here. First of all, it is widely recognised that, in models with tree-level FCNC, the most stringent bounds are usually associated with Δm_K. Regarding the B_d sector, it has also been argued that in the absence of a predictive theory for the Yukawa couplings, the bounds associated with Δm_{B_d} should be considered as a more reliable constraint, since they do not involve the mixing between the first two generations [50]. Although we include it in our analysis, the B_s mass difference is not expected to add any new information. In the SM, this mixing is already maximal, and the addition of a new contribution would have little effect, the only exception occurring if new contributions matched exactly those of the SM, but had opposite sign, in which case a cancellation could take place. Still, this is a very fine-tuned scenario, and hardly significant, given the uncertainties associated with the computation. Finally, we turn

[6] In all cases, we are only computing an estimate value, not taking into account neither theoretical uncertainties (as those associated with the computation of the matrix elements), nor experimental errors.

our attention to the D^0 mass difference. As pointed out in [46, 49] and [86], models allowing for FCNC at the tree-level may present the possibility of very large contributions to Δm_D, thus emerging as an excellent probe of new physics effects. The latter contributions are often harder to control than those associated with, for example, Δm_K. In fact, and as discussed in [49], the contribution of tree-level FCNCs to Δm_D could even exceed by a factor 20 those to Δm_K. On the other hand, mixing in the D^0 sector is very sensitive to the hadronic model used to estimate the transition amplitudes, and there is still a very large uncertainty in deriving its decay constants, etc. Therefore, the constraints on a given model arising from Δm_D should not be over-emphasised.

Another interesting issue is that of rare decays. It has been argued that, again when no theory for the full Yukawas is available, some rare decays may become very sensitive to flavour changing contributions induced by Higgs exchange at the tree-level. In Ref. [50], the authors have identified that the most promising decay modes involve the leptonic sector, are the $l_i \to 3l_j$ tree-level decays. We will not pursue this issue in the present chapter, reserving its study to the case of Z_3 orbifold compactifications [54], analysed in Chapter 4.

2.6 Flavour violation in SUSY models with three families: results and discussion

2.6.1 Yukawa couplings: the simple Fritzsch scheme

We have carried out in the previous Section a general analysis of FCNC contributions. This can be applied to any particular model with three Higgs families, provided that the Yukawa couplings are known. Lead by simplicity, and following the analysis of [49], we take as an illustrative example the so-called "simple Fritzsch scheme" [75, 76]. Taking this ansatz for each of the Yukawa couplings presents two main advantages: it leads to mass matrices with a fairly hierarchical structure, and allows to fit experimental data on quark masses and mixings for a reasonable number of free parameters.

The "simple Fritzsch scheme" essentially consists in having all the weak quark eigenstates adopt identically structured couplings, which display suppressed flavour-changing elements for the first two generations in each family. More explicitly one has

$$Y_i = \frac{1}{w_i} \begin{pmatrix} 0 & A_i & 0 \\ A_i & 0 & B_i \\ 0 & B_i & C_i \end{pmatrix} , \tag{2.62}$$

where $i = 1, ..., 6$, and the entries are given by[7]

$$A_i = a_i \sqrt{m_1^q \, m_2^q}\,, \qquad B_i = b_i \sqrt{m_2^q \, m_3^q}\,, \qquad C_i = c_i \, m_3^q\,, \tag{2.63}$$

with a_i, b_i and c_i coefficients of order one, and m_j^q the quark masses of the $j^{\rm th}$ generation and $q = d\,(u)$ for $i = 1, 3, 5\,(2, 4, 6)$. One further advantage of this choice, which will become more evident in the subsequent discussion, is that under the above ansatz, the quark masses and mixings are independent of the chosen VEV regime (although the Yukawas are not). This means that for a given successful choice of the parameters a_i, b_i and c_i, one can study a number of distinct VEV schemes, corresponding to different $\tan\beta$ scenarios.

Let us now present a specific numerical example. Taking the values for the input quark masses, m_i^q entering in the ansatz of Eq. (2.63) as $m_u = 3$ MeV, $m_d = 6.5$ MeV, $m_c = 1.25$ GeV, $m_s = 0.1$ GeV, $m_t = 178$ GeV, m_b =4.5 GeV, and using the following choice of coefficients

$$\begin{aligned} a &= \{0.45, 0.30, 0.35, 0.45, 0.20, 0.50\}\,, \\ b &= \{0.25, 0.40, 0.45, 0.30, 0.20, 0.35\}\,, \\ c &= \{0.30, 0.45, 0.30, 0.30, 0.40, 0.25\}\,, \end{aligned} \tag{2.64}$$

one obtains the following set of output quark masses

$$\begin{aligned} &m_u = 0.0042 \text{ GeV}\,, \quad m_c = 1.37 \text{ GeV}\,, \quad m_t = 179.4 \text{ GeV} \\ &m_d = 0.0073 \text{ GeV}\,, \quad m_s = 0.087 \text{ GeV}\,, \quad m_b = 4.5 \text{ GeV} \end{aligned} \tag{2.65}$$

and the associated mixing matrix

$$|V_{\rm CKM}| = \begin{pmatrix} 0.9742 & 0.2255 & 0.0031 \\ 0.2251 & 0.9733 & 0.0438 \\ 0.0129 & 0.0420 & 0.9990 \end{pmatrix}\,, \tag{2.66}$$

which is in good agreement with experimental data. Having the relevant data (Yukawa couplings and CKM matrix), we can now proceed to estimate the contributions to neutral meson mass differences. As stressed before, we are considering a general multi-Higgs model, so that we have no definite scheme for the μ-terms and soft SUSY breaking masses. Therefore, and as done in Section 2.2, we will assume simple textures for the Higgs sector.

2.6.2 Tree-level FCNC in neutral mesons: numerical results

The first step in evaluating the contributions to tree-level FCNC is to parameterise the Higgs sector, and thus obtain the mixing matrices and mass eigenstates entering in Eqs. (2.58,2.59).

[7]For simplicity, and since our main concern is to illustrate the contributions to meson mass difference, we will assume that the Yukawa couplings are real, so that we will not examine the contributions to CP violation observables.

As discussed in Section 2.2, the Higgs basis is far more intuitive to work in than the original superpotential basis. Working in Higgs-basis notation (see Eqs. (2.14-2.24)), let us assume that the free parameters m_{ij}^2 and b_{ij} obey the following simple patterns:

$$m_{ij}^{(d)} = \begin{pmatrix} \otimes & \otimes & \otimes \\ \otimes & x_3 & y \\ \otimes & y & x_5 \end{pmatrix} \times 1\text{TeV}\,, \quad m_{ij}^{(u)} = \begin{pmatrix} \otimes & \otimes & \otimes \\ \otimes & x_4 & y \\ \otimes & y & x_6 \end{pmatrix} \times 1\text{TeV}\,, \quad \sqrt{b_{ij}} = \sqrt{b} \times 1\text{TeV}\,, \tag{2.67}$$

where the $\otimes$ denotes an entry which is fixed by the minimisation conditions (cf. Eqs. (2.22,2.23)). The above parametrisation can be further simplified by taking $x_3 = x_4$ and $x_6 = x_5$. Therefore, we have the following free parameters associated with the Higgs sector:

$$x_3\,, \quad x_5\,, \quad \sqrt{b}\,, \quad \tan\beta\,, \tag{2.68}$$

and the pattern of VEVs, namely whether they are degenerate or hierarchical. In the numerical examples we will thus consider the following textures for m_{ij}^2 and b_{ij}.

$$\begin{aligned} &\text{(A)}: \quad x_3 = 1\,, \quad x_5 = 5\,, \quad y = 0.4\,, \quad \sqrt{b} = 0.3\,, \\ &\text{(B)}: \quad x_3 = 10\,, \quad x_5 = 10\,, \quad y = 0.6\,, \quad \sqrt{b} = 0.5\,. \end{aligned} \tag{2.69}$$

In each case, we will consider several values for $\tan\beta$, taking it to lie in the range $3 \lesssim \tan\beta \lesssim 12$. Moreover, for every $\tan\beta$ we take to very distinct schemes of VEVs, that while respecting the electroweak symmetry breaking conditions and being in agreement with the chosen $\tan\beta$ value, exhibit either a degenerate pattern ($w_1 = w_3 = w_5$, $w_2 = w_4 = w_6$) or a strongly hierarchical one ($w_5 = 10\,w_3 = 100\,w_1$, $w_6 = 10\,w_4 = 100\,w_2$).

For the above range of $\tan\beta$, the Higgs spectra (lightest and heaviest scalar, pseudoscalar and charged states) is within the following ranges [8]:

$$\begin{aligned} &\text{Texture (A)}: \\ &79\,\text{GeV} \lesssim m_1^s \lesssim 90\,\text{GeV}\,, \quad 198\,\text{GeV} \lesssim m_2^p \lesssim 409\,\text{GeV}\,, \quad 417\,\text{GeV} \lesssim m_2^\pm \lesssim 203\,\text{GeV}\,, \\ &\qquad 5009\,\text{GeV} \lesssim m_6^s,\ m_6^p,\ m_5^\pm \lesssim 5011\,\text{GeV}\,. \\ &\text{Texture (B)}: \\ &79\,\text{GeV} \lesssim m_1^s \lesssim 90\,\text{GeV}\,, \quad 908\,\text{GeV} \lesssim m_2^p \lesssim 1547\,\text{GeV}\,, \quad 909\,\text{GeV} \lesssim m_2^\pm \lesssim 1549\,\text{GeV}\,, \\ &\qquad 10043\,\text{GeV} \lesssim m_6^s,\ m_6^p,\ m_5^\pm \lesssim 10047\text{GeV}\,. \end{aligned} \tag{2.70}$$

[8] In both cases m_1^s and the masses of the heaviest states grow monotonically with $\tan\beta$. However, in the case of Texture (A), since the mixing induced by b and the diagonal mass x_3 are of comparable magnitude, as $\tan\beta$ grows, so does the mixing between the states, and thus, as pointed out in Section 2.3, the states h_2^p and $h_2^\pm$ can become lighter with increasing $\tan\beta$.

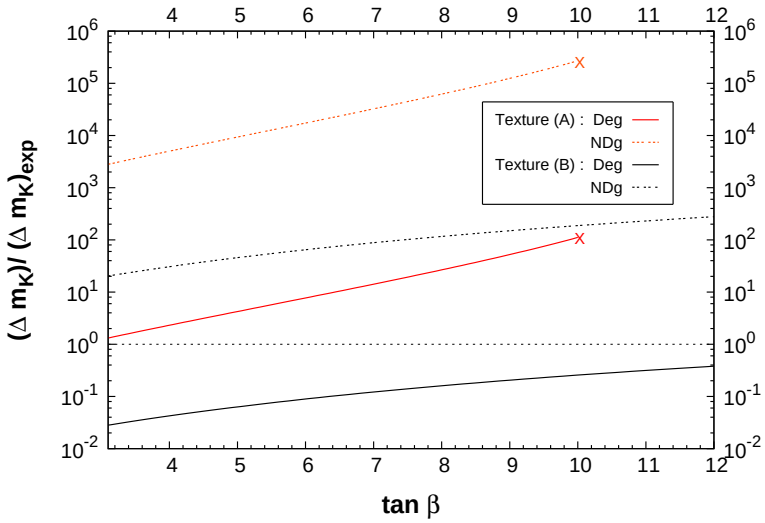

Figure 2.7: $\Delta m_K/(\Delta m_K)_{\rm exp}$ as a function of $\tan\beta$. Full (dashed) red line denotes texture (A) for degenerate (hierarchical) VEVs, while a black full (dashed) line refers to texture (B) with degenerate (hierarchical) VEVs. For Texture (A) a cross marks the appearance of tachyonic states. The experimental bound is depicted via a dotted horizontal line.

Let us begin by addressing the observable which is associated to most stringent constraints for this class of models: Δm_K. In Fig. 2.7, we plot ratio $\Delta m_K/(\Delta m_K)_{\rm exp}$ as a function of $\tan\beta$ for textures (A) and (B), considering in each case a pattern of degenerate (Deg) or non-degenerate (NDeg) VEVs. Fig. 2.7 clearly reflects the most problematic aspect of this class of multi-Higgs doublet models. Without a symmetry forbidding some of the Yukawa couplings, and if the Yukawas themselves do not exhibit a strong hierarchical character, the contributions to the neutral kaon mass difference can only be brought down to the experimental value via a set of very heavy Higgses, as those of texture (B). A Higgs spectrum closer to the electroweak scale, with a typical mass scale of 500 GeV, would generate, for the case of degenerate (non-degenerate) VEVs, contributions to Δm_K of around 30 (3×10^4) $(\Delta m_K)_{\rm exp}$. It is also manifest that smaller values of $\tan\beta$ favour smaller contributions. This is due to having the Yukawa couplings for the down quarks proportional to $\sec\beta$. The relevance of the VEV regime should also be emphasised, since the latter plays a very important role. Even though the Yukawas enter in the contribution to $\mathcal{M}_{12}^K$ already rotated by the matrices that diagonalise the quark mass matrices, it is clear that the smaller the VEVs associated to the first and second quark generations, the more enhanced will be the (12) matrix elements. In the case of degenerate VEVs, all the Yukawas are identically suppressed/enhanced[9]. Naturally, assuming such a large

[9]This is also related to the specific ansatz for the Yukawa couplings.

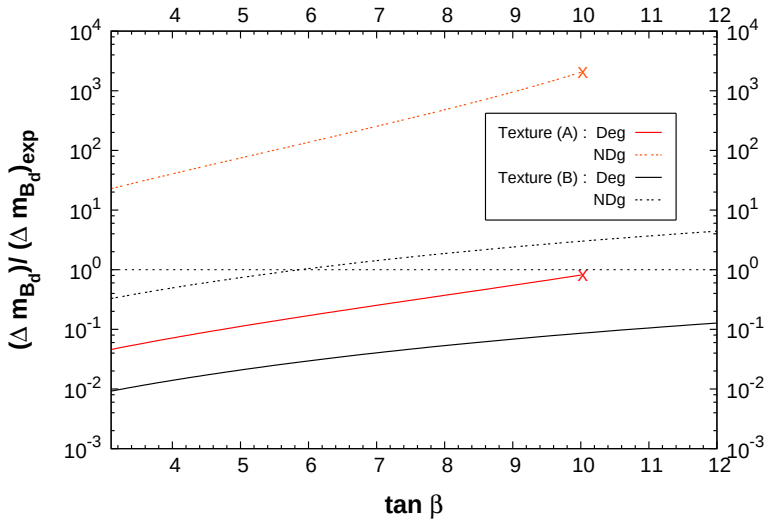

Figure 2.8: $\Delta m_{B_d}/(\Delta m_{B_d})_{\rm exp}$ as a function of $\tan\beta$. Line and colour codes as in Fig. 2.7.

scale for the soft-breaking terms potentially leads to a fine tuning problem. As pointed out in Section 2.2.3, and even though the discussion was conducted for a distinct basis, masses above the few TeV scale are in principle within range of a more than 1% fine tuning.

When compared to some previous studies, our results are more severe. However, let us stress that in our analysis we have taken a few distinct steps. Firstly, and in comparison to the ansätze used in [49], our Yukawa couplings are quite different, since accommodating the current CKM matrix data leads to values of a_i, b_i and c_i quite smaller than those previously considered. This implies that the present Yukawas are less hierarchic. Moreover, we have explicitly taken into account the values of the VEVs, and considered the contributions from the exchange of all physical scalar and pseudoscalar Higgses (not weak interaction eigenstates), taking into account not only their masses, but also their mixings. It is also important to mention that the values of the hadronic matrix elements have been revised in the past years.

In Fig. 2.8, we present the contributions to the mass difference of the B_d mesons. As expected, in this case it is far easier to comply with the experimental bounds. For the case of degenerate VEVs, even the "lightest" texture (A) succeeds in complying with the experimental bounds throughout the whole range of $\tan\beta$ considered, while for the heavier Higgs set (B), with non-degenerate VEVs. compatibility is obtained for the low $\tan\beta$ regime ($\tan\beta \lesssim 6$).

To complete our study, we display in Fig. 2.9 the same analysis for the case of the B_s meson system. In this case, the experimental bound is a lower (rather than upper bound). As discussed in Section 2.5, the SM already has maximal mixing in the B_s system, and even though the new

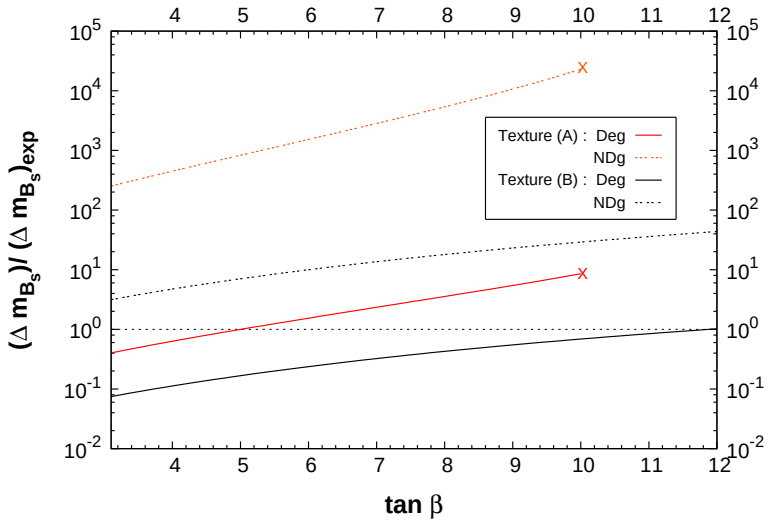

Figure 2.9: $\Delta m_{B_s}/(\Delta m_{B_s})_{\rm exp}$ as a function of $\tan\beta$. Line and colour codes as in Fig. 2.7.

contributions may be of identical magnitude, there is no reason to expect a cancellation between SM and tree-level contributions, which would be associated to an extremely fine tuned scenario for all the parameters involved.

From the meson systems so far discussed, the most severe constraints arise, as expected, from the $K_L - K_S$ mass difference. As a final remark, and following the discussion of Section 2.5, we briefly comment on the predicted scenario involving the D^0 mesons. A study similar to those conducted for the K^0 and B sectors is of less interest, since there is little dependence of $\Delta m_D/(\Delta m_D)_{\rm exp}$ on $\tan\beta$. This is due to having the up-type quarks Yukawa couplings associated to $\csc\beta$, as seen from Eq. (2.62). Rather than presenting a plot, we will briefly summarise the situation. With the exception of Texture (A), with non-degenerate VEVs, which induces contributions to Δm_D around 10 times its experimental value, all other cases predict contributions below the experimental bound, ranging from 10^{-3} to 10^{-1} $(\Delta m_D)_{\rm exp}$.

To summarise, ansätze for the Yukawa couplings of the "simple Fritzsch" type, when generalised to multi-Higgs doublet models, typically induce tree-level FCNC's, and require a Higgs spectrum at least of order 10 TeV, in order to ensure compatibility with experiment. Notice however that the results presented here are very dependent on the assumed scheme for the Yukawa couplings, and are only to be taken as an illustrative example, in the absence of a full theory for the Higgs-quark-quark interactions.

2.7 Conclusions

Models that predict family replication in the Higgs sector offer a very aesthetic and phenomenologically interesting scenarios. Although there is abundant motivation for extending the Higgs sector (in non-minimal SUSY models, GUTs or string constructions, for example), in most cases the viability of these models is challenged by the occurrence of potentially dangerous FCNCs at the tree-level.

We have analysed the most general form of the SUSY potential with three Higgs families, studying its minimisation, and deriving the tree-level expressions for the neutral (scalar and pseudoscalar) and charged Higgses mass matrices.

The main goal of our study was to derive a model-independent evaluation of the tree-level contributions to neutral meson mass differences. We have computed the most general expression for the tree-level neutral Higgs mediated contributions to the mass difference of the neutral mesons. We took into account the exchange of all Higgs states, included the effects of mixing in the Higgs sector, and made no approximation with respect to dominant/sub-dominant contributions. This analysis is completely general, and can be applied to any given model with three Higgs families, independently of its Yukawa structure. As an example, in Section 2.6 we have assumed a simple ansatz for the Yukawa couplings (in analogy to what had previously been done), and have considered the contributions of two distinct Higgs spectra to the K^0, B_d, B_s and D^0 mass differences, finding that the strongest bound - which as expected arises from Δm_K - requires a spectrum of order 10 TeV.

We again remark that the results for the Higgs masses are strongly dependent on the specific ansatz for the Yukawa couplings. Other ansätze, that account for a stronger hierarchy in the quark sector and still accommodate experimental data on quark masses and mixings, may generate quite smaller contributions to Δm_K, and thus require a lighter Higgs spectrum. This possibility is analysed in the following Chapter in the context of Z_3 compatifications [53], where we will show that a Higgs spectra of order 1 TeV can be accommodated. On the other hand, it is also possible that while generating smaller contributions to Δm_K, the different ansätze induce larger Δm_B, or Δm_D.

In addition to the contributions to neutral meson mass difference, within the quark sector there are other processes that also deserve further investigation. For example, let us mention, at the one loop level, the very suppressed SM and MSSM B_s decays. Processes involving the lepton sector also offer an even wider field for testing the new contributions induced by the additional Higgses (neutral and charged). CP violation, given the potential tree-level contributions to ε_K, may also become a stringent bound.

Chapter 3

Phenomenological viability of the quark sector in Z_3 scenarios with three Higgs families

3.1 Introduction

The understanding of the observed pattern of quark and lepton masses and mixings remains as one of the most important open questions in particle physics. From experiment, we believe that Nature contains three families of quarks and leptons, with peculiar mass hierarchies. Moreover, there is firm evidence that the flavour structure in both quark and lepton sectors is far from trivial, as exhibited by the current bounds on the quark [82] and lepton [87–89] mixing matrices.

As previously commented in the general introduction, the Standard Model fails in explaining some important issues such as the fermion flavour structure or the number of fermion families we encounter in Nature. Moreover, the mechanism of mass generation for quarks and leptons remains still unconfirmed until the future discovery of the Higgs boson in a collider.

Supersymmetry, supergravity or grand unified theories (GUTs) may repair some deficiencies of the SM, but they still fail in providing a clear understanding of the nature of masses, mixings and number of families. In this sense, a crucial ingredient to relate theory and observation is the precise knowledge of how fermions and Higgs scalars interact, in other words, the Yukawa couplings of the fundamental theory.

If we want string theory to be the theory of everything, it must therefore necessarily contain the SM as its low-energy limit. In this sense, string theory must provide an answer to the above mentioned questions. In Chapter 1 we have seen that the compactification of the $E_8 \times E_8$

heterotic string [13] on six-dimensional orbifolds [17] turns out to be a very attractive method to obtain a four dimensional effective theory, and this has proved to be a very successful attempt at finding the superstring standard model [18–21, 23–25, 29, 51, 62, 64–66, 90–105] As it was shown in [19, 20], the use of two Wilson lines [17, 18] on the torus defining a symmetric Z_3 orbifold can give rise to SUSY models with $SU(3) \times SU(2) \times U(1)^n$ gauge group and three families of chiral particles with the correct $SU(3) \times SU(2)$ quantum numbers. These models present very attractive features from a phenomenological point of view. One of the $U(1)$s of the extended gauge group is in general anomalous, and it can induce a Fayet-Iliopoulos (FI) D-term [22] that would break SUSY at very high energies (FI scale $\sim \mathcal{O}(10^{16-17}$ GeV)). To preserve SUSY, some fields will develop a vacuum expectation value (VEV) to cancel the undesirable D-term. The FI mechanism allows to break the gauge group down to $SU(3)_c \times SU(2)_L \times U(1)_Y$ and obtain the mass spectrum of the minimal supersymmetric standard model (MSSM), plus some exotic matter, as extra singlets, doublets or vector-like triplets, depending on the model, as shown in Refs. [21, 24, 25].

Orbifold compactifications have other remarkable properties. For instance, they provide a geometric mechanism to generate the mass hierarchy for quarks and leptons [26–28, 30, 33] through renormalisable Yukawa couplings. Z_n orbifolds have twisted fields which are attached to the orbifold fixed points. Fields at different fixed points may communicate with each other only by world sheet instantons. The resulting renormalisable Yukawa couplings can be explicitly computed [26, 27, 31, 32, 34, 35] and they receive exponential suppression factors that depend on the distance between the fixed points to which the relevant fields are attached. These distances can be varied by giving different VEVs to the T-moduli associated with the size and the shape of the orbifold.

However, the major problem that one encounters when trying to obtain models with entirely renormalisable Yukawas lies at the phenomenological level, and is deeply related to obtaining the correct quark mixing. Summarising the analyses of Refs. [30, 33], for prime orbifolds the space group selection rules and the need for a fermion hierarchy forces the fermion mass matrices to be diagonal at the renormalisable level. Thus, in these cases, the Cabibbo-Kobayashi-Maskawa (CKM) parameters must arise at the non-renormalisable level. For analyses of non-prime orbifolds see Refs. [30, 33, 120, 121].

For example, since the FI breaking generates VEVs for fields of order $\langle \chi_j \rangle \sim 10^{16-17}$ GeV, if one has terms in the superpotential of the type $\frac{1}{M_P^m}\, \chi_1 \cdots \chi_m\, \xi\, \xi\, \xi$, these would produce couplings of order $(M_{FI}/M_P)^m$. Therefore, depending on m, different values for the couplings might be generated. Obviously, the presence of these couplings is very model-dependent and introduces a high degree of uncertainty in the computation. However, it is important to remark that having the latter couplings is not always allowed in string constructions. First of all, they must be gauge-invariant, something that is not easy to achieve, due to the large number of $U(1)$

charges which are associated to the particles in these models. Even if the couplings fulfil this condition, this does not mean that they are automatically allowed. They must still fulfil the so-called "stringy" selection rules. For example in the $SU(3) \times SU(2) \times U(1)_Y \times SO(10)_{hidden}$ model of Ref. [24], where renormalisable couplings are present, only a small number of non-renormalisable terms are allowed by gauge invariance. Nevertheless, even the latter terms turn out to be forbidden by string selection rules.

Clearly, purely renormalisable Yukawa couplings are preferable, because, in general, due to the arbitrariness of the VEVs of the fields entering the non-renormalisable couplings, the predictivity is lost. Furthermore, as discussed above, higher-order operators such as those induced by the FI breaking are very model-dependent. One possibility of avoiding the necessity of these non-renormalisable couplings is to relax the requirement of a minimal matter content (with just two Higgs doublets) in a Z_3 orbifold with two Wilson lines. Since these models naturally contain three families of everything, including Higgses, additional Yukawa couplings will be present, with the possibility of leading to realistic fermion masses and mixings, entirely at the renormalisable level (with a key role being played by the FI breaking) [66]. In addition, and given the existence of three families of quarks and leptons, having also three families of Higgses renders these models very aesthetic. In fact, let us recall that experimental data imposes no constraints on the number of Higgs families. Moreover, this non-minimal Higgs content, provided that the extra doublets are light enough to be present at low-energies, also favours the unification of gauge couplings in heterotic string constructions. Due to the FI scale, the gauge couplings may unify at the string scale [64].

Thus, this class of string compactifications is one of the scenarios where one can obtain a SM/MSSM compatible low-energy theory, albeit with an extended Higgs sector. Furthermore it offers a solution to the flavour problem of the SM and MSSM, since the structure of the Yukawa couplings is completely derived from the geometry of the high-energy string construction. Given the increasing experimental accuracy, accommodating the data on quark masses and mixings is not straightforward. In this chapter, we propose to investigate in detail whether or not it is possible to obtain Z_3 orbifold configurations that successfully reproduce the observed flavour pattern in Nature. In this sense, having additional Yukawa couplings presents several advantages, as for example a greater flexibility when fitting the data from the quark masses and mixings.

On the other hand, as analysed in Chapter 2, when working in a multi-Higgs context we should also take into account the potential appearance of FCNCs at the tree level, which could contribute to a wide variety of Higgs decays and interactions with other particles As we will see, the Yukawa couplings of this Z_3 scenario exhibit a strongly hierarchical structure, and this property is instrumental in circumventing the FCNC problem without the need for an excessively heavy Higgs sector.

Z_3 orbifolds are also very attractive when addressing the lepton sector, and in fact offer an appealing scenario to study the problem of neutrino masses. We postpone this analysis for Chapter 4 [54].

In this chapter we describe the main properties of the Yukawa couplings in Z_3 orbifold models. We study the relations between the several orbifold parameters induced from the quark mass hierarchy and from electroweak symmetry breaking. Finally, the numerical analyses of the orbifold parameter space and FCNCs in association with specific Higgs textures is given, addressing the possibility of new contributions to indirect CP violation.

3.2 Yukawa couplings in Z_3 orbifold models

In this section we will briefly review the characteristics of Yukawa couplings between twisted fields in the Z_3 orbifold. As it was previously discussed in Chapter 1 we showed that the Z_3 orbifold is constructed by dividing R^6 by the $[SU(3)]^3$ root lattice modded by the point group (P) with generator θ, where the action of θ on the lattice basis e_i (with $i = 1, 3, 5$) is

$$\theta e_i = e_{i+1}\,, \qquad \theta e_{i+1} = -(e_i + e_{i+1})\,. \tag{3.1}$$

The two-dimensional sublattices associated to $[SU(3)]^3$ are presented in Fig. 3.1. Let us employ the following definition for the orfifold radii and angles

$$R_k \equiv |e_k|\,, \qquad \alpha_{kl} \equiv \cos\theta_{kl}, \tag{3.2}$$

where $k, l = 1, ..., 6$ and $e_k e_l = R_k R_l \cos\theta_{kl}$. Initially, the six-torus of the Z_3 orbifold has 21 degrees of freedom (six radii and fifteen angles). However, taking into account the relations that P-invariance imposes reduces these to only nine. Indeed, preserving the magnitude of the lattice basis leads to the relations

$$R_i = R_{i+1}\,, \qquad \alpha_{i,i+1} = -1/2\,. \tag{3.3}$$

If we also want to preserve the angles under the action of P then we will obtain

$$\alpha_{i,j+1} + \alpha_{i+1,j} + \alpha_{i,j} = 0\,, \qquad \alpha_{i,j} = \alpha_{i+1,j+1}. \tag{3.4}$$

Taking into account the previous constraints, only the following nine deformation parameters are left [30]:

$$R_1\ ,\quad R_3\ ,\quad R_5\ ,\quad \alpha_{13}\ ,\quad \alpha_{15}\ ,\quad \alpha_{35}\ ,\quad \alpha_{14}\ ,\quad \alpha_{16}\ ,\quad \alpha_{36}\ . \tag{3.5}$$

In the Z_3 orbifold without deformations the angles between complex planes are vanishing, however this need not be the case. These nine deformation parameters are associated to the VEVs

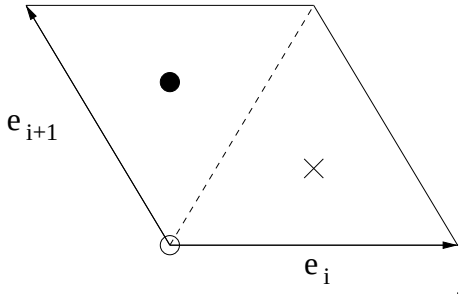

Figure 3.1: Two dimensional sublattice of the Z_3 orbifold, symbolically denoting the fixed points as $(\circ, \bullet, \times)$.

of the nine singlet moduli fields, denoted by T, that appear in the spectrum of the untwisted sector.

As commented in Chapter 1, twisted strings in orbifolds appear attached to fixed points under the point group. In the case of the Z_3 orbifold there are 27 fixed points under P, and therefore 27 twisted sectors. We will denote the three fixed points of each two-dimensional sublattice as shown in Fig. 3.1. It was shown in Ref. [17] that given two fields associated to two fixed points f_1, f_2, they can only couple to a unique third fixed point f_3 as a consequence of the so-called space group selection rules (thus there are $27\times\ 27 = 729$ allowed Yukawa couplings). In particular, the components of the three fixed points in each sublattice must be either equal or different.

The expressions for the different Yukawa couplings can be found for example in the Appendix of Ref. [34]. They contain suppressions factors that depend on the relative positions of the fixed points to which the fields involved in the coupling are attached (i.e. f_1, f_2, f_3) and on the size and shape of the orbifold (i.e. the deformation parameters in Eq. (3.5)). In fact, it is possible to show that only 14 couplings out of the 729 allowed are different. In the particular case of an orthogonal lattice, i.e. when the six angles in Eq. (3.5) are zero, there are only 8 distinct couplings. We will show in the following sections that these three radii are sufficient to fit the whole quark masses, and so we henceforth restrict the discussion to this case.

Let us begin by presenting the general form of the Yukawa couplings. They are given by the Jacobi theta function [34],

$$Y_{\theta\theta\theta} = g\ N \sum_{\mathbf{u}\in Z^6} exp\ [-2\pi(\mathbf{f}_{23}+\mathbf{u})^T M(\mathbf{f}_{23}+\mathbf{u})]\ , \tag{3.6}$$

with g being the heterotic gauge coupling constant and

$$N = \sqrt{V}\ \frac{3^{3/4}}{8\pi^3}\frac{\Gamma^6(\frac{2}{3})}{\Gamma^3(\frac{1}{3})}\ . \tag{3.7}$$

V is the volume of the unit cell for the Z_3 lattice and Γ is the Euler's *Gamma* function. The vector $\mathbf{f}_{23}$ represents the six components of $(f_2 - f_3)$. One can check that the only eight inequivalent possibilities are

$$(0,0,0,0,0,0)\ ,\ (\frac{1}{3},\frac{2}{3},0,0,0,0)\ ,\ (0,0,\frac{1}{3},\frac{2}{3},0,0)\ ,\ (0,0,0,0,\frac{1}{3},\frac{2}{3})\ ,$$
$$(\frac{1}{3},\frac{2}{3},\frac{1}{3},\frac{2}{3},0,0)\,,(\frac{1}{3},\frac{2}{3},0,0,\frac{1}{3},\frac{2}{3})\,,(0,0,\frac{1}{3},\frac{2}{3},\frac{1}{3},\frac{2}{3})\,,(\frac{1}{3},\frac{2}{3},\frac{1}{3},\frac{2}{3},\frac{1}{3},\frac{2}{3})\,, \tag{3.8}$$

corresponding to three fields with the same fixed point components in three sublattices, two sublattices, one sublattice, and no sublattice, respectively.

Under the simplest assumption of an orthogonal lattice, the matrix M takes the form

$$M = \begin{pmatrix} T_1 & -\frac{1}{2}T_1 & 0 & 0 & 0 & 0 \\ -\frac{1}{2}T_1 & T_1 & 0 & 0 & 0 & 0 \\ 0 & 0 & T_3 & -\frac{1}{2}T_3 & 0 & 0 \\ 0 & 0 & -\frac{1}{2}T_3 & T_3 & 0 & 0 \\ 0 & 0 & 0 & 0 & T_5 & -\frac{1}{2}T_5 \\ 0 & 0 & 0 & 0 & -\frac{1}{2}T_5 & T_5 \end{pmatrix} . \tag{3.9}$$

In the latter, T_i are the diagonal moduli VEVs whose real parts are associated to the internal metric $g_{ii} = e_i e_i$, with

$$Re\ T_i = \frac{\sqrt{3}}{16\pi^2} R_i^2\,. \tag{3.10}$$

It turns out that for values of the moduli of order one, all terms in the sum of Eq. (3.6) are negligible with respect to those corresponding to the shortest distance between fixed points. For example, for the fourth vector in Eq. (3.8) the sum, say ε_5, is given by

$$\varepsilon_5 = 3\ e^{-\frac{2\pi}{3}T_5}\ (1 + 6\ e^{-2\pi T_1} + 6\ e^{-2\pi T_3} + \dots)\ , \tag{3.11}$$

where the dots denote terms with larger suppression factors, which can therefore be approximated as

$$\epsilon_5 \approx 3\ e^{-\frac{2\pi}{3}T_5}. \tag{3.12}$$

Taking this into account, the sums in Eq. (3.6) corresponding to the different vectors in Eq. (3.8) can be approximated respectively as

$$1\,,\ \varepsilon_1\,,\ \varepsilon_3\,,\ \varepsilon_5\,,\ \varepsilon_{13}\,,\ \varepsilon_{15}\,,\ \varepsilon_{35}\,,\ \varepsilon_{135}\,, \tag{3.13}$$

where $\varepsilon_i = 3\ e^{-\frac{2\pi}{3}T_i}$, $\varepsilon_{ij} = \varepsilon_i\varepsilon_j$, and $\varepsilon_{135} = \varepsilon_1\varepsilon_3\varepsilon_5$. Let us stress that in the case without deformations, i.e. assuming an orthogonal lattice with $T_i = T$, there are only four different couplings, with the sums in Eq. (3.6) given by 1, ε, ε^2, ε^3, where $\varepsilon = 3\ e^{-\frac{2\pi}{3}T}$.

Through the following sections we will analyse how the suppression factors ε_i can be employed to provide the desired hierarchies between the different fermion Yukawa couplings, with the aid of the FI breaking.

3.3 Masses and mixings before the Fayet-Iliopoulos breaking

With the previous results we can now turn proceed to analyse the construction of fermion mass matrices in models with two Wilson lines. As a first approach to the problem, let us study the case prior to the FI breaking (as presented in [66]), assuming that the two non-vanishing Wilson lines (a_1, a_3) correspond to the first and second sublattices. Then the 27 twisted sectors come in nine sets with three equivalent sectors in each one. The three generations of matter (including Higgses) correspond to changing the third sublattice component ($\times$, $\bullet$, $\circ$) of the fixed point whilst keeping the other two fixed. In what follows we shall consider a particular assignment of Standard Model matter to different fixed point components. This is a "bottom-up" approach in that we do not explicitly construct the models but are asking which assignment is appropriate for the observed masses and mixings.

$$\begin{array}{lll} Q \leftrightarrow \circ\ \circ & u^c \leftrightarrow \circ\ \circ & d^c \leftrightarrow \times\ \circ \\ L \leftrightarrow \bullet\ \bullet & e^c \leftrightarrow \bullet\ \times & \nu^c \leftrightarrow \times\ \times \\ H^u \leftrightarrow \circ\ \circ & H^d \leftrightarrow \bullet\ \circ & . \end{array} \tag{3.14}$$

Assuming three different radii for the orbifold, and before taking into account the effect of the FI breaking, the fermion Yukawa mass matrices will be given by the following expression [66]:

$$\begin{aligned} \mathcal{M}^u &= g\,N\,A^u\,, \qquad \mathcal{M}^d = g\,N\,\varepsilon_1\,A^d\,, \\ \mathcal{M}^\nu &= g\,N\,\varepsilon_1\,\varepsilon_3\,A^u\,, \qquad \mathcal{M}^e = g\,N\varepsilon_3\,A^d\,, \end{aligned} \tag{3.15}$$

where

$$A^u = \begin{pmatrix} w_2 & w_6\,\varepsilon_5 & w_4\,\varepsilon_5 \\ w_6\,\varepsilon_5 & w_4 & w_2\,\varepsilon_5 \\ w_4\,\varepsilon_5 & w_2\,\varepsilon_5 & w_6 \end{pmatrix}\,, \qquad A^d \begin{pmatrix} w_1 & w_5\,\varepsilon_5 & w_3\,\varepsilon_5 \\ w_5\,\varepsilon_5 & w_3 & w_1\,\varepsilon_5 \\ w_3\,\varepsilon_5 & w_1\,\varepsilon_5 & w_5 \end{pmatrix}\,, \tag{3.16}$$

Here w_i^u, w_i^d denote the VEVs of the Higgses H_i^u, H_i^d respectively. For simplicity we will assume for the moment that these VEVs, as well as those of the moduli T_i, are real. Of course, in general they can be complex numbers, and later on we will address the importance that this may have for CP violation.

The elements in the above matrices can be obtained straightforwardly. For example, if the Higgs H_1^u corresponds to ($\circ$,$\circ$,$\circ$), then since the three generations of (3,2) quarks Q correspond to ($\circ$,$\circ$,($\circ$,$\times$,$\bullet$)) and the three generations of ($\bar{3}$,1) quarks u^c to ($\circ$,$\circ$,($\circ$,$\times$,$\bullet$)), there are only three allowed couplings,

$$\{(\circ,\circ,\circ)(\circ,\circ,\circ)(\circ,\circ,\circ)\}\,,\ \{(\circ,\circ,\circ)(\circ,\circ,\times)(\circ,\circ,\bullet)\}\,,\ \{(\circ,\circ,\circ)(\circ,\circ,\bullet)(\circ,\circ,\times)\}\ .$$

The corresponding suppression factors are given by 1, ε_5, ε_5 respectively, and are associated with the elements 11, 23, 32 in the matrix M^u.

Now let us consider the first two mass matrices in Eq. (3.15), and ask ourselves wheter we can fit the observed quark masses and mixings with them. As we will show, these matrices are very constrained, and indeed it is possible to see that they are incompatible with a successful CKM matrix.

In order to prove this we can use the following procedure to find the CKM matrix. The symmetric matrices $A^{u,d}$ of Eq. (3.16) can be diagonalised by the matrices $V_{u,d}$

$$A^{u,d}_{\rm diag} = V_{u,d}\ A^{u,d}\ V^T_{u,d}\ , \tag{3.17}$$

The CKM matrix is then

$$V_{\rm CKM} = V_u\ V_d^T\ . \tag{3.18}$$

The matrices $V_{u,d}$ may be thought as a product of three orthogonal rotations [66]. It can be checked that, assuming ε_5 sufficiently small, the quark mass eigenvalues and diagonalization of $A^{u,d}$ can be expanded in series as

$$V_{u,d}\ A^{u,d}\ V^T_{u,d} = \begin{pmatrix} w_{1,2} & 0 & 0 \\ 0 & w_{3,4} & 0 \\ 0 & 0 & w_{5,6} \end{pmatrix} + \mathcal{O}(\varepsilon_5)\ , \tag{3.19}$$

where the matrices V_u and V_d can be expressed as

$$V_u = \begin{pmatrix} 1 & \frac{w_6}{w_3-w_4}\varepsilon_5 & \frac{w_3}{w_2-w_5}\varepsilon_5 \\ -\frac{w_6}{w_2-w_4}\varepsilon_5 & 1 & \frac{w_2}{w_4-w_6}\varepsilon_5 \\ -\frac{w_4}{w_2-w_6}\varepsilon_5 & -\frac{w_2}{w_4-w_6}\varepsilon_5 & 1 \end{pmatrix} + \mathcal{O}(\varepsilon_5^2) \tag{3.20}$$

and

$$V_d = \begin{pmatrix} 1 & \frac{w_5}{w_1-w_3}\varepsilon_5 & \frac{w_3}{w_1-w_5}\varepsilon_5 \\ -\frac{w_5}{w_1-w_3}\varepsilon_5 & 1 & \frac{w_1}{w_3-w_5}\varepsilon_5 \\ -\frac{w_3}{w_1-w_5}\varepsilon_5 & -\frac{w_1}{w_3-w_5}\varepsilon_5 & 1 \end{pmatrix} + \mathcal{O}(\varepsilon_5^2)\,. \tag{3.21}$$

Without FI breaking therefore, the mass hierarchies must be provided entirely by the Higgs VEVs, and we have

$$\begin{aligned} \{w_1,\, w_3,\, w_5\} &\propto \{m_d,\, m_s,\, m_b\}\ , \\ \{w_2,\, w_4,\, w_6\} &\propto \{m_u,\, m_c,\, m_t\}\ . \end{aligned} \tag{3.22}$$

The CKM matrix is then given by

$$V_{\rm CKM} \approx \begin{pmatrix} 1 & \varepsilon_5\left(\frac{m_b}{m_s}-\frac{m_t}{m_c}\right) & \varepsilon_5\left(\frac{m_s}{m_b}-\frac{m_c}{m_t}\right) \\ -\varepsilon_5\left(\frac{m_b}{m_s}-\frac{m_t}{m_c}\right) & 1 & \varepsilon_5\left(\frac{m_d}{m_b}-\frac{m_u}{m_t}\right) \\ -\varepsilon_5\left(\frac{m_s}{m_b}-\frac{m_c}{m_t}\right) & -\varepsilon_5\left(\frac{m_d}{m_b}-\frac{m_u}{m_t}\right) & 1 \end{pmatrix} + O(\varepsilon_5^2)\ . \tag{3.23}$$

From the $V_{\rm CKM}$ matrix elements we can derive those values of ε compatible with a realistic mixing for the quarks. For $(V_{\rm CKM})_{12} \approx 0.22$, a value of $\varepsilon_5 \approx$ can be obtained. However, the rest of the matrix elements are generally not well fitted, leading to the conclusion that the orbifold model considered without the effects of FI breaking fails at the quark mixing stage [66]. In the next section we will see how the presence of the FI mixing can affect the previous results in a crucial way, allowing for the matching of model with the experiment.

3.4 Quark mass matrices and Yukawa couplings after the Fayet-Iliopoulos breaking

As discussed in Chapter 1, the anomalous $U(1)$ of the extended $SU(3) \times SU(2) \times U(1)^n$ gauge group generates a Fayet-Iliopoulos D-term which can in principle break SUSY at energies close to the string scale. This term can be cancelled when scalar fields (C_i), which are singlets under $SU(3) \times SU(2)$, develop large VEVs (10^{16-17} GeV). The VEVs of these fields (c_i), have several important effects. Firstly, they break the original $SU(3) \times SU(2) \times U(1)^n$ gauge group down to the (MS)SM $SU(3) \times SU(2) \times U(1)$. Secondly, they induce very large effective mass terms for many particles (vector-like triplets and doublets, as well as singlets), which thus decouple from the low-energy theory. After the breaking, many particles, which we will refer to as ξ, are expected to acquire a high mass because of the generation of effective mass terms. These come for example from operators of the type $C\xi\xi$. In this way vector-like triplets and doublets and also singlets become heavy and disappear from the low-energy spectrum. Even so, the Standard Model matter remain massless, surviving through certain combinations with other states. Let us consider the simplest example studied in [66], a model with the Yukawa couplings

$$C_1\xi_1 f \ , \quad C_2\xi_1\xi_2 \, , \tag{3.24}$$

where f denotes a Standard Model field, $\xi_{1,2}$ denote two extra matter fields (triplets, doublets or singlets), and $C_{1,2}$ are the fields developing large VEVs denoted by $\langle C_{1,2}\rangle = c_{1,2}$. It is worth noting here that f can be an u^c, d^c, L, ν^c or e^c field, but not a Q field. This is because in these orbifold models no extra (3,2) representations are present, and therefore the Standard Model field Q cannot mix with other representations through Yukawas.

Clearly the 'old' physical particle f will combine with $\xi_{1,2}$. It is now straightforward to diagonalize the mass matrix arising from the mass terms in Eq. (3.24) to find two very massive and one massless combination. The latter is given by

$$f' \equiv \frac{1}{\sqrt{|c_1|^2 + |c_2|^2}} \left(c_2^* f - c_1^* \xi_2\right) \ . \tag{3.25}$$

Notice for example that the mass terms (3.24) can be rewritten as $\sqrt{|c_1|^2 + |c_2|^2}\ \xi_1\xi_2'$, where

$\xi_2' \equiv \frac{1}{\sqrt{|c_1|^2+|c_2|^2}}\,(c_1 f + c_2\xi_2)$. Indeed the unitary combination is the massless field in Eq. (3.25). The Yukawa couplings and hence mass matrices of the effective low energy theory are modified accordingly. For example, consider a model where we begin with a Yukawa coupling HQf. Since we have

$$f = \frac{1}{\sqrt{|c_1|^2+|c_2|^2}}\left(c_2 f' + c_1^*\xi_2'\right)\ , \tag{3.26}$$

then the 'new' coupling (involving the light state) will be

$$\frac{c_2}{\sqrt{|c_1|^2+|c_2|^2}} HQf'\,.$$

The situation in realistic models is more involved since the fields appear in three copies. Thus the mass matrix for the example in Eq.(3.24) is (using the results above)

$$gN(\xi_1^1\ \xi_1^2\ \xi_1^3)\left\{\varepsilon'\begin{pmatrix} c_1^1 & c_1^3\varepsilon_5 & c_1^2\varepsilon_5 \\ c_1^3\varepsilon_5 & c_1^2 & c_1^1\varepsilon_5 \\ c_1^2\varepsilon_5 & c_1^1\varepsilon_5 & c_1^3 \end{pmatrix}\begin{pmatrix} f^1 \\ f^2 \\ f^3 \end{pmatrix} + \varepsilon''\begin{pmatrix} c_2^1 & c_2^3\varepsilon_5 & c_2^2\varepsilon_5 \\ c_2^3\varepsilon_5 & c_2^2 & c_2^1\varepsilon_5 \\ c_2^2\varepsilon_5 & c_2^1\varepsilon_5 & c_2^3 \end{pmatrix}\begin{pmatrix} \xi_2^1 \\ \xi_2^2 \\ \xi_2^3 \end{pmatrix}\right\} \tag{3.27}$$

where $\varepsilon', \varepsilon''$ can take different values

$$\varepsilon', \varepsilon'' \equiv 1\ ,\ \varepsilon_1\ ,\ \varepsilon_3\ ,\ \varepsilon_1\varepsilon_3\ \ , \tag{3.28}$$

depending on the particular case. For example, if the field f corresponds to the down quark with the assignment as in Eq. (3.14), and the fields C_1, C_2, ξ_1, ξ_2 have the assignments for the first two sublattices $(\times\ \circ)$, $(\circ\ \times)$, $(\times\ \circ)$, $(\bullet\ \bullet)$, respectively, then $\varepsilon' = 1$ and $\varepsilon'' = \varepsilon_1\varepsilon_3$.

Now, in order to simplify the analysis, let us consider the following VEVs for the $C_{1,2}^i$ fields[1]

$$\begin{aligned} c_1^1 \equiv c_1\ , \qquad & c_1^2 = c_1^3 = 0\ , \\ c_2^1 = c_2^3 = 0\ , \qquad & c_2^2 \equiv c_2\ . \end{aligned} \tag{3.29}$$

Then Eq. (3.27) gives rise to the mass terms

$$\sqrt{|\hat{c}_1|^2+|\hat{c}_2\varepsilon_5|^2}\ \xi_1^1\xi_2'^1\ +\ \sqrt{|\hat{c}_1\varepsilon_5|^2+|\hat{c}_2|^2}\ \xi_1^2\xi_2'^2\ +\ \varepsilon_5\sqrt{|\hat{c}_1|^2+|\hat{c}_2|^2}\ \xi_1^3\xi_2'^3 \tag{3.30}$$

where

$$\begin{aligned} \xi_2'^1 &\equiv \frac{1}{\sqrt{|\hat{c}_1|^2+|\hat{c}_2\varepsilon_5|^2}}\left(\hat{c}_1 f_1 + \hat{c}_2\varepsilon_5\xi_2^3\right)\ , \\ \xi_2'^2 &\equiv \frac{1}{\sqrt{|\hat{c}_1\varepsilon_5|^2+|\hat{c}_2|^2}}\left(\hat{c}_1\varepsilon_5 f_3 + \hat{c}_2\xi_2^2\right)\ , \\ \xi_2'^3 &\equiv \frac{1}{\sqrt{|\hat{c}_1|^2+|\hat{c}_2|^2}}\left(\hat{c}_1 f_2 + \hat{c}_2\xi_2^1\right)\ , \end{aligned} \tag{3.31}$$

[1] In principle we are allowed to do this since the cancellation of the FI D-term only imposes $\sum_i Q_i^{(a)}(|c_i^1|^2+|c_i^2|^2+|c_i^3|^2) = const$, where $Q_i^{(a)}$ are the charges of the C_i fields under the anomalous $U(1)$, and therefore flat directions arise. As for the T-moduli, these VEVs can eventually be determined dynamically through supersymmetry breaking.

and

$$\hat{c}_1 \equiv \varepsilon' c_1 \quad , \qquad \hat{c}_2 \equiv \varepsilon'' c_2 \; . \tag{3.32}$$

All these effects modify the mass matrices of the low-energy effective theory (see Eq. (3.15)), which, are now given by[2]

$$\begin{aligned} \mathcal{M}^u &= g\, N\, a^{u^c}\, A^u\, B^{u^c} \,, \\ \mathcal{M}^d &= g\, N \varepsilon_1\, a^{d^c}\, A^d\, B^{d^c} \,, \end{aligned} \tag{3.33}$$

where $A^{u,d}$ are the quark mass matrices prior to FI breaking (see Eq. (3.16)), a^f is given by

$$a^f \;=\; \frac{\hat{c}_2^f}{\sqrt{|\hat{c}_1^f|^2 + |\hat{c}_2^f|^2}} \,, \tag{3.34}$$

with $f = u^c, d^c$, and B^f is the diagonal matrix defined as

$$B^f \;=\; \mathrm{diag}\,(\,\beta^f\,\varepsilon_5,\, 1\,, \alpha^f/\varepsilon_5\,)\,. \tag{3.35}$$

Finally

$$\alpha^f = \varepsilon_5 \sqrt{\frac{|\hat{c}_1^f|^2 + |\hat{c}_2^f|^2}{|\hat{c}_1^f \varepsilon_5|^2 + |\hat{c}_2^f|^2}} \,, \qquad \beta^f = \sqrt{\frac{|\hat{c}_1^f|^2 + |\hat{c}_2^f|^2}{|\hat{c}_1^f|^2 + |\hat{c}_2^f \varepsilon_5|^2}} \,. \tag{3.36}$$

In the above, $\hat{c}_i^f$ are derived from the VEVs of the heavy fields responsible for the FI breaking as

$$\hat{c}_1^f \;\equiv\; \varepsilon'^{(f)}\, c_1^f \,, \qquad \hat{c}_2^f \;\equiv\; \varepsilon''^{(f)}\, c_2^f \,, \tag{3.37}$$

where in each case ε' and ε'' can take any of the following values:

$$\varepsilon' \,,\; \varepsilon'' \equiv 1,\, \varepsilon_1,\, \varepsilon_3,\, \varepsilon_1\, \varepsilon_3 \,. \tag{3.38}$$

Let us also stress that one should not take α^f, β^f, ε_5 and a^f as independent parameters. In fact, Eqs. (3.34) and (3.36) imply that

$$a^f \;=\; \frac{\left(1 - \alpha^{f\,2}\right)^{1/2}}{\alpha^f} \, \frac{\varepsilon_5}{\left(1 - \varepsilon_5^2\right)^{1/2}} \;=\; \left(1 - \frac{1}{\beta^{f\,2}}\right)^{1/2} \, \frac{1}{\left(1 - \varepsilon_5^2\right)^{1/2}} \,, \tag{3.39}$$

[2]Note that although the c_i are in general complex VEVs, they only introduce a global and therefore unphysical phase in the mass matrix. More complicated examples would in principle give rise to a contribution to the CP phase [66]. This mechanism to generate the CP phase through the VEVs of the fields cancelling the FI D-term was used first, in the context of non-renormalisable couplings, in Ref. [30]. For a recent analysis, see Ref. [122].

so that for given values of ε_5 and α^f, β^f is fixed as

$$\beta^f \;=\; \frac{1}{\sqrt{1+\varepsilon_5^2\left(1-\frac{1}{\alpha^{f\,2}}\right)}}\,. \tag{3.40}$$

Eqs. (3.33) and (3.35) become more transparent when the terms that encode the flavour structure are explicitly displayed:

$$A^u B^{u^c} = \begin{pmatrix} w_2\,\varepsilon_5\,\beta^{u^c} & w_6\,\varepsilon_5 & w_4\,\alpha^{u^c} \\ w_6\,\varepsilon_5^2\,\beta^{u^c} & w_4 & w_2\,\alpha^{u^c} \\ w_4\,\varepsilon_5^2\,\beta^{u^c} & w_2\,\varepsilon_5 & w_6\,\alpha^{u^c}/\varepsilon_5 \end{pmatrix},\;\; A^d B^{d^c} = \begin{pmatrix} w_1\,\varepsilon_5\,\beta^{d^c} & w_5\,\varepsilon_5 & w_3\,\alpha^{d^c} \\ w_5\,\varepsilon_5^2\,\beta^{d^c} & w_3 & w_1\,\alpha^{d^c} \\ w_3\,\varepsilon_5^2\,\beta^{d^c} & w_1\,\varepsilon_5 & w_5\,\alpha^{d^c}/\varepsilon_5 \end{pmatrix}. \tag{3.41}$$

Given that the mass matrices are related to the Yukawa couplings as

$$\mathcal{M}^u = \sum_{i=2,4,6} w_i\,Y_i^u\,, \qquad \mathcal{M}^d = \sum_{i=1,3,5} w_i\,Y_i^d\,, \tag{3.42}$$

the structure of the Yukawa couplings is easily derived from Eq. (3.41). For the down sector, the latter read:

$$Y_1^d = gN\varepsilon_1 a^{d^c}\begin{pmatrix} \varepsilon_5\,\beta^{d^c} & 0 & 0 \\ 0 & 0 & \alpha^{d^c} \\ 0 & \varepsilon_5 & 0 \end{pmatrix},\quad Y_3^d = gN\varepsilon_1 a^{d^c}\begin{pmatrix} 0 & 0 & \alpha^{d^c} \\ 0 & 1 & 0 \\ \varepsilon_5^2\,\beta^{d^c} & 0 & 0 \end{pmatrix},$$

$$Y_5^d = gN\varepsilon_1 a^{d^c}\begin{pmatrix} 0 & \varepsilon_5 & 0 \\ \varepsilon_5^2\,\beta^{d^c} & 0 & 0 \\ 0 & 0 & \alpha^{d^c}/\varepsilon_5 \end{pmatrix}. \tag{3.43}$$

The Yukawa couplings for the up-type quarks can be also obtained by doing the appropriate replacements: $(\varepsilon_1 a^{d^c}) \to a^{u^c}$ and $\alpha^{d^c}, \beta^{d^c} \to \alpha^{u^c}, \beta^{u^c}$.

Expanding the eigenvalues of the quark mass matrices up to leading order in ε_5, one can derive the following relation[3] for the Higgs VEVs in terms of the quark masses[4] [66]

$$\begin{aligned} \text{down-quarks}:\;\{w_1,w_3,w_5\}\,(gN\,\varepsilon_1\,a^{d^c}) \;&=\; \left\{\frac{1}{\varepsilon_5\beta^{d^c}}\left(m_d+\varepsilon_5^5\frac{m_b^2}{m_s}\right), m_s, \frac{m_b\varepsilon_5}{\alpha^{d^c}}\right\}, \\ \text{up-quarks}:\;\{w_2,w_4,w_6\}\,(gN\,a^{u^c}) \;&=\; \left\{\frac{1}{\varepsilon_5\beta^{u^c}}\left(m_u+\varepsilon_5^5\frac{m_t^2}{m_c}\right), m_c, \frac{m_t\varepsilon_5}{\alpha^{u^c}}\right\}. \end{aligned} \tag{3.44}$$

The most striking effect of the FI breaking is that it enables the reconciliation of the Yukawa couplings predicted by this scenario with experiment. In particular, and as we will see in Section 3.5.1, the quark spectra and a successful CKM matrix can now be accommodated.

[3] Regarding quark mixing, it is also possible to obtain analytical expressions (up to second order in ε_5) for the several CKM matrix elements, as done in Ref. [66].

[4] Notice that there is a misprint in these equations in Ref. [66], where in the corresponding version of Eq. (3.44) the factor ε_5^5 appeared as ε_5^2.

3.4.1 Electroweak symmetry breaking and the orbifold parameter space

In addition to the hierarchy constraint imposed by the observed pattern of quark masses, the VEVs must further comply with other constraints as those arising from electroweak symmetry breaking:

$$w_1^2 + w_2^2 + w_3^2 + w_4^2 + w_5^2 + w_6^2 = 2\,M_Z^2/(g^2 + g'^2) \approx (174\ \text{GeV})^2\,. \tag{3.45}$$

In particular, we have that

$$\begin{aligned}&\frac{1}{(gNa^{u^c})^2}\left[\frac{1}{(\varepsilon_5\beta^{u^c})^2}\left(m_u + \varepsilon_5^5\frac{m_t^2}{m_c}\right)^2 + m_c^2 + \left(\frac{m_t\varepsilon_5}{\alpha^{u^c}}\right)^2\right] + \\ &\frac{1}{(gN\varepsilon_1 a^{d^c})^2}\left[\frac{1}{(\varepsilon_5\beta^{d^c})^2}\left(m_d + \varepsilon_5^5\frac{m_b^2}{m_s}\right)^2 + m_s^2 + \left(\frac{m_b\varepsilon_5}{\alpha^{d^c}}\right)^2\right] \approx (174\,\text{GeV})^2\,.\end{aligned} \tag{3.46}$$

We notice that the above condition can always be fulfilled since the quark Yukawa matrix prefactors, ε_1 and gN, have not yet been used. At this point, let us introduce a generalised definition for $\tan\beta$:

$$\tan\beta \;=\; \frac{v_u}{v_d} \;\equiv\; \frac{\sqrt{w_2^2 + w_4^2 + w_6^2}}{\sqrt{w_1^2 + w_3^2 + w_5^2}}\,. \tag{3.47}$$

Using Eq. (3.44), Eq. (3.47) can be rewritten as

$$\tan\beta \;=\; \varepsilon_1\frac{a^{d^c}}{a^{u^c}}\sqrt{\frac{\frac{1}{(\varepsilon_5\beta^{u^c})^2}\left(m_u + \varepsilon_5^5\frac{m_t^2}{m_c}\right)^2 + m_c^2 + \left(\frac{m_t\varepsilon_5}{\alpha^{u^c}}\right)^2}{\frac{1}{(\varepsilon_5\beta^{d^c})^2}\left(m_d + \varepsilon_5^5\frac{m_b^2}{m_s}\right)^2 + m_s^2 + \left(\frac{m_b\varepsilon_5}{\alpha^{d^c}}\right)^2}}\,. \tag{3.48}$$

From the above equation it becomes manifest that by considering a given value for $\tan\beta$ we are implicitly defining ε_1, for fixed values of ε_5 and α^f. This in turn implies that according to Eq. (3.46), $g\,N$ is in fact a function of $\tan\beta$, ε_5 and α^f, and its value, $g\,N \approx 1$, suffers tiny fluctuations (of order 1% - 10%) in order to accommodate the correct electroweak symmetry breaking. The latter statements become more transparent noticing that by bringing together Eqs. (3.46) and (3.48), one can derive useful relations that allow to express gN and ε_1 as a function of the quark masses and orbifold parameters for a given value[5] of $\tan\beta$:

$$gN = \frac{1}{a^{u^c}}\,\frac{\left(1+\tan^2\beta\right)^{1/2}}{\tan\beta}\,\frac{\sqrt{\frac{1}{(\varepsilon_5\beta^{u^c})^2}\left(m_u + \varepsilon_5^5\frac{m_t^2}{m_c}\right)^2 + m_c^2 + \left(\frac{m_t\varepsilon_5}{\alpha^{u^c}}\right)^2}}{174\,\text{GeV}}\,,$$

$$\varepsilon_1 gN = \frac{1}{a^{d^c}}\left(1+\tan^2\beta\right)^{1/2}\,\frac{\sqrt{\frac{1}{(\varepsilon_5\beta^{d^c})^2}\left(m_d + \varepsilon_5^5\frac{m_b^2}{m_s}\right)^2 + m_s^2 + \left(\frac{m_b\varepsilon_5}{\alpha^{d^c}}\right)^2}}{174\,\text{GeV}}\,. \tag{3.49}$$

[5]Whenever referring to a parameter whose value was estimated using the electroweak symmetry breaking conditions, and which is a function of $\tan\beta$, we will use the designation "EWSB fit".

The first equality of Eq. (3.49) provides a clear insight to understanding the smallness of the fluctuations of $g\,N$. Assuming the limit where $\alpha^{u^c}, \varepsilon_5 \ll 1$, $a^{u^c} \sim \varepsilon_5/\alpha^{u^c}$, so that $g\,N \approx m_t/(174$ GeV).

It is also important to comment on the relative size of the VEVs $\hat{c}_1$ and $\hat{c}_2$. From the definition of a^f (Eq. (3.34)) we can derive an additional relation

$$|c_1^f| \,=\, \frac{\varepsilon''^{(f)}}{\varepsilon'^{(f)}} \sqrt{\frac{1-a^{f\,2}}{a^{f\,2}}}\, |c_2^f|\,, \tag{3.50}$$

where we have used the definitions of Eqs. (3.37) and (3.38). If, for example, one assumes the VEVs to be of the same order of magnitude, i.e. $c_1 \sim c_2$, then one should further ensure that

$$\frac{\varepsilon''^{(f)}}{\varepsilon'^{(f)}} \sqrt{\frac{1-a^{f\,2}}{a^{f\,2}}} \,\sim 1\,. \tag{3.51}$$

To conclude this section, let us make a few remarks regarding two topics so far not discussed. Firstly, and since it is well known that the CP symmetry is not conserved in nature, it is important to comment on the sources of CP violation present in this class of models. The Yukawa couplings have been defined through real quantities, so that no physical phase appears via the CKM mechanism. However, this need not be the most general scenario. Dismissing for the present time the possibility of spontaneous CP violation, associated with non-trivial phases of the Higgs VEVs, there still remains another source of CP violation, in addition to the one already mentioned in footnote 2. Should the VEV of the moduli field have a phase, then CP (which is a gauge symmetry of the model) would be spontaneously broken at very high energies. The phases would be fed into ε_i (thus also appearing in α^f), and would be present in the Yukawa couplings. Therefore, in the low-energy theory, CP would be explicitly violated via the usual CKM mechanism [123, 124].

It is also relevant to mention the effect of the renormalisation group equations (RGE) on the mass matrices presented in this section. The flavour structure of Eqs. (3.33) and (3.41) is associated with a mechanism taking place at a very high energy scale. However, and given the clearly hierarchical structure of the quark mass matrices, one does not expect that RGE running will significantly affect the predictions of the model.

3.5 Numerical results

In the present scenario, most of the observables addressed in the previous section receive their dominant contributions from tree-level processes. This situation strongly diverges from the usual scenarios of both SM and MSSM, where FCNCs only occur at the 1-loop level. Given

the increasing experimental accuracy, it is important to investigate to which extent the present scenario is compatible with current experimental data.

We divide the numerical approach in two steps. Firstly, we focus on the string sector of the model, and for each point in the space generated by the free parameters of the orbifold $(\varepsilon_5, \alpha^f)$, we derive the up- and down-quark mass matrices[6] and compute the CKM matrix. This procedure allows us to investigate the several regimes of parameters that translate into viable quark spectra, and discuss the implications of the relations between the several parameters. At this early stage, we consider only real values for the orbifold parameters. Further imposing the conditions associated to electroweak symmetry breaking given in Eq. (3.46), and fixing a value[7] for $\tan\beta$, one can then determine the values of $g\,N$ and ε_1 (cf. Eqs. (3.48) and (3.49)). Another possible approach would be to scan over the space generated by the moduli (T_i) and the VEVs of the $SU(3)\times SU(2)$ singlet fields (c_i), but this would translate in less straightforward relations between the orbifold parameters and the experimental data. A secondary step requires specifying the several Higgs parameters, which must obey the minimum criteria of Eqs. (2.22 and 2.23). Finally, the last step comprehends the analysis of how each of the Yukawa patterns constrains the Higgs parameters in order to have compatibility with the FCNC data. In particular, we want to investigate how heavy the scalar and pseudoscalar eigenstates are required to be in order to accommodate the observed values of Δm_K, Δm_{B_d}, etc.

3.5.1 Quark Yukawa couplings and the CKM matrix

As discussed in [66], there are three regimes for the values of α^f and β^f, depending on the specific orbifold configuration :

(a) $\alpha^f \sim \varepsilon_5$ and $\beta^f \sim 1$;

(b) $\alpha^f \approx \varepsilon_5$ and $\beta^f \approx 1/\varepsilon_5$;

(c) $\alpha^f \sim 1$ and $\beta^f \sim 1$.

In any case, it is clear from Eq. (3.36) that α^f and β^f must obey, by construction, the following bounds:

$$\varepsilon_5 \lesssim \alpha^f \lesssim 1\,, \qquad 1 \lesssim \beta^f \lesssim \frac{1}{\varepsilon_5}\,. \tag{3.52}$$

In what follows we investigate whether each point in the orbifold parameter space can be associated with a consistent quark spectrum and mixings. For given values of the input quark masses,

[6] It is worth emphasising here that the quark masses appearing in Eq. (3.44) (and in all subsequent relations) are used on the sole purpose of obtaining an approximate determination of the VEVs. Afterwards, the actual values of m_{q_i} are exactly computed.

[7] We recall here that $\tan\beta$ is a necessary parameter to specify the Higgs sector, which in turn is mandatory to investigate the issue of FCNCs in the present model.

Set	m_u	m_d	m_c	m_s	m_t	m_b
A	0.004	0.008	1.35	0.13	180	4.4
B	0.0035	0.008	1.25	0.1	178	4.5
C	0.0035	0.004	1.15	0.08	176	4.1
D	0.004	0.006	1.2	0.105	178	4.25

Table 3.1: Sets of input quark masses (in GeV) used in the numerical analysis.

one fixes the ratio of the several Higgs VEVs, which in turn allows to reconstruct the full quark mass matrices, and obtain the mass eigenstates and CKM matrix. In particular, throughout this analysis we shall focus on four sets of input quark masses, whose values are listed in Table 3.1.

Throughout, we require the CKM matrix elements to lie within the following ranges [82]:

$$V_{\rm CKM} = \begin{pmatrix} 0.9739 - 0.9751 & 0.221 - 0.227 & 0.0029 - 0.0045 \\ 0.221 - 0.227 & 0.9730 - 0.9744 & 0.039 - 0.044 \\ 0.0048 - 0.014 & 0.037 - 0.043 & 0.9990 - 0.9992 \end{pmatrix} . \tag{3.53}$$

Regarding the effect of the orbifold parameters on quark mixing, let us notice that both ε_5 and α^{u^c} are crucial in obtaining the Cabibbo angle. As expected, the down-sector parameters are those directly responsible for the mixings between generations, and their role is particularly relevant in determining V_{td} (α^{d^c} - and to a lesser extent, also α^{u^c}), V_{ts}, V_{ub} and V_{cb}. Once these elements are fixed in accordance with experiment, the others are usually also in agreement. Finally, let us recall that from choosing a concrete value for $\tan\beta$, and complying with the bound on M_Z from electroweak symmetry breaking, Eqs. (3.46) and (3.48), one is implicitly fixing for each set of $\{\varepsilon_5, \alpha^f, \beta^f\}$, the values of ε_1 and $g\,N$.

In Fig. 3.2, we present the correlation between the orbifold parameters, for the four sets of input quark masses given in Table 3.1. We only present points that are associated with viable quark masses and that are in agreement with current bounds on $|V_{\rm CKM}|$ (from Eq. (3.53)). Rather than scatter plots, in Fig. 3.2 we present sets of points. This is due to having very narrow intervals of fluctuation for all the parameters. As an example, let us mention that for constant values of ε_5, α^{d^c} and β^f, α^{u^c} is fixed within a 2% interval. From Fig. 3.2 it is clear that for a given set of Higgs VEVs (determined by the associated set of input quark masses - Table 3.1) the allowed orbifold parameter space is very constrained. This is a direct consequence of the increasing accuracy in the experimental determination of the $V_{\rm CKM}$. In each set (A–D), moving outside the displayed ranges would translate in violating the experimental bounds on (at least) one of the CKM matrix elements. Larger values of ε_5 would also (typically) be associated

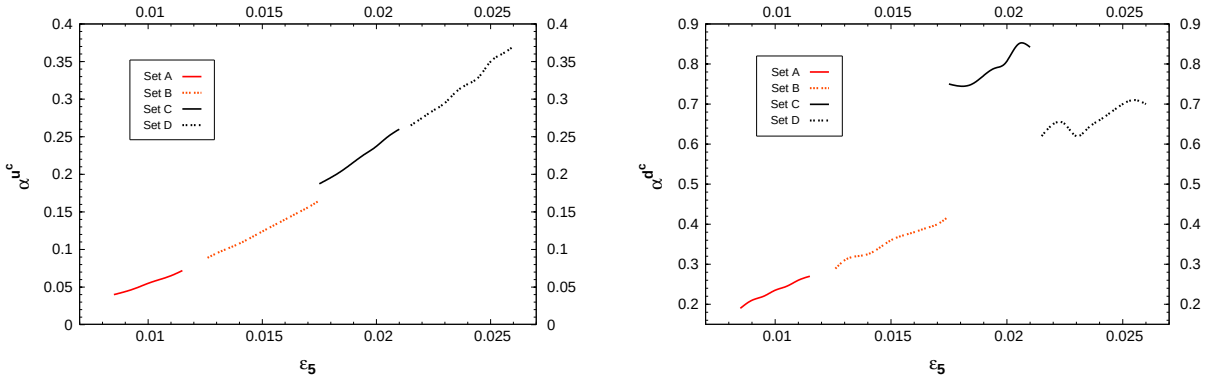

Figure 3.2: Correlation between the orbifold parameters (α^{u^c}, ε_5) and (α^{d^c}, ε_5), for distinct sets of input quark masses, A-D (red full lines, red dashed lines, full black and dashed black lines, respectively).

with an up-quark mass below the current accepted range. Regarding the values of β^f, these are constrained to be $\beta^f \approx 1$ throughout the allowed parameter space (cf. Eq. (3.40)). From the direct inspection of Fig. 3.2, together with the fact that $\beta^f \approx 1$, it appears that at least two regimes for α^f are present. For the up sector, one would suggest that the orbifold configuration is such that α^{u^c} is roughly $\mathcal{O}(\varepsilon_5)$, so that one is faced with regime (a). The same would happen for sets A and B in the down sector, although sets C and D appear to favour a regime with $\alpha^{d^c} \sim 1$, thus suggesting regime (c).

Let us now aim at understanding the behaviour of both α^{u^c,d^c} as a function of ε_5. In Ref. [66], several analytical relations for the CKM matrix elements as a function of $\{\varepsilon_5, \alpha^f, \beta^f\}$ were derived. Although those relations were computed for the case of hermitic mass matrices, where $V_L^f = V_R^f$, and are thus not truly valid for the present case, they are quite useful in understanding Fig. 3.2. For instance, the Cabibbo angle is given, to a very good approximation, by

$$V_{us} \approx -\varepsilon_5^2 \left(\frac{m_t}{m_c} \frac{1}{\alpha^{u^c}} - \frac{m_b}{m_s} \frac{1}{\alpha^{d^c}} \right) , \tag{3.54}$$

and the above expression is clearly dominated by the first term on the right-hand side (r.h.s). From Eq. (3.54), it becomes transparent that the dependence of α^{u^c} on ε_5 should indeed be parabolic, as clearly displayed in Fig. 3.2. Regarding α^{d^c}, its evolution is strongly influenced by the allowed regions of ε_5 (as dictated by the quark mass regimes taken as input, especially m_s/m_b). For sets A and B, the ratio of down-type quark masses is such that the leading term

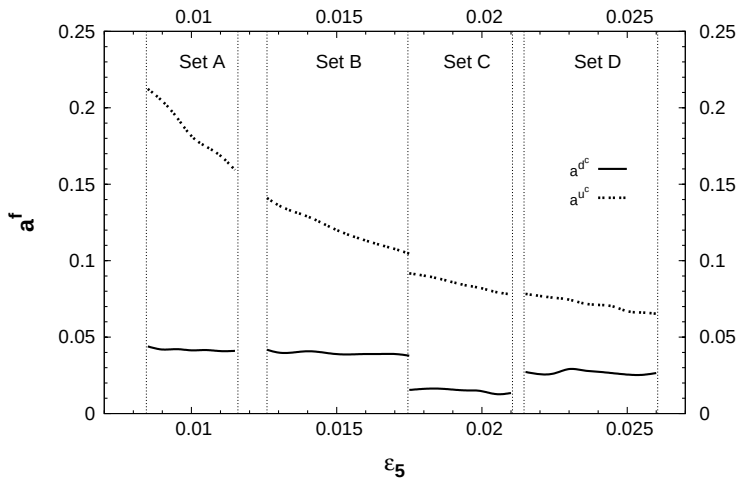

Figure 3.3: Values of a^{d^c} and a^{u^c} (full and dashed lines, respectively) as a function of ε_5. Vertical dotted lines isolate the ranges of ε_5 associated with each set A-D.

in the analytical expression of V_{ub},

$$V_{ub} \approx \left(\frac{m_s}{m_b}\alpha^{d^c} - \frac{m_c}{m_t}\alpha^{u^c}\right) - \varepsilon_5 \left(\frac{m_d}{m_b}\frac{m_t}{m_c}\frac{\alpha^{d^c}}{\alpha^{u^c}\beta^{d^c}} - \frac{m_u}{m_t}\frac{1}{\beta^{u^c}}\right) + \mathcal{O}(\varepsilon_5^6)\,, \tag{3.55}$$

provides a reasonable understanding of $\alpha^{d^c}(\varepsilon_5)$. For sets C and D, the situation is more involved, and the second term on the r.h.s. of Eq. (3.55) plays an important role. In fact, α^{d^c} receives contributions which display a near-resonant behaviour for the input quark mass ratios in the correspondent ε_5 range. This is the origin of the unexpected positioning of set C in Fig. 3.2. We now address the behaviour of a^{u^c} and a^{d^c}. By construction, and as clearly seen from Eq. (3.39), once ε_5 and α^f (or equivalently ε_5 and β^f) are set, one is implicitly fixing a^f. Moreover, satisfying the electroweak symmetry breaking conditions for the VEVs, together with imposing a given value of $\tan\beta$ also translates in determining $g\,N$ and ε_1. In Fig. 3.3, we plot the values of a^{u^c} and a^{d^c} as a function of ε_5, as determined from Eq. (3.39).

As seen from Fig. 3.3, the behaviour of set C regarding a^{d^c} is slightly misaligned with what one would expect from the analysis of sets A, B and D. Notice however that this is due to the dependence of a^{d^c} on α^{d^c} (cf. Eq. (3.39)). Recall from Fig. 3.2 that for set C, the allowed values of α^{d^c} were somewhat higher than for the other cases, and this is the source of the suppression displayed in Fig. 3.3, set C.

In Fig. 3.4, we present the values of ε_1 as a function of ε_5 for the four sets of quark masses, and distinct regimes of $\tan\beta$. From Fig. 3.4 we can also verify that the values of ε_1 are, in general, larger than those of ε_5. The "misaligned" behaviour of set C is again a consequence of

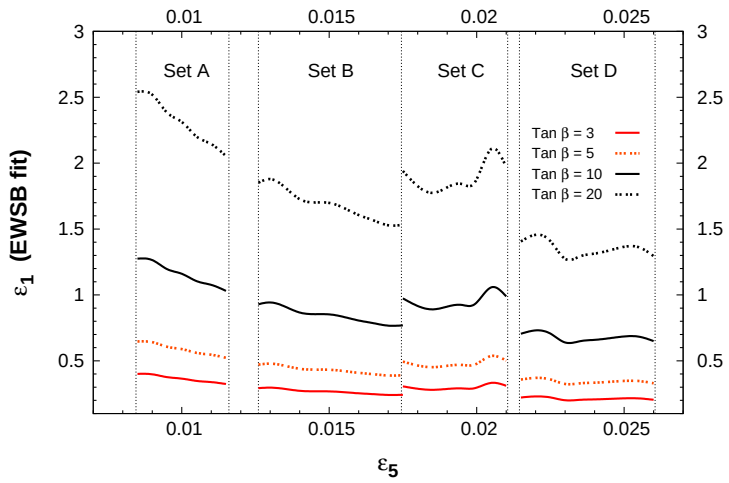

Figure 3.4: ε_1 as a function of ε_5 for $\tan\beta$ =3, 5, 10 and 20 (red full lines, red dashed lines, full black and dashed black lines, respectively). Vertical dotted lines isolate the ranges of ε_5 associated with each set A-D.

the effects already discussed. Regarding the actual value of $g\,N$ it suffices to mention that for the orbifold parameter space here investigated, and for the values of $\tan\beta$ here selected, one has $1.03 \lesssim g\,N \lesssim 1.16$.

Since we now have the relevant information, we can further compute the value of the lattice's diagonal moduli, T_1 and T_5, as defined in Eq. (3.10). The value of T_5 is unambiguously determined. Nevertheless, and since the determination of ε_1 is a direct consequence of complying with the electroweak symmetry breaking conditions for a fixed value of $\tan\beta$, its determination varies accordingly. In Fig. 3.5 we display the diagonal moduli as a function of ε_5, for $\tan\beta$ =3, 5, 10 and 20. From Fig. 3.5, it is manifest that for the parameter space investigated, the values of the diagonal moduli, T_1 and T_5, are never degenerate. This confirms our original assumption that distinct moduli are indeed required to accommodate the experimental data. Although we have allowed for non-degenerate T_i, this remains quite a restrictive choice. We recall that we still have six additional degrees of freedom, namely the angles between the complex planes, which we have taken as zero in the present analysis.

To conclude the study of the orbifold parameter space, let us just plot the values of the Higgs VEVs, again as a function of ε_5. As an illustrative example, depicted in Fig. 3.6, we take $\tan\beta = 5$. It is interesting to comment that in the up-sector, the VEVs exhibit a clearly hierarchical pattern, $w_2 < w_4 < w_6$ while in the down-type VEVs we encounter a not so definite pattern, with $w_3 < w_5 < w_1$. This is a direct consequence of the relations given in Eq. (3.44).

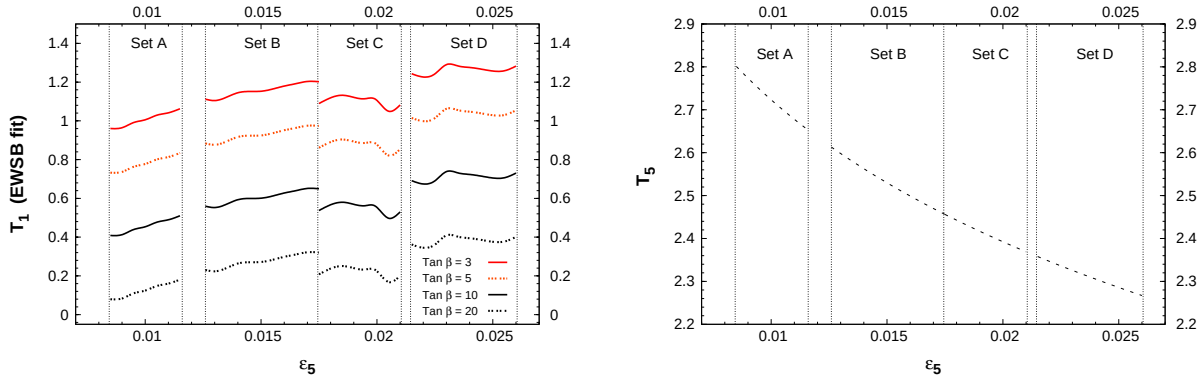

Figure 3.5: Diagonal lattice moduli, T_1 (left) and T_5 (right), as a function of ε_5. For the case of T_1, we plot it for several values of $\tan\beta$ =3, 5, 10 and 20 (following the line and colour scheme of Fig. 3.4). For T_5 the dotted line denotes the prediction of the orbifold.

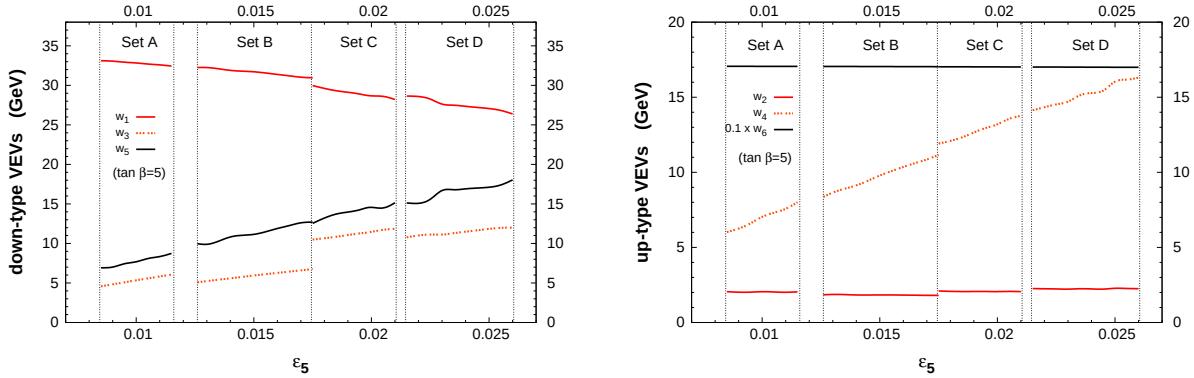

Figure 3.6: Down- and up-type Higgs VEVs, $w_{1,3,5}$ and $w_{2,4,6}$, as a function of ε_5, for $\tan\beta$ =5. For convenience, we plot $w_6/10$. As before, vertical dotted lines isolate the ranges of ε_5 associated with each set A-D.

Finally, let us summarise our analysis of the orbifold parameter space by commenting on the relative number of input parameters and number of observables fitted. Working with the six Higgs VEVs (w_i), and the orbifold parameters ε_1, ε_5, α^{u^c} and α^{d^c}, one can obtain the correct electroweak symmetry breaking (M_Z), as well as the correct quark masses and mixings (six masses and three mixing angles).

3.5.2 Tree-level FCNCs in neutral mesons

The present orbifold model does not include a specific prediction regarding the Higgs sector. For instance, we have no hint regarding the value of the several bilinear terms, nor towards their origin. Concerning the soft breaking terms, the situation is identical. Since the FI D-term, which could have broken SUSY at the string scale, was cancelled, one must call upon some other mechanism to ensure that supersymmetry is indeed broken in the low-energy theory. In the absence of further information, we merely assume that the structure of the soft breaking terms is as in Eq. (2.20), taking the Higgs soft breaking masses and the $B\mu$-terms as free parameters (provided that the electroweak symmetry breaking and minimisation conditions are verified).

Before proceeding, it is important to stress that the Higgs spectrum (i.e. the scalar and pseudoscalar physical masses) cannot be a direct input when investigating the occurrence of FCNCs. In some previous studies of FCNCs in multi-Higgs doublets models (see for example [49]) the bounds were derived for the diagonal entries in the scalar and pseudoscalar mass matrices. However, this approach neglects mixings between the several fields R_i, I_i, and excludes the exchange of some scalar and pseudoscalar states.

Although it is possible to begin the analysis from the original basis (where all neutral Higgses develop VEVs), we prefer to define the Higgs parameters on the Higgs-basis, relying on the minima conditions (and associated inequalities) to ensure that we are on the presence of true minima. Therefore, the parameters that must be specified are:

$$\tan\beta\,, \quad m_{ij}^2\,, \quad b_{ij}\,, \tag{3.56}$$

entering in Eqs. (2.22 and 2.23). In the absence of orbifold predictions for the Higgs sector parameters, and motivated by an argument of simplicity, we begin our analysis by considering textures for the above parameters as simple as possible.

To avoid rewriting the Higgs soft-breaking masses, we adopt the following parameterisation:

$$m_{ij}^{(d)} = \begin{pmatrix} \otimes & \otimes & \otimes \\ \otimes & x_3 & y \\ \otimes & y & x_5 \end{pmatrix} \times 1\text{TeV}\,, \quad m_{kl}^{(u)} = \begin{pmatrix} \otimes & \otimes & \otimes \\ \otimes & x_4 & y \\ \otimes & y & x_6 \end{pmatrix} \times 1\text{TeV}\,, \quad \sqrt{b_{ij}} = b \times 1\text{TeV}\,. \tag{3.57}$$

In the above, $m^{d(u)}$ should be understood as the $i,j = 1,3,5$ ($k,l = 2,4,6$) submatrices of the 6×6 matrix that encodes the rotated soft-breaking Higgs masses in the Higgs basis (see [52]). The symbol $\otimes$ denotes an entry which is fixed by the minima equations of Eq. (2.22 and 2.23). This parametrisation allows to easily define the Higgs sector via six dimensionless parameters. We begin by taking a near-universality limit for the Higgs-sector textures introduced in Eq. (3.57).

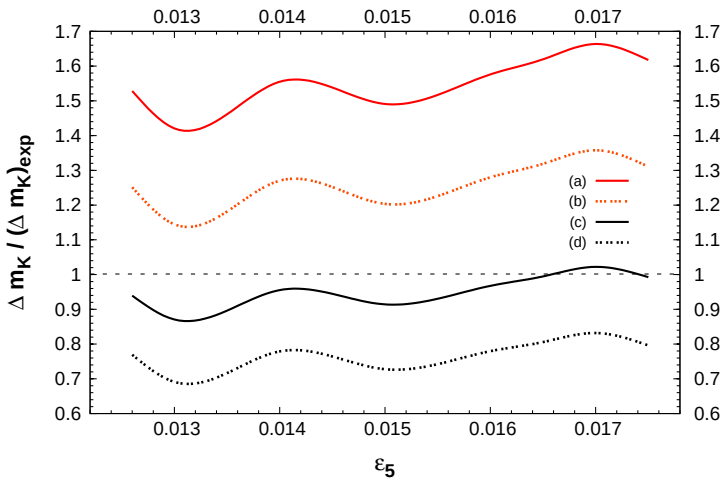

Figure 3.7: $\Delta m_K/(\Delta m_K)_{\rm exp}$ as a function of ε_5 for set B and $\tan\beta = 5$. The Higgs parameters correspond to textures (a)-(d).

Regarding the value of $\tan\beta$, and if not otherwise stated, we shall take $\tan\beta = 5$ in the subsequent analysis. We first consider the following four cases, presenting the associated scalar and pseudoscalar Higgs spectra:

(a) $x_3 = x_4 = 0.5\,, x_5 = x_6 = 0.75\,, y = 0.1\,, b = 0.1$

$m^s = \{82.5, 190.6, 493.9, 515.9, 744.4, 760.2\}$ GeV ;

$m^p = \{186.8, 493.9, 515.9, 744.4, 760.2\}$ GeV .

(b) $x_3 = x_4 = 0.4\,, x_5 = x_6 = 0.8, y = 0.15\,, b = 0.2$

$m^s = \{84.6, 213.9, 387.4, 560.8, 785.9, 879.1\}$ GeV ;

$m^p = \{215.2, 387.3, 560.5, 785.9, 878.9\}$ GeV .

(c) $x_3 = x_4 = 0.75\,, x_5 = x_6 = 1, y = 0.25\,, b = 0.2$

$m^s = \{83.6, 292.9, 733.6, 785.9, 987.6, 1057.0\}$ GeV ;

$m^p = \{291.1, 733.6, 785.9, 987.6, 1057.0\}$ GeV .

(d) $x_3 = x_4 = 0.3\,, x_5 = x_6 = 0.8, y = 0.1\,, b = 0.1$

$m^s = \{79.4, 121.5, 296.9, 354.3, 794.6, 808.8\}$ GeV ;

$m^p = \{114.8, 296.9, 353.7, 794.6, 808.8\}$ GeV .

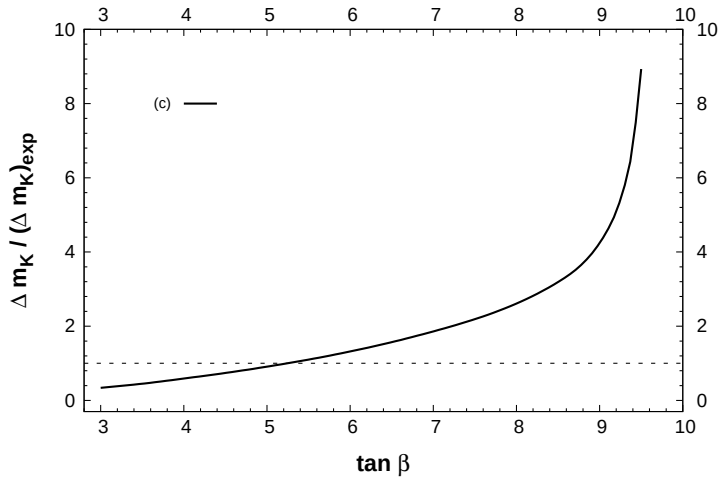

Figure 3.8: $\Delta m_K/(\Delta m_K)_{\rm exp}$ as a function of $\tan\beta$ for set B. The Higgs parameters correspond to texture (c).

In Fig. 3.7 we plot the ratio $\Delta m_K/(\Delta m_K)_{\rm exp}$ versus ε_5, for cases (a)-(d). We considered $\tan\beta = 5$ and, since the other sets of input quark masses were in general associated to smaller FCNC effects, we take the quarks masses as in "set B" (Table 3.1). Once again, all the points displayed comply with the bounds from the CKM matrix. From Fig. 3.7 it is clear that it is quite easy for the orbifold model to accommodate the current experimental values for Δm_K. Even though the model presents the possibility of important tree-level contributions to the kaon mass difference, all the textures considered give rise to contributions very close to the experimental value. Although (a) and (b) are not in agreement with the measured value of Δm_K, their contribution is within order of magnitude of $(\Delta m_K)_{\rm exp}$. As seen from Fig. 3.7, with a considerably light Higgs spectrum (i.e. $m_{h_i^0} < 1$ TeV), one is safely below the experimental bound, as exhibited by cases (c) and (d). This is not entirely unexpected given the strongly hierarchical structure of the Yukawa couplings (notice from Eq. (3.43) that Y^d_{21} is suppressed by ε_5^2).

One important aspect clearly manifest in Fig. 3.7, and which has been overlooked in some previous analyses, is that the Higgs mixings can be as relevant as the Higgs eigenvalues in determining the contributions to Δm_K. This is patent in the comparison of curves (c) and (d). From a naïve inspection of the Higgs spectra associated to each case, one would expect that (c) would induce a much stronger suppression to the model's contribution to Δm_K. Nevertheless, case (d), with a spectrum quite similar to case (b), and indeed much lighter than that of (d), but with much smaller mixings, is the one associated with the strongest suppression of Δm_K. It is also important to comment on the effect of changing $\tan\beta$ regarding the contributions to the

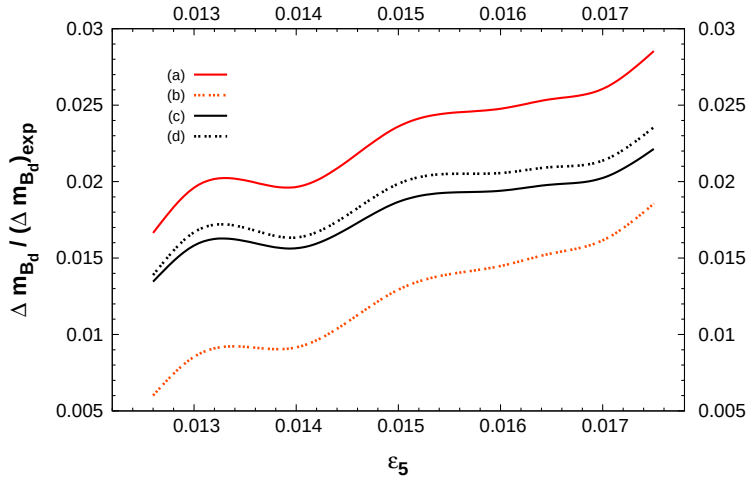

Figure 3.9: $\Delta m_{B_d}/(\Delta m_{B_d})_{\rm exp}$ as a function of ε_5 for set B and $\tan\beta = 5$. The Higgs parameters correspond to textures (a)-(d).

kaon mass difference. For the specific case of texture (c), let us investigate the effect of varying $\tan\beta$. We take the quark masses as in set B, and while keeping the Higgs parameters fixed, $\tan\beta$ is taken in the range $3 \lesssim \tan\beta \lesssim 9.5$. As it becomes clear from Fig. 3.8, larger values of $\tan\beta$ produce increasingly larger contributions to Δm_K. This is a direct consequence of the fact that, due to larger off-diagonal terms in the Higgs mass matrices, the mixing is larger, and the corresponding eigenstates become lighter. Even though the masses of the heaviest states remain stable, the intermediate states become lighter, and the FCNC contributions are less suppressed. Close to $\tan\beta$=10, it is no longer possible to find physical minima of the Higgs potential, and tachyonic states emerge. This effect has been already pointed out in the general analysis of [52].

B_d and B_s meson mass difference

For the several parameterisations of the Higgs sector used for the analysis of Δm_K, we display in Fig. 3.9 the contributions of Higgs textures (a)-(d) to the B_d mass difference. As one would expect, given the structure of the mass matrices (and thus the Yukawa couplings), the present model generates very small contributions to Δm_{B_d}. All the textures analysed, even those associated with excessive contributions to Δm_K are in good agreement with the experimental data on the B_d mass difference. Notice that the behaviour of the textures is now quite distinct: as an example, texture (b), which generated the second largest contribution to the Δm_K is now the one associated with the strongest suppression. This stems from the fact that the leading

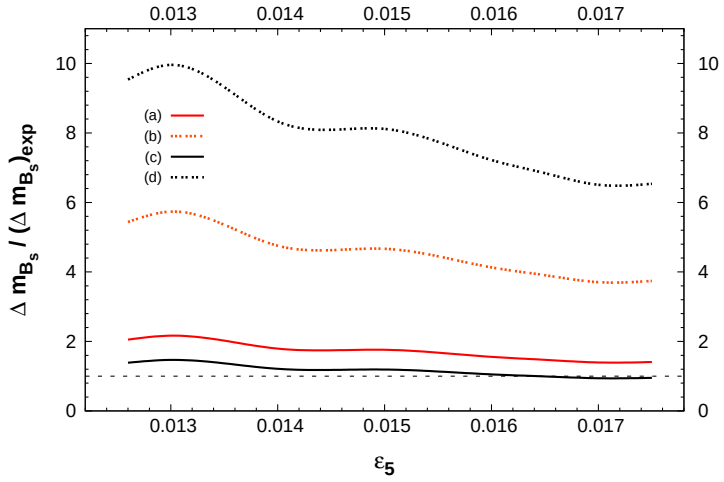

Figure 3.10: $\Delta m_{B_s}/(\Delta m_{B_s})_{\rm exp}$ as a function of ε_5 for set B and $\tan\beta = 5$. The Higgs parameters correspond to textures (a)-(d).

contributions are now given by distinct Higgses, whose couplings to the quarks need not be identical.

Likewise, in Fig. 3.10 we plot the contributions to the B_s mass difference. In this case experiment only provides a lower bound, so that any ratio larger than 1 is in agreement with current data. As we would expect from the discussion of Section 2.4, this model's contributions to Δm_{B_s} are well above the current limit.

$D^0 - \bar{D}^0$ mass difference

The cases (a)-(d) considered in the previous subsections generate contributions to Δm_D that exceed the experimental bounds by at least a factor 10. As discussed in Section 2.4, this is not surprising, nor excessively worrying. Nevertheless, and for the sake of completing the analysis, let us consider four additional Higgs patterns, in order to derive a bound on the mass of the heaviest Higgs boson that would render the model compatible with the data from the D^0 sector.

The new Higgs textures are defined as follows:

(e) $x_3 = x_4 = 0.75\,, x_5 = 2.5\,, x_6 = 7.5\,, y = 0.5\,, b = 0.5$

$m^s = \{84.2, 672.7, 704.9, 1414, 2573, 7501\}$ GeV ;

$m^p = \{673.1, 704.9, 1414, 2573, 7501\}$ GeV .

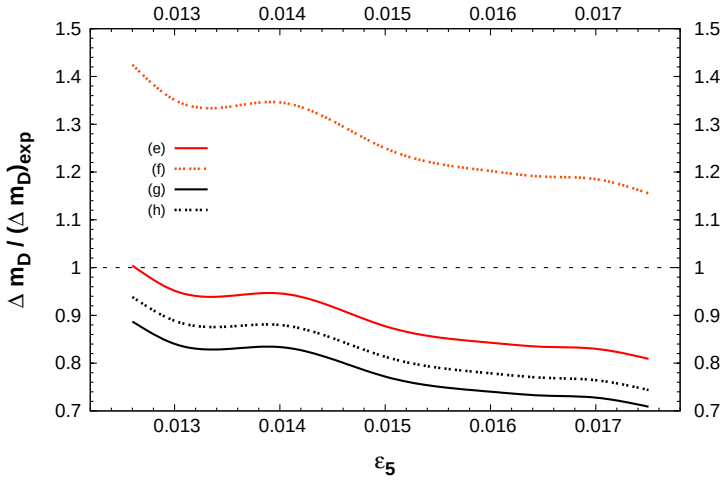

Figure 3.11: $\Delta m_D/(\Delta m_D)_{\rm exp}$ as a function of ε_5 for set B and $\tan\beta = 5$. The Higgs parameters correspond to textures (e)-(h).

(f) $x_3 = x_4 = 0.5\,, x_5 = 5\,, x_6 = 7.5\,, y = 0.5\,, b = 0.1$

$m^s = \{82.7, 201.4, 492.4, 516.4, 5000, 7500\}$ GeV ;

$m^p = \{197.9, 492.4, 516.4, 5000, 7500\}$ GeV .

(g) $x_3 = x_4 = 1\,, x_5 = x_6 = 7.5\,, y = 0.5\,, b = 0.5$

$m^s = \{82.3, 378.5, 958.9, 1578, 7483, 7518\}$ GeV ;

$m^p = \{379.2, 958.9, 1578, 7484, 7518\}$ GeV .

(h) $x_3 = x_4 = 3\,, x_5 = x_6 = 7\,, y = 1\,, b = 0.5$

$m^s = \{84.1, 1032, 2964, 3059, 6984, 7022\}$ GeV ;

$m^p = \{1031, 2964, 3059, 6984, 7022\}$ GeV .

For the cases (e) to (h) we present in Fig. 3.11 the contributions to Δm_D. Compatibility with experiment can be obtained for any of the sets (e), (g) or (h), thus suggesting that one of the Higgses (a state mostly dominated by an up-type Higgs field) must be at least of around 7.5 TeV. Notice that no major hierarchy is required from the Higgs spectrum - case (e) is an excellent example of the latter statement, in the sense that one obtains states softly ranging from 600 to 7500 GeV. One may wonder if such a choice of Higgs soft-breaking terms may lead to a fine-tuning problem. In [52], it was pointed out that for non-degenerate VEVs, soft-breaking terms above the few TeV range typically induced a fine tuning stronger than 1%. Nevertheless,

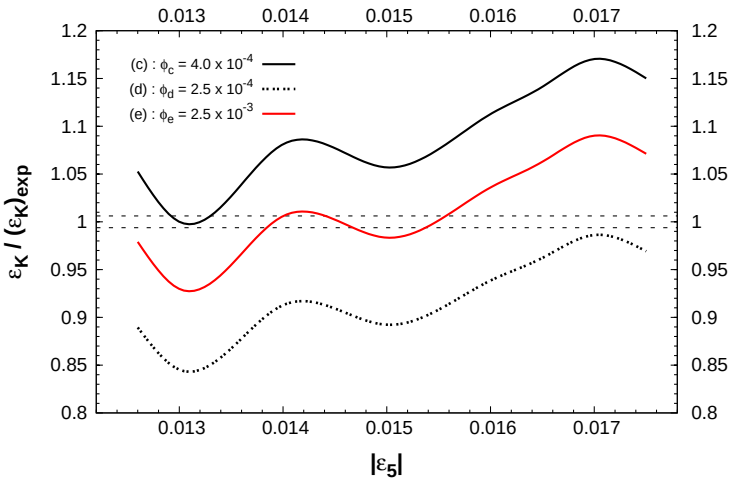

Figure 3.12: $\varepsilon_K/(\varepsilon_K)_{\rm exp}$ as a function of $|\varepsilon_5|$ for set B and $\tan\beta = 5$. The Higgs parameters correspond to textures (c)-(e).

we again stress that these values for the Higgs masses (as derived from the D^0 mass difference analysis) should not be interpreted from a very strict point of view.

3.5.3 Tree-level CP violation: ε_K

Finally, we turn our attention to the issue of CP violation. So far, we have seen that accommodating the several $\Delta F = 2$ observables is not an excessively hard task (especially if we choose to set aside the D^0 sector). Nevertheless, a successful model of particle physics must also comply with the observed CP violation in the kaon sector. As we mentioned in Section 2.4, we will only consider the specific contribution of the present model to indirect CP violation in the kaon sector (ε_K). Therefore, we now assume ε_5 (and thus α^f) to be a complex quantity, and parameterise it as $\varepsilon_5 = |\varepsilon_5|\, e^{i\phi}$.

In Fig. 3.12 we present the tree-level contributions to ε_K (normalised by its experimental value) as a function of $|\varepsilon_5|$. We take the input quark masses as in set B, fix $\tan\beta = 5$, and analyse the Higgs textures associated with cases (c), (d) and (e). For each texture, the phase is assumed to be $\phi_c = 4.0 \times 10^{-4}$, $\phi_d = 2.5 \times 10^{-4}$ and $\phi_e = 2.5 \times 10^{-3}$. These phases are taken as illustrative examples; we choose values that for a specific set of input quark masses (set B, in this case) and a given Higgs texture (c)-(e) simultaneously succeed in generating an amount of ε_K close to the value experimentally measured (range delimited by dotted grey lines in Fig. 3.12), and still have a compatible CKM. One should bare in mind that once $\arg\varepsilon_5$ (and thus

$\arg \alpha^f$) is no longer a small number, it will significantly affect the computation of the Yukawa couplings, and thus the CKM matrix. We have considered one texture that accommodates all FCNC observables, namely texture (e), which already has a somewhat heavy Higgs spectrum. In this case, the phase required to saturate $(\varepsilon_K)_{\rm exp}$ is $\mathcal{O}(10^{-3})$. Since we do not wish to view the D^0 sector as a very stringent constraint, we also consider two other Higgs patterns, (c) and (d), which only succeed in complying with both kaon and B-meson data. In these cases, the phases necessary to obtain $(\varepsilon_K)_{\rm exp}$ are now $\mathcal{O}(10^{-4})$, as one would expect, since a lighter set of Higgs bosons typically enhances the contributions.

In the range of parameters analysed in this plot, the amount of CP violation stemming from the CKM matrix is $J_{CP} \sim \mathcal{O}(10^{-8} - 10^{-6})$, i.e. at least one order of magnitude below the SM value that is associated with the observed ε_K [82]. The possibility of obtaining an orbifold configuration that saturates the observed value of ε_K and at the same time allows to reproduce the J_{CP} required by the unitarity triangle fits should not be discarded. It is clear that the phase of ε_5 must be quite large, and such values would push us to distinct areas of the orbifold parameter space. It is worth emphasising that there are still other sources of CP violation in addition to the one we have studied in this section. As mentioned in footnote 2, a more complicated choice of the VEVs c_i could lead to physical phases in the quark masses matrices, which would in turn contribute to the physical CKM phase.

3.6 Conclusions

In this chapter we have investigated whether it is possible to find abelian Z_3 orbifold configurations associated with an experimentally viable low-energy scenario.

Orbifolds provide a beautiful geometric mechanism for the generation of the fermion mass hierarchy. The Yukawa couplings are explicitly calculable, and thus a solution to the elusive flavour problem of the SM and MSSM can be explored. We have concentrated here in Z_3 orbifold compactifications with two Wilson lines, which naturally include three families for fermions and Higgses. The fact that additional Yukawas are present opens the possibility of obtaining realistic fermion masses and mixings, entirely at the renormalisable level.

Our analysis here has been a phenomenological "bottom-up" one [66]. That is the particles were assigned to fixed points in a way that can reproduce the experimental data. In addition the scheme relies on the mixing between fields due to the FI breaking. We have not completed a full analysis of minimising the potential along D- and F- flat directions after the breaking, but we have made use of the very general features that such a minimization should have, namely mixing of the would-be MSSM fields with other singlet, doublet and triplet fields that couple to heavy fields [24, 25]. Under these assumptions, we have successfully reproduced the observed

pattern of quark masses and mixings. Let us remark, however, that this severely constrains the orbifold parameters.

On the other hand, having six Higgs doublets (and thus six quark Yukawa couplings) poses the potential problem of having tree-level FCNCs. By assuming simple textures for the Higgs free parameters, we have verified that the experimental data on the neutral kaon mass difference, as well as on Δm_{B_d} and Δm_{B_s} can be easily accommodated for a quite light Higgs spectra, namely $m_{h_i^0} \lesssim 1$ TeV. The data from the D^0 sector proves to be a more difficult challenge, requiring a Higgs spectrum of at least 7 TeV, but we again stress that, in view of the theoretical and experimental uncertainties associated with the D^0 sector, this constraint should not be over-emphasised.

CP violation can be also embedded into the low-energy theory. Although CP is a gauge symmetry of the full theory, it can be spontaneously broken at the string scale, if the VEVs of the moduli have a non-vanishing phase. We have parameterised these effects by assuming the presence of a phase in ε_5, and we have verified that one can also obtain a value for ε_K in agreement with current experimental data.

Z_3 orbifold compactifications with two Wilson lines are equally predictive regarding the lepton sector. This analysis, especially that of the neutrino sector, will be addressed in the next chapter.

Chapter 4

Lepton masses and mixings in Z_3 scenarios with three Higgs families

4.1 Introduction

In Chapter 3 we addressed the phenomenology of the Higgs and quark sectors of Z_3 models with two Wilson lines. We have verified that quark masses and mixings can be reproduced, and that dangerous tree-level FCNC contributions in the neutral K-, B- and D-sectors can be avoided by a fairly light Higgs spectrum. It is worth recalling that, after fitting the quark data, the free parameters defining the orbifold geometry are already very constrained.

In this chapter we complete our previous analyses, by investigating whether or not the Z_3 orbifolds can also succeed in accommodating present data [82] on charged lepton masses, while avoiding conflict with the most relevant lepton flavour violating processes at the tree-level, such as three-body decays.

With the whole orbifold parameter space completely constrained by the obtention of quark and lepton masses, we will comment on the implications of the phenomenologically derived constraints in the properties of the compact space and its effect on the value of the heterotic gauge coupling constant.

In addition, we will study the viability of orbifold scenarios to comply with experimental data on neutrino mass squared differences and mixing angles [87–89, 129]. The analysis of the latter turns out to be particularly challenging. Let us note that the experimental observation of neutrino oscillations has led to extend the SM in order to accommodate non-vanishing neutrino masses. In the absence of a predictive theory for the Yukawa couplings, it is only common to argue that purely Dirac neutrinos pose a naturalness problem, in the sense that the associated couplings are extremely tiny. Moreover, and contrary to what is observed in the quark sector,

the leptonic mixing, parameterised by the Maki-Nagakawa-Sakata matrix, $U_{\rm MNS}$ [130, 131], is nearly maximal. As we will see, Z_3 orbifolds offer a variety of possibilities to account for the generation of neutrino masses and mixings, ranging from a purely Dirac formulation, to several implementations of a type-I seesaw mechanism [132]. Here we will argue on the viability of each possibility.

4.2 Charged leptons

As mentioned in the Introduction, the previous analysis [53] of the orbifold parameter space has already severely constrained the free parameters of the orbifold. As discussed, we have verified that one could successfully reproduce the observed hierarchy and mixings in the quark sector, and avoid potentially dangerous tree-level FCNCs with a fairly light Higgs boson spectrum. In what follows, we extend our analysis to the lepton sector. In this section we address how reproducing the charged lepton masses further constrains the orbifold parameters, and also discuss possible tree-level lepton flavour violation, arising from the exchange of neutral Higgses.

4.2.1 Charged lepton masses

We start by considering the mass matrix for the charged leptons, which after FI breaking is given by[1]

$$\mathcal{M}^e \;=\; g\,N\,\epsilon_3\,a^L\,a^{e^c}\,B^L\,A^d\,B^{e^c} \;=\; g\,N\,\epsilon_3\,a^L\,a^{e^c}\,\begin{pmatrix} v_1\,\varepsilon_5^2\,\beta^L\,\beta^{e^c} & v_5\,\varepsilon_5^2\,\beta^L & v_3\,\epsilon_5\,\alpha^{e^c}\,\beta^L \\ v_5\,\varepsilon_5^2\,\beta^{e^c} & v_3 & v_1\,\alpha^{e^c} \\ v_3\,\varepsilon_5\,\alpha^L\,\beta^{e^c} & v_1\,\alpha^L & v_5\,\alpha^L\,\alpha^{e^c}/\varepsilon_5^2 \end{pmatrix}, \quad (4.1)$$

where A^d, a^{L,e^c} and B^{L,e^c} have been defined in Eqs. (3.16, 3.34-3.36), setting $f = L, e^c$. The next step in the analysis is to determine whether one can find regions of the parameter space where the charged lepton masses can be obtained. We recall that most of the variables appearing in Eq. (4.1), namely g, N, ε_5 and the Higgs VEVs w_i are also related to the quark sector of the model, and are thus already tightly constrained [53]. We consider the quark input sets studied in Ref. [53], used to fix the six Higgs VEVs, and which correctly reproduce the correct mass

[1] Note that the expression for the matrix $\mathcal{M}^e$ in Eq. (4.1) corrects the misprint in Ref. [66], Eq. (69), where the matrix product was taken in the order ABB. A similar correction for neutrino masses will be subsequently taken into account in Eqs. (4.19) and (4.29).

spectrum for both the up- and down-quarks $\{m_u,\, m_d,\, m_c,\, m_s,\, m_t,\, m_b\}$:

$$\text{SET A} = \{0.0040,\, 0.008,\, 1.35,\, 0.130,\, 180,\, 4.40\}\ \text{GeV}, \tag{4.2}$$

$$\text{SET B} = \{0.0035,\, 0.008,\, 1.25,\, 0.100,\, 178,\, 4.50\}\ \text{GeV}, \tag{4.3}$$

$$\text{SET C} = \{0.0035,\, 0.004,\, 1.15,\, 0.080,\, 176,\, 4.10\}\ \text{GeV}, \tag{4.4}$$

$$\text{SET D} = \{0.0040,\, 0.006,\, 1.20,\, 0.105,\, 178,\, 4.25\}\ \text{GeV}, \tag{4.5}$$

and scan over the ε_5, α^{u^c} and α^{d^c} intervals compatible with realistic quark masses and mixings,

$$0.0085 \,\leq\, \varepsilon_5 \,\leq\, 0.0260\,, \qquad 0.040 \,\leq\, \alpha^{u^c} \,\leq 0.370\,, \qquad 0.190 \,\leq\, \alpha^{d^c} \,\leq\, 0.842\,, \tag{4.6}$$

The value of $\tan\beta$, which is also crucial, is tightly related to ε_1 [53]. From the previous values, and employing Eqs. (3.44), (2.17) and (2.18), we can also derive the value of gN, which is obtained from the following expression:

$$g\,N = \frac{1}{a^{u^c}}\,\frac{\left(1+\tan^2\beta\right)^{1/2}}{\tan\beta}\,\frac{\sqrt{\frac{1}{(\varepsilon_5\,\beta^{u^c})^2}\left(m_u+\varepsilon_5^5\frac{m_t^2}{m_c}\right)^2+m_c^2+\left(\frac{m_t\,\varepsilon_5}{\alpha^{u^c}}\right)^2}}{174\,\text{GeV}}\,. \tag{4.7}$$

Thus, once the several orbifold parameters are determined, one can derive information on the intrinsic orbifold properties, such as the value of the orbifold normalisation constant N, or the heterotic coupling constant g. The numerical analysis of this subsection is instrumental in obtaining the latter information.

Having set the quark parameters and choosing $\tan\beta = 5$ as an example, we proceed to determine ε_3, α^L, and α^{e^c}. These values will in turn allow to derive the mass matrix for the charged leptons. In agreement with experimental data [82], the latter eigenvalues should be

$$\{m_e,\, m_\mu,\, m_\tau\} = \{0.511,\, 105.41,\, 1778.45\}\ \text{MeV}. \tag{4.8}$$

In Figures 4.1 and 4.2 we present the values of α^{L,e^c} and a^{L,e^c} giving rise to the correct masses for both the quark and the charged-lepton sectors. The scan over ε_5 has been conducted for the four quark sets in Eqs. (4.2-4.5). We can see that the behaviour of α^{L,e^c} is completely analogous to what had been observed for the quark sector [53], which is not unexpected, given that the Yukawa couplings for the charged leptons closely follow those of the down-type quarks.

Let us comment on the suppression factor ε_3. As seen from Eq. (4.1), ε_3 is a global factor in the charged-lepton mass matrix. This allows its value to be modified without affecting the mass eigenstates, provided that $\tan\beta$ (i.e. the ratio of the Higgs VEVs) is accordingly changed. In other words, $\tan\beta$ is still an unconstrained degree of freedom, a fact that is particularly useful for the analysis involving the Higgs sector (as discussed in [52]). In Figure 4.3 we display the relation between ε_3 and ε_5 for four different values of $\tan\beta$. It is worth mentioning here that,

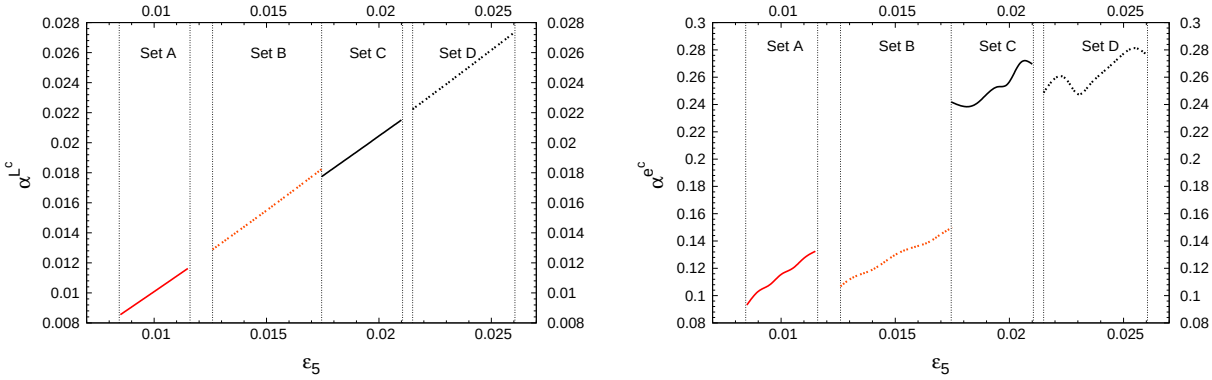

Figure 4.1: Correlation between the orbifold parameters $(\alpha^{L^c}, \varepsilon_5)$ and $(\alpha^{e^c}, \varepsilon_5)$, for $\tan\beta = 5$ and the distinct sets of input quark masses, A-D (red full lines, red dashed lines, full black and dashed black lines, respectively).

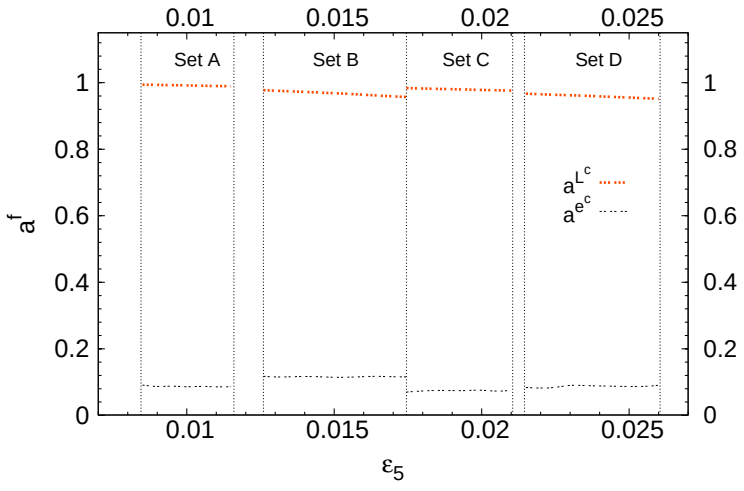

Figure 4.2: Correlation between the orbifold parameters a^{L^c}, a^{e^c} and ε_5, for the quark sets A-D and $\tan\beta = 5$.

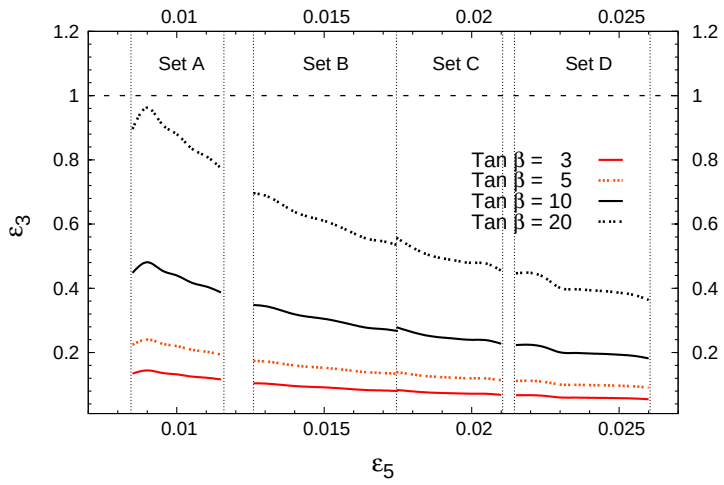

Figure 4.3: Correlation between ε_3 and ε_5 for different values of $\tan\beta$.

given a particular quark input set, the value of $\tan\beta$ is bounded from above in order to avoid $\varepsilon_3 > 1$. For example, for set A this bound is close to $\tan\beta = 20$. In fact, and as already noticed in the study of the quark sector, the phenomenological viability of these orbifold constructions favours lower values of $\tan\beta$ (not only based on reproducing a viable spectrum, but also related with avoiding excessive FCNCs).

Not only can the quantities ε_i be understood as suppression factors which affect the Yukawa couplings (providing the desired mass hierarchy between fermions), but they are also subject to perturbativity constraints. Concerning the latter, for example ε_3 is actually given by [66]

$$\varepsilon_3 \;=\; 3\,e^{-\frac{2\pi}{3}T_3}(1+6\,e^{-2\pi T_1}+6\,e^{-2\pi T_5}+...) \;\approx\; 3\,e^{-\frac{2\pi}{3}T_3}\,, \tag{4.9}$$

where the last approximation corresponds to the assumption of Eq. (3.12). Clearly, if ε_i are in general large, T_i have to be small, and therefore perturbativity is spoiled. Under the approximation of Eq. (3.12), one can write

$$T_i \;=\; -\frac{3}{2\,\pi}\,\ln\frac{\varepsilon_i}{3}\,, \tag{4.10}$$

and, as a consequence, we verify that ε_i cannot be larger than 3, since the T_i VEVs are proportional to R_i^2, and therefore positive. From the analysis of the orbifold parameters, one can obtain useful information about the high-energy configuration of the string model, namely the size and properties of the compact space, as well as its relation with the gauge unification scale. The allowed regimes for the three T_i and their physical implications will be studied in detail in Section 4.3.

4.2.2 Tree-level lepton flavour violation

Identical to what occurs for the quark sector, having a model with Higgs family replication opens the possibility of tree-level FCNCs in the lepton sector, contrary to what occurs in the SM or in the MSSM. Given the fact that flavour-violating interactions are very suppressed in Nature, one should ensure that the present model does not induce excessively large contributions to these processes. In a general multi-Higgs model, it is widely recognised that the most stringent bounds arise from the smallness of the masses of the long- and short-lived neutral kaons. It has been previously verified [53] that for a relatively light Higgs boson spectrum of order $\sim 1-5$ TeV, the present orbifold model is in very good agreement with experimental data. The analysis was also extended to the B- and D-meson systems, leading to similar bounds for the Higgs masses. With the inclusion of the charged lepton sector in our analysis, it is only natural to expect dangerous lepton flavour-violating interactions. Regarding these interactions, here we have focused on the branching ratios (BRs) of pure leptonic decays of the type $l_i \to 3l_j$, which have been identified in the literature as the less suppressed processes [46, 47]. In the context of the present orbifold model, these decays are going to be generated by Yukawa interactions mediated by neutral Higgs bosons[2]. As shown in recent studies of LFV in SUSY models with one Higgs family [133–135], the one-loop contributions to flavour violating processes can be extremely large for sizable values of $\tan\beta$ and a Higgs mass of order 100 -150 GeV. In our case, and as will be shortly confirmed, the requirement that the Higgs bosons are heavy enough to suppress the dangerous quark FCNC interactions indeed ensures that the leptonic processes remain several orders of magnitude below the respective experimental bounds.

In order to study the occurrence of tree-level LFV in the charged-lepton sector we consider the branching ratios of three-body decays, $l_i \to 3l_j$, mediated by a neutral physical Higgs eigenstate (φ_k). The transition amplitudes and BRs of these processes are then given by

$$\Gamma(l_i \to 3l_j|\varphi_k) = \frac{|\mathcal{Y}^k_{ji}|^2\,|\mathcal{Y}^k_{jj}|^2}{128\,m^4_{\varphi_k}}\,\frac{m^5_{l_i}}{192\,\pi^3} \qquad \mathrm{BR}(l_i \to 3l_j|\varphi_k) = \frac{1}{128\,G_F^2}\,\frac{|\mathcal{Y}^k_{ji}|^2\,|\mathcal{Y}^k_{jj}|^2}{m^4_{\varphi_k}}\,, \quad (4.11)$$

where m_l is the lepton mass, m_{φ_k} the mass of the mediating scalar/pseudoscalar neutral Higgs, and $\mathcal{Y}^k_{ij}$ is the i,j element of the Yukawa coupling matrix, in the physical mass-eigenstate basis, defined as

$$\mathcal{Y}^k_{ij} = (S^\dagger)_{kl}\,(V^e_R\,Y^e_l\,V^{e\dagger}_L)_{ij}\,. \quad (4.12)$$

In the above, the Higgs physical states are related to the original interaction eigenstates by $\varphi_k = S_{kl}\,h^0_l$, where h^0_l are the neutral components of the Higgs doublets (see Eq. (2.1)). V^e_R and $V^{e\dagger}_L$ are the matrices which diagonalise the charged-lepton mass matrix, and Y^e_l (with $l = 1, 2, 3$)

[2]We stress here that there are no tree-level contributions to other LFV processes, like radiative decays of the type $l_i \to l_j\gamma$, which only occur at one-loop level.

are the three charged-lepton Yukawa matrices associated to the down-type Higgses, as shown in Eq. (2.2). Using the above expressions, we can now compute the contributions of the full Higgs spectrum (six scalars and five pseudoscalars) to the LFV decays. To do so, we choose three distinct Higgs mass textures, already considered in a previous study [53]. Working in the Higgs basis (see Chapter 2, Section 2.2) these can be summarily defined via the following parametrisation, which allows to define the Higgs sector via six dimensionless parameters as

$$m_{ij}^{(d)} = \begin{pmatrix} \otimes & \otimes & \otimes \\ \otimes & x_3 & y \\ \otimes & y & x_5 \end{pmatrix} \times 1\text{TeV}\,, \quad m_{kl}^{(u)} = \begin{pmatrix} \otimes & \otimes & \otimes \\ \otimes & x_4 & y \\ \otimes & y & x_6 \end{pmatrix} \times 1\text{TeV}\,, \quad \sqrt{b_{ij}} = b \times 1\text{TeV}\,. \tag{4.13}$$

In the above, $m_{ij}^{d(u)}$ should be understood as the $i,j = 1,3,5$ ($k,l = 2,4,6$) submatrices of the 6×6 matrix that encodes the rotated soft-breaking Higgs masses in the Higgs basis (see [52]). The symbol $\otimes$ denotes an entry which is fixed by the minima conditions of Eqs. (2.22, 2.23). For the Yukawa matrices, we will employ the quark Set A of Eq. (4.2) and those values of ε_5, α^{L^c} and α^{e^c} compatible with realistic masses for the charged leptons (as analysed in Section 4.2). Other sets for the quark masses will lead to similar results. For simplicity, we will take a near-universality limit for the Higgs-sector textures introduced in Eq. (4.13). Regarding the value of $\tan\beta$, and unless otherwise stated, we shall take $\tan\beta = 5$ in the subsequent analysis. We consider the following cases, with the associated tree-level scalar and pseudoscalar Higgs spectra:

(1) $x_3 = x_4 = 0.5\,, x_5 = x_6 = 0.75\,, y = 0.1\,, b = 0.1$
$m^s = \{82.5, 190.6, 493.9, 515.9, 744.4, 760.2\}$ GeV ;
$m^p = \{186.8, 493.9, 515.9, 744.4, 760.2\}$ GeV .

(2) $x_3 = x_4 = 0.75\,, x_5 = x_6 = 1, y = 0.25\,, b = 0.2$
$m^s = \{83.6, 292.9, 733.6, 785.9, 987.6, 1057.0\}$ GeV ;
$m^p = \{291.1, 733.6, 785.9, 987.6, 1057.0\}$ GeV .

(3) $x_3 = x_4 = 0.5\,, x_5 = 5\,, x_6 = 7.5, y = 0.5\,, b = 0.1$
$m^s = \{82.7, 201.4, 492.4, 516.4, 5000, 7500\}$ GeV ;
$m^p = \{197.9, 492.4, 516.4, 5000, 7500\}$ GeV .

In the above, m^s and m^p respectively denote the values for the physical scalar and pseudoscalar masses. The results for the decays $\mu \to 3e$, $\tau \to 3\mu$ and $\tau \to 3e$ are summarised in Figs. 4.4, 4.5 and 4.6. From the latter, we immediately observe that the Higgs-mediated contributions to the $l_i \to 3l_j$ branching ratios always lie several orders of magnitude below the experimental limits (collected in Table 4.1). This occurs even for Texture (1), associated with a spectrum containing only light (below 1 TeV) Higgs particles.

LFV process	Present bound	Future sensitivity
$\mathrm{BR}(\mu \to 3\,e)$	1.0×10^{-12}	10^{-13}
$\mathrm{BR}(\tau \to 3\,e)$	2.0×10^{-7}	10^{-8}
$\mathrm{BR}(\tau \to 3\,\mu)$	1.9×10^{-7}	10^{-8}

Table 4.1: Present bounds and future sensitivities for the LFV processes [136–138].

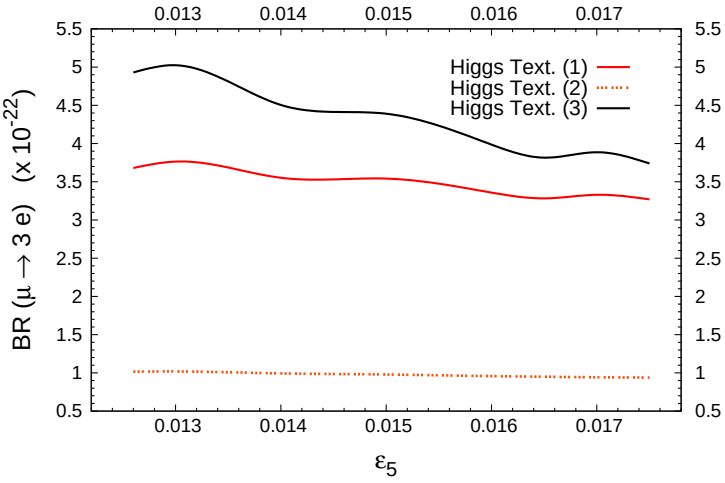

Figure 4.4: BRs for the Higgs-mediated $\mu \to 3e$ decay as a function of ε_5, for quark set A and Textures (1-3).

Regarding other relevant LFV processes, as for example leptonic conversion processes in heavy nuclei, which could in principle also receive important tree-level contributions, we have not discussed them here, as these conversion processes are always assumed to be of the same order or even sub-dominant with respect to the leptonic decays (see, for example, [46], [47] or [139]). The extremely low contribution to the purely leptonic decays previously studied (between 5-10 orders of magnitude below the present experimental bounds) renders the impact of these LFV processes clearly negligible, when compared to the flavour-changing processes occurring in the quark sector.

4.3 Orbifold analysis at the string scale

With the full determination of the quark and charged-lepton sectors we are now ready to address the implications of imposing phenomenological viability at the string level. As previously discussed, the characterisation of the orbifold model is tightly related to the determination of

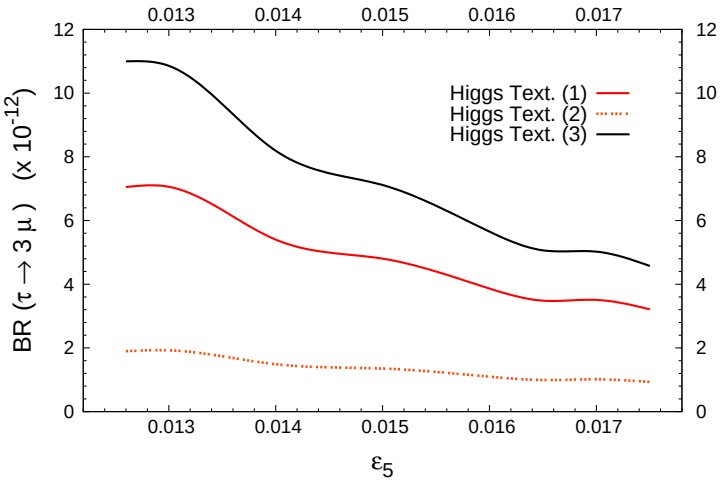

Figure 4.5: BRs for the Higgs-mediated $\tau \to 3\mu$ decay as a function of ε_5, for quark set A and Textures (1-3).

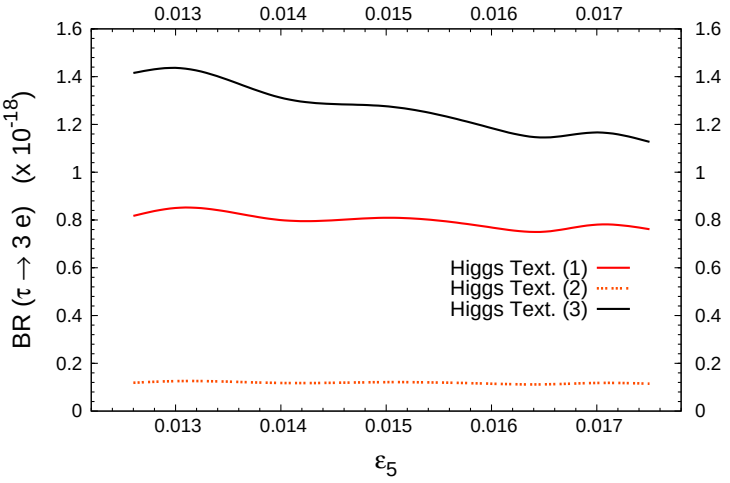

Figure 4.6: BRs for the Higgs-mediated $\tau \to 3e$ decay as a function of ε_5, for quark set A and Textures (1-3).

the geometrical suppression factors, ε_i, which in turn are instrumental in complying with the different fermion mass hierarchies. As we will discuss in Section 4.4, ε_i will further affect the neutrino Yukawa couplings, with an important impact on the seesaw scale. At this point, it is also relevant to mention that we will not take into account the effect of the renormalisation group equations (RGE) on the quark and lepton mass matrices presented in the previous sections. The flavour structure for the masses is associated with a mechanism taking place at a very high energy scale. However, and given the clearly hierarchical structure of the mass matrices, one does not expect that RGE running will significantly affect the predictions of the model.

In this section, we briefly comment on the information about the shape and size of the compact space, and also discuss the hints on the gauge properties of the string model, which can be inferred from the already constrained values of ε_i.

Let us firstly consider the value of the product of the heterotic coupling constant, g, by the orbifold normalisation constant N, defined in Eq. (4.7). The normalisation constant is given by

$$N \,=\, \sqrt{V}\,\frac{3^{3/4}}{8\,\pi^3}\,\frac{\Gamma^6(\frac{2}{3})}{\Gamma^3(\frac{1}{3})}\,. \tag{4.14}$$

In the latter, V denotes the volume of the unit cell of the Z_3 lattice,

$$V \,=\, (R_1\,R_3\,R_5)^2\,\left(\sin\frac{2\,\pi}{3}\right)^3 \tag{4.15}$$

where $R_{1,3,5}$ are the unit cell radii in each sublattice, defined in terms of the three T-moduli as

$$R_i \,=\, \frac{4\,\pi}{3^{1/4}}\,\sqrt{\mathrm{Re}\,T_i}\,. \tag{4.16}$$

From Eq. (4.7), taking only the dominant terms into account, we can verify that the assumption of $g\,N \,\approx 1$ [66] is indeed valid for values of ε_5, $\alpha^{u^c} \ll 1$ and $\tan\beta \geq 3$, since

$$g\,N \,\approx\, \frac{\varepsilon_5}{\alpha^{u^c}\,a^{u^c}}\,\frac{(1+\tan^2\beta)^{1/2}}{\tan\beta}\,\frac{m_t}{174\,\mathrm{GeV}} \,\approx\, \frac{(1-\varepsilon_5)^{1/2}}{(1-\alpha^{u^c})^{1/2}} \,\approx\, 1\,, \tag{4.17}$$

where we have used the relation between the orbifold parameters given by Eq. (3.39). In Fig. 3.5 we display (as presented in Ref. [53]) the diagonal moduli T_1 and T_5 for different values of $\tan\beta$. In Figure 4.8 we show the correlation between those values of the moduli T_3 compatible with correct charged-lepton masses and ε_5, for different values of $\tan\beta$. From all plots we are led to verify that $T_i \sim 1$, implying that the sizes of the radii in each orbifold sublattice are comparable and of order

$$R_i \,\approx\, \frac{4\,\pi}{3^{1/4}} \,\approx\, 10\,. \tag{4.18}$$

As it was previously shown in Section 4.2.1, Eq. (4.10), the upper bound for the suppression factors ε_i is 3, above which the moduli are no longer a positive quantity. In the case of T_1 and

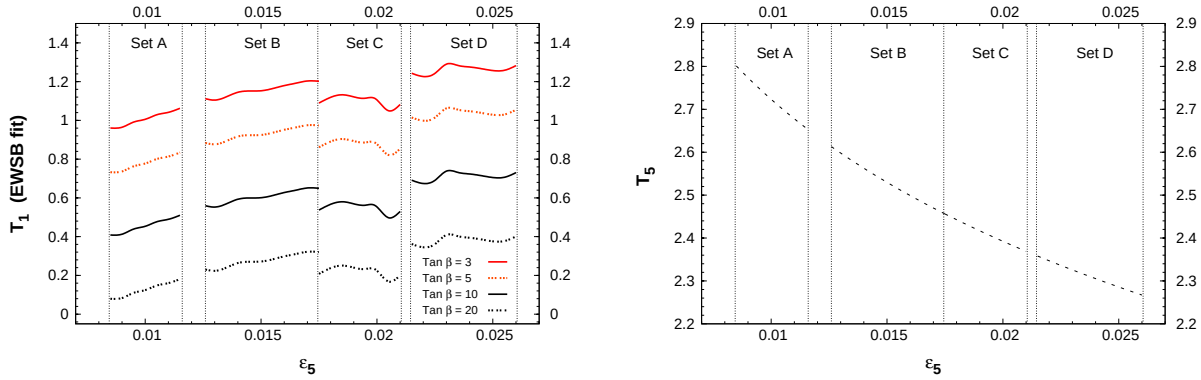

Figure 4.7: Diagonal lattice moduli, T_1 (left) and T_5 (right), as a function of ε_5 [53]. For the case of T_1, we consider several values of $\tan\beta$ =3, 5, 10 and 20. For T_5 the dotted line denotes the prediction of the orbifold.

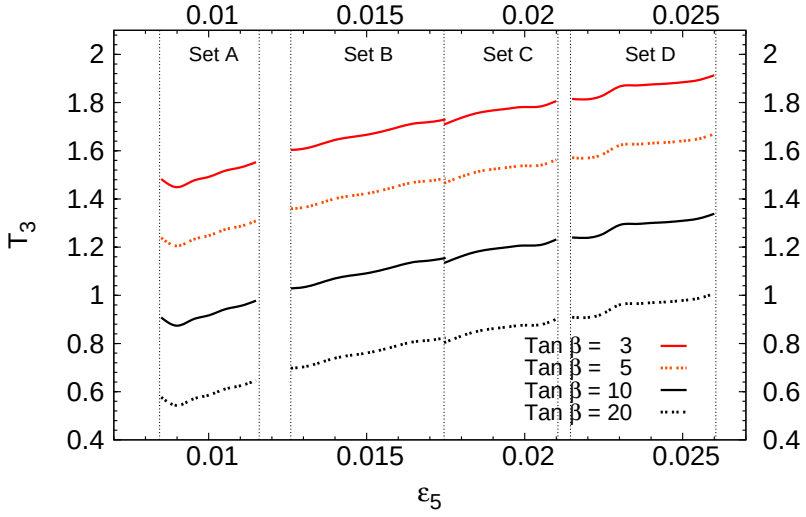

Figure 4.8: T_3-moduli dependence on ε_5, for $\tan\beta = 3, 5, 10, 20$.

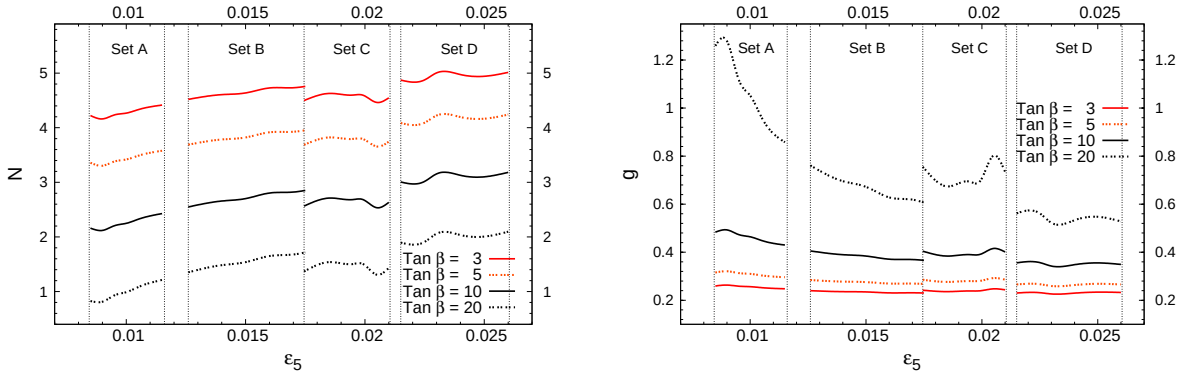

Figure 4.9: Orbifold normalisation constant N for $\tan\beta = 3, 5, 10, 20$ as a function of ε_5 (left), and corresponding values of the heterotic gauge coupling constant g (right).

T_3, the values are always fixed by the choice of a given $\tan\beta$, as we can see in the previous plots. This in turn implies the existence of an upper limit for $\tan\beta$, above which the moduli become zero. In general, this occurs for values of $\tan\beta$ between 30 and 40, depending on the choice of the remaining orbifold parameters.

In the first analysis of Ref. [53], the constraints on the orbifold parameters derived from the quark sector had already allow to hint towards a range for the product gN, $1.03 \lesssim g\,N \lesssim 1.16$. The inclusion of the bounds arising from considering the lepton sector finally allows to refine the knowledge of these orbifold parameters. On the left hand-side of Fig. 4.9 we show the value of the orbifold normalisation constant N for different values of $\tan\beta$ as a function of ε_5. From this plot, using Eq. (4.17), we can derive the value of the heterotic gauge coupling constant g. The result is presented on the right hand-side of Fig. 4.9. As we observe, for the chosen regimes of $\tan\beta$, the value of g varies between $\approx (0.2 - 1.2)$. It is worth noticing here that a value of g of order 1, which is compatible with the above result, was obtained in the orbifold models with three Higgs families analysed in [64], in order to solve the discrepancy between the unification scale predicted by the heterotic superstring ($\approx g\,5.27 \times 10^{17}$ GeV) and the value deduced from LEP experiments ($\approx 2 \times 10^{16}$ GeV).

4.4 Neutrinos

As seen from the previous sections, after having imposed the requirements of viable quark masses and mixings, as well as the correct charged lepton masses, many of the orbifold parameters have already been constrained. The question that remains to be answered is whether or not the

present neutrino data can be reproduced. In the following subsections, we will discuss how the orbifold model allows us to deal with the problem of neutrino masses, providing several mechanisms that can potentially account for an experimentally viable mass spectrum and MNS matrix, including in some of the cases the generation of an effective seesaw mechanism.

4.4.1 Dirac neutrino masses without seesaw

In the present orbifold model, the simplest way of obtaining massive neutrinos is to assume that the latter are Dirac particles, and introduce a Yukawa term, coupling left- and right-handed neutrinos to the up-type Higgs fields. Accordingly, the Dirac mass matrix for the neutral leptons is given by:

$$\mathcal{M}^{\nu} = gN\varepsilon_1\varepsilon_3\, a^L a^{\nu^c} B^L A^u B^{\nu^c} = gN\varepsilon_1\varepsilon_3\, a^L a^{\nu^c} \begin{pmatrix} v_2\,\varepsilon_5^2\,\beta^L\,\beta^{\nu^c} & v_6\,\varepsilon_5^2\,\beta^L & v_4\,\epsilon_5\,\alpha^{\nu^c}\,\beta^L \\ v_6\,\varepsilon_5^2\,\beta^{\nu^c} & v_4 & v_2\,\alpha^{\nu^c} \\ v_4\,\varepsilon_5\,\alpha^L\,\beta^{\nu^c} & v_2\,\alpha^L & v_6\,\alpha^L\,\alpha^{\nu^c}/\varepsilon_5^2 \end{pmatrix}, \tag{4.19}$$

where A^u, a^{L,ν^c} and B^{L,ν^c} are defined in Eqs. (3.16) and (3.34 - 3.36). As shown in [66], unless some fine-tuning is introduced in the model the use of these terms without the addition of Majorana couplings gives rise to excessively heavy neutrinos. This can be easily understood by noticing that all the parameters involved in Eq. (4.19) are completely determined from the quark and charged-lepton sectors, the only exception being α^{ν^c} (and thus β^{ν^c} and a^{ν^c}). Thus, the mass eigenvalues of the Dirac neutrinos can be approximately written as:

$$m_{\nu_i} \;\approx\; \varepsilon_1\,\frac{a^{\nu^c}}{a^{e^c}}\,m_{l_i}\,, \tag{4.20}$$

leading to the relation

$$\frac{m_{\nu_i}}{m_{l_i}} \;\approx\; \varepsilon_1\,\frac{a^{\nu^c}}{a^{e^c}} \;\sim 10^{-7}\,. \tag{4.21}$$

Regarding the three parameters appearing in the previous equation, ε_1 is defined by the chosen value of $\tan\beta$ (see [53]). For $\tan\beta$ between 3 and 20, values of ε_1 compatible with realistic quark masses lie in the range $\varepsilon_1 \approx 0.2 - 2$. The factor a^{e^c} has been determined from the charged-lepton sector, $a^{e^c} \approx 0.1$. Thus the remaining free parameter in Eq. (4.21) is a^{ν^c}, which depends on α^{ν^c} and ε_5 in the following way (see Eq. (3.39)):

$$a^{\nu^c} \;=\; \frac{(1-\alpha^{\nu^c{}^2})^{1/2}}{\alpha^{\nu^c}}\,\frac{\varepsilon_5}{(1\,-\,\varepsilon_5)^{1/2}}\,. \tag{4.22}$$

Suppression of the light neutrino masses requires values of α^{ν^c} very close to 1, forcing a^{ν^c} to be very small. In turn, this would imply that there are additional fields entering the FI breaking, with a very distinct mass hierarchy (much lighter VEVs), giving rise to terms of the form

$$a^{\nu^c} \;=\; \frac{\hat{c}_2^{\nu^c}}{\sqrt{|\hat{c}_1^{\nu^c}|^2 + |\hat{c}_2^{\nu^c}|^2}} \;\approx\; 10^{-7} - 10^{-6}\,. \tag{4.23}$$

To clarify the latter statement, and as an example, let us consider the case in which the factors $\varepsilon'^{(\nu^c)}$ and $\varepsilon''^{(\nu^c)}$, defined in Eq. (3.37), are taken to be $\varepsilon'^{(\nu^c)} = 1$ and $\varepsilon''^{(\nu^c)} = \varepsilon_1\varepsilon_3 \approx 0.01$. In this case, Eq. (4.23) may be rewritten as

$$\frac{c_2^{\nu^c}}{c_1^{\nu^c}} \approx 10^{-5} - 10^{-4}\,. \tag{4.24}$$

In order to fulfil the above condition, we are compelled to modify the original hypothesis of assuming the VEVs c_i^f to be of the order of the FI breaking scale, i.e. $10^{16\text{-}17}$ GeV. One possibility of obtaining the desired hierarchy between $c_1^{\nu^c}$ and $c_2^{\nu^c}$ is to invoke the existence of effective non-renormalisable couplings of the form

$$\frac{\langle C^2\rangle}{M_{\rm string}^2}\, C_2^{\nu^c}\,\xi_1\,\xi_2 \approx 10^{-4} \times C_2^{\nu^c}\,\xi_1\,\xi_2\,, \tag{4.25}$$

where ξ_1, ξ_2 denote two extra-matter fields which should later mix with the ν^c field, as explained in Section 3.4. Although this possibility may solve the discrepancy between the FI-breaking scale and the one needed to comply with realistic neutrinos, the introduction of non-renormalisable couplings sets an undesired arbitrariness in the mass scales used to generate the fermion masses. In this sense, it seems preferable to find another way to generate neutrino masses without the addition of higher-order operators.

Another possible solution to this problem could lie in the assumption of a more involved mixing of the fields participating in the FI breaking, as will be presented in Section 4.4.3. Nevertheless, a more straightforward and simple possibility consists of assuming that the neutrinos are Majorana particles. In this case, one allows the presence of Majorana terms in the superpotential, leading to a type-I seesaw mechanism. There are several possible ways of implementing a seesaw mechanism in the context of these orbifold models, and we pursue this topic in the following subsections.

4.4.2 Neutrino masses via a type-I seesaw

As first proposed in [66], the introduction of a seesaw mechanism can be easily achieved by considering a Majorana term in the superpotential, arising from the coupling of three extra scalars (of the low-energy spectrum) as follows:

$$W^{\nu} \sim H^u\, L\, \nu^c + S\, \nu^c\, \nu^c\,, \tag{4.26}$$

where S are singlets assigned to the following fixed-point components in the first two sublattices:

$$S \quad \times \ \times \tag{4.27}$$

Under this assumption, when the singlets develop a VEV, a Majorana mass for the right-handed neutrinos is generated. In the seesaw limit, where the latter VEVs are much heavier than the electroweak scale, the effective mass matrix for the light neutrinos is then

$$m_\nu^{\rm eff} \approx \mathcal{M}^\nu \, (\mathcal{M}^{\nu^c})^{-1} \, \mathcal{M}^{\nu T} , \tag{4.28}$$

where $\mathcal{M}^\nu$ is given in Eq. (4.19) and $\mathcal{M}^{\nu^c}$ arises from the coupling $S\,\nu^c\nu^c$, and is thus defined as

$$\mathcal{M}^{\nu^c} \;=\; g\, N a^{\,\nu^c}\, a^{\nu^c}\, B^{\nu^c}\, A^s\, B^{\nu^c} \tag{4.29}$$

with

$$A^s \;=\; \begin{pmatrix} s_1 & s_3\varepsilon_5 & s_2\varepsilon_5 \\ s_3\varepsilon_5 & s_2 & s_1\varepsilon_5 \\ s_2\varepsilon_5 & s_1\varepsilon_5 & s_3 \end{pmatrix} , \tag{4.30}$$

$s_{1,2,3}$ being the singlet VEVs. Note that in Eq. (4.28) the mixing B^{ν^c} cancels, so that the only free parameters in the mass matrix will be the VEVs s_i. It is also important to stress at this point that the Majorana mass term in Eq. (4.28) is clearly non-diagonal, with a structure which is determined from the orbifold (analogous to what occurs for all the Dirac mass terms).

The study of the parameter space generated by s_i (for different regimes of the other parameters) reveals that it is possible to generate light neutrino masses of the desired order of magnitude, in good agreement with the experimentally measured mass squared differences between the three species, Δm^2_{21} and $|\Delta m^2_{31}|$ (see, for example, [129]),

$$\Delta m^2_{21} \;=\; 7.9\,{}^{+0.27}_{-0.28}\,\left({}^{+1.1}_{-0.89}\right)\ \mathrm{eV}^2, \tag{4.31}$$

$$\left|\Delta m^2_{31}\right| \;=\; 2.6 \pm 0.2\,(0.6) \times 10^{-3}\,\mathrm{eV}^2 . \tag{4.32}$$

To illustrate this mechanism, let us define the seesaw mass matrix as it would arise from the following point in the orbifold parameter space, compatible with realistic quark (Set B, Eq. (4.3)) and charged-lepton masses,

$$\begin{aligned} \varepsilon_5 = 0.0126, \qquad \varepsilon_3 = 0.170, \qquad \varepsilon_1 = 0.450\,, \\ \alpha^{u^c} = 0.089, \qquad \alpha^{d^c} = 0.295, \qquad \alpha^{L} = 0.129\,. \end{aligned} \tag{4.33}$$

Setting $\tan\beta = 5$, the only remaining parameters in the model are the singlet VEVs s_1, s_2, s_3. The choice of the following values

$$\{s_1,\, s_2,\, s_3\} = \{2.45 \times 10^9,\, 8.89 \times 10^{12},\, 1.32 \times 10^{12}\}\ \ \mathrm{GeV}\,, \tag{4.34}$$

gives us a "normal hierarchy" light neutrino spectrum,

$$\{m_{\nu_1},\, m_{\nu_2},\, m_{\nu_3}\} \;=\; \{5.39 \times 10^{-8},\, 9.13 \times 10^{-3},\, 5.65 \times 10^{-2}\}\ \ \mathrm{eV}, \tag{4.35}$$

leading to mass squared differences in good agreement with the experimental range of Eqs. (4.31, 4.32). Even though this implementation of a type-I seesaw mechanism can lead to a viable light neutrino spectrum, there are two drawbacks to this formulation. The first one comes from the high scale required by the Majorana singlets (10^{9-12} GeV). Again, a possible explanation of this high scale is to assume the fields S_i as effective non-renormalisable FI fields (analogous to the ones suggested in Eq. (4.25)) or to allow a more complicated FI mixing which would translate into a further suppression of the Yukawa couplings (see Section 4.4.3, below). The second shortcoming stems from a failure in reproducing the observed mixing in the leptonic sector, as parameterised by the the $U_{\rm MNS}$ matrix

$$U_{\rm MNS} = \begin{pmatrix} c_{12}c_{13} & s_{12}c_{13} & \pm s_{13} \\ -s_{12}c_{23} \mp s_{23}s_{13}c_{12} & c_{12}c_{23} \mp s_{23}s_{13}s_{12} & s_{23}c_{13} \\ s_{12}s_{23} \mp s_{13}c_{23}c_{12} & -s_{123}c_{12} \mp s_{13}c_{23}c_{12} & c_{23}c_{13} \end{pmatrix} , \tag{4.36}$$

where, for simplicity, we use the CP-conserving parametrisation. The mixing angles θ_{12}, θ_{23}, θ_{13}, are experimentally[3] given by

$$\theta_{12} = \ 33.7 \pm 1.3 \left(^{+4.3}_{-3.5}\right) , \tag{4.37}$$

$$\theta_{23} = \ 43.3 \, ^{+4.3}_{-3.8} \left(^{+9.8}_{-8.8}\right) , \tag{4.38}$$

$$\theta_{13} = \ 0 \, ^{+5.2}_{-0.0} \left(^{+11.5}_{-0.0}\right) , \tag{4.39}$$

where the angles are expressed in degrees. With the choice of orbifold parameters used in the previous example, Eq. (4.33), we find that in this case the mixing angles in the $U_{\rm MNS}$ matrix are

$$\{\theta_{12}^{\rm orbifold}, \theta_{23}^{\rm orbifold}, \theta_{13}^{\rm orbifold}\} \ = \ \{48.4,\, 54.5,\, 17.9\} . \tag{4.40}$$

As can be verified, the above values lie considerably above the ones allowed by the experimental bounds. The associated $U_{\rm MNS}$ would then be given by

$$U_{\rm MNS}^{\rm orbifold} = \begin{pmatrix} 0.998 & 0.045 & 0.022 \\ 0.050 & 0.87 & 0.48 \\ 0.002 & 0.48 & 0.88 \end{pmatrix} . \tag{4.41}$$

This matrix contains nearly the desired mixing for the second and third generations, but fails in reproducing the mixing for the first generation of neutrinos. This behaviour is generic to the surveyed orbifold parameter space, where we have systematically found that no more than two-generation mixing can be satisfied. By varying the singlet VEVs other mixing possibilities can be achieved, but one generation of neutrinos never has a viable mixing with the other two. This appears to be a general feature of the present orbifold model, in the sense that it is extremely

[3] We employ the values given in [129].

difficult to simultaneously accommodate the observed near-maximal mixing in the lepton sector and the small one evidenced in the CKM matrix.

A second possibility of implementing a type-I seesaw, without the need of considering a more intricate FI breaking, consists in assuming the existence of an intermediate scale. In principle this scale is not predicted by the orbifold formulation, but it would nevertheless allow to accommodate the experimental data in view of orbifold-derived neutrino Yukawa couplings. In particular, in this case one is allowing for additional sources of unconstrained mixing in the lepton sector, stemming from heavy Majorana neutrino interactions. Thus the effective light neutrino mass matrix is obtained from the seesaw equation, and given by

$$m_\nu \,=\, \mathcal{M}^\nu \,(M_R)^{-1}\, \mathcal{M}^{\nu T}\,, \tag{4.42}$$

$$U_{\rm MNS}^T\, m_\nu\, U_{\rm MNS} \,=\, m_\nu^{\rm diag}\,, \tag{4.43}$$

where $\mathcal{M}^\nu$ is defined in Eq. (4.19) and M_R is the Majorana mass matrix, whose values are not determined by orbifold considerations. In general, $U_{\rm MNS}$, $m_\nu^{\rm diag}$ are known and a very simple structure is adopted for M_R (namely a diagonal matrix) in order to derive the unknown Yukawa couplings. In the present approach, we do know the Yukawa couplings (from the orbifold construction, which at this stage has become strongly constrained), and phenomenological viability of the orbifold scenario indirectly suggests the structure of M_R. Noticing that the seesaw equation can be rewritten as

$$\mathcal{M}^\nu\, U_{\rm MNS}\, (m_\nu^{\rm diag})^{-1}\, U_{\rm MNS}^T\, \mathcal{M}^{\nu T} \,=\, M_R\,, \tag{4.44}$$

we obtain M_R as required to comply with data on neutrino masses and mixings. It is important to notice that we are not working in a basis where the charged lepton Yukawa couplings are diagonal, implying that the $U_{\rm MNS}$ matrix is defined as

$$U_{\rm MNS} \,=\, V_L^{E\dagger}\, U^n\,, \tag{4.45}$$

where V_L^E is the unitary matrix that rotates the left-handed charged lepton fields, so to diagonalise $\mathcal{M}^e$, while U^n is the matrix that diagonalises the symmetric neutrino mass matrix, m_ν.

In Fig. 4.10, we depict the eigenvalues of M_R, as a function of ε_5, for the input orbifold parameter sets A, B, C and D. Leading to this figure we have assumed $\tan\beta = 5$, $\theta_{13} = 8^\circ$, a regime of $\alpha^{\nu^c} \approx \varepsilon_5$, and a normal hierarchy for the light neutrino spectrum, namely

$$m_{\nu_i} \,=\, \{10^{-5}, 0.0089, 0.0509\}\,\text{eV}\,. \tag{4.46}$$

As can be seen from Fig. 4.10, the orbifold structure would indeed suggest the existence of

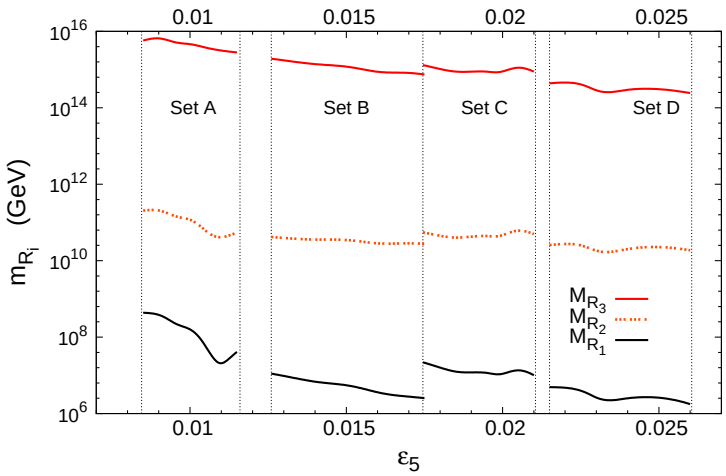

Figure 4.10: Eigenvalues of M_R (in GeV) as a function of ε_5, for the input parameter sets A, B, C and D. We take $\tan\beta = 5$, $\theta_{13} = 8°$, and $m_{\nu_i} = \{10^{-5}, 0.0089, 0.0509\}$ eV.

heavy Majorana neutrinos, whose masses would lie in the $10^6 - 10^8$ GeV and $10^{14} - 10^{16}$ GeV ranges for the lightest and heaviest states, respectively. Naturally, the heavy spectrum strongly reflects the input parameters, with the most important role being played by α^{ν^c}, $\tan\beta$ and the hierarchy of the light neutrinos. Essentially $\tan\beta$ translates in an overall factor, and having normal/inverted hierarchy or quasi-degenerate light neutrinos mostly affects the m_{R_i} pattern. On the other hand, the chosen α^{ν^c} range can have a crucial impact: while values of $\alpha^{\nu^c} \approx \varepsilon_5$ (as used for Fig. 4.10) lead to m_{R_1} masses in the $10^6 - 10^8$ GeV range, larger values, close to 1, can even give rise to masses as small as $\mathcal{O}$(TeV). The phenomenological implications of the latter regime would be extensive, and we do not address them here.

Finally, and as an illustrative example, we present the complete M_R matrix structure, for the orbifold set of parameters taken in Eq. (4.33), $\tan\beta = 5$, $\theta_{13} = 1°$, $\alpha^{\nu^c} = \varepsilon_5$ and the light-neutrino spectrum of Eq. (4.46):

$$M_R = \begin{pmatrix} 3.86\times10^{11} & 1.73\times10^{12} & -3.35\times10^{13} \\ 1.73\times10^{12} & 7.73\times10^{12} & -1.50\times10^{14} \\ -3.35\times10^{13} & -1.50\times10^{14} & 2.92\times10^{15} \end{pmatrix} \text{GeV}\,. \tag{4.47}$$

Using this matrix one can check that both a high seesaw scale and additional mixings involving the right-handed neutrinos should be invoked in order to reproduce the correct neutrino masses and mixings. The eigenvalues for the Majorana mass matrix (which correspond to the masses

of the heavy neutrinos) are

$$\{m_{R_1},\, m_{R_2},\, m_{R_3}\} = \{1.43\times 10^{7},\, 2.12\times 10^{10},\, 2.93\times 10^{15}\}\ \text{GeV}, \tag{4.48}$$

From these values one can see that, due to the mixing in the upper-left 2×2 block matrix in Eq. (4.47), we encounter a very suppressed mass eigenvalue. For different regimes in the relevant parameters considered ($\tan\beta$, $\theta_{13}^{\rm MNS}$, α^{ν^c} and the light-neutrino mass spectrum) one can check that this eigenvalue may be even sufficiently small to lie at the TeV scale, being thus potentially detectable. The other eigenvalues, as can be seen in Fig. 4.10, remain always heavy, between 10^{10} and 10^{16} GeV.

Although phenomenological viable, these last implementation of a type-I seesaw is, as previously mentioned, neither related to the geometry of the orbifold, nor to the dynamics associated with FI breaking. In what follows, we pursue one final avenue, possibly leading to a more appealing seesaw realisation.

4.4.3 A viable seesaw from the FI breaking

As mentioned, a third possibility for reproducing the observed neutrino masses and mixings may be related with assuming a more complex FI breaking. Here, we briefly outline the idea, for the simplest case of one generation. Let us then assume that in addition to the L and ν^c fields, which have the standard location

$$L \leftrightarrow \bullet\ \bullet \qquad\qquad \nu^c \leftrightarrow \times\times\,, \tag{4.49}$$

there are additional matter fields (triplets, doublet or singlets) ζ_i, coupled to the C_i fields which develop very large VEVs, thus inducing FI breaking. One can assume that these fields have the following assignments with respect to the first two sublattices:

$$\begin{array}{lll} \zeta_1 \leftrightarrow \bullet\ \bullet & \zeta_2 \leftrightarrow \times\ \circ & \zeta_3 \leftrightarrow \bullet\ \times \\ C_1 \leftrightarrow \bullet\ \bullet & C_2 \leftrightarrow \circ\ \times & C_3 \leftrightarrow \bullet\ \times \end{array} \tag{4.50}$$

The latter C_i develop VEVs, $c_i = \langle C_1\rangle$, with $c_i \approx \mathcal{O}(10^{16-17})$ GeV. In principle, one can also have the following terms in the superpotential

$$C_1\,\zeta_1\,L + C_2\,\zeta_2\,\zeta_1 + C_2\,\nu^c\,\zeta_3 + C_3\,\zeta_3\,\zeta_3\,. \tag{4.51}$$

With the above proposed lattice assignments, and after FI breaking, this would lead to

$$c_1\,\zeta_1\,L + \varepsilon_1\,\varepsilon_3\,c_2\,\zeta_2\,\zeta_1 + \varepsilon_1\,c_2\,\nu^c\,\zeta_3 + c_3\,\zeta_3\,\zeta_3\,. \tag{4.52}$$

In the basis defined by $(L\,\nu^c\,\zeta_1\,\zeta_2\,\zeta_3)^T$, one would then arrive at the following "mass matrix" (again neglecting family dependence as a first approach),

$$M^{\nu}{}_{\rm FI} = \begin{pmatrix} 0 & 0 & c_1 & 0 & 0 \\ 0 & 0 & 0 & 0 & \varepsilon_1 c_2 \\ c_1 & 0 & 0 & \varepsilon_1\varepsilon_3 c_2 & 0 \\ 0 & 0 & \varepsilon_1\varepsilon_3 c_2 & 0 & 0 \\ 0 & \varepsilon_1 c_2 & 0 & 0 & c_3 \end{pmatrix}, \tag{4.53}$$

with eigenvalues given by

$$m_i^{\rm FI} = \left\{ 0\,, \pm\sqrt{c_1^2 + \varepsilon_1^2\,\varepsilon_3^2\,c_2^2}\,, \frac{1}{2}\left(c_3 \pm \sqrt{c_3^2 + 4\,\varepsilon_1^2\,c_2^2} \right) \right\}. \tag{4.54}$$

Further assuming that we are in the limit where $\tan\beta$ is low (favoured from several arguments, as discussed throughout this work), ε_1 is smaller than unity. In this limit, and given that $c_2 \sim c_3$, one would find

$$m_4 \approx c_3 + \varepsilon_1^2\,c_3\,, \quad m_5 \approx -\varepsilon_1^2\,c_3\,, \tag{4.55}$$

thus implying the presence of a term in the superpotential behaving like

$$-\varepsilon_1^2\,c_3\,\nu^{c\prime}\,\nu^{c\prime}\,, \tag{4.56}$$

with

$$\nu^{c\prime} \propto \left(-c_3 + \sqrt{c_3^2 + 4\,\varepsilon_1^2\,c_2^2} \right) \nu^c + (2\,\varepsilon_1\,c_2)\;\zeta_3. \tag{4.57}$$

In the superpotential involving the MSSM fields, the term in Eq. (4.56) would effectively generate a Majorana mass term for the neutrino field. Thus, an intermediate Majorana scale (lower than the FI breaking scale, and much heavier than the electroweak scale) would naturally appear, induced from the dynamics of FI breaking. Other mixings between ζ_i and the remaining matter fields could in principle occur, but can be suppressed by some appropriate symmetry.

4.5 Conclusions

In this chapter we have aimed at completing the analysis of the phenomenological viability of Z_3 orbifold compactifications with two Wilson lines, addressing in detail the implications of this class of scenarios for the lepton sector. Regarding the charged leptons, we verified that the still unconstrained orbifold parameters, after the analysis of the quark sector in Chapter 3, could easily account for the observed spectrum. Moreover, and even though one is equally likely to encounter tree-level contributions to three-body LFV decays, the typical choices of Higgs soft-breaking masses (taken as to comply with the bounds on neutral meson FCNC) ensure that the predicted BRs lie several orders of magnitude below the experimental bounds.

Regarding the neutrino sector, after having imposed the requirements of viable quark masses and mixings, as well as the correct charged lepton masses, many of the orbifold parameters have already been constrained. Nevertheless, the orbifold scenarios still offer several possibilities. Albeit promising, we verified that the hypothesis of strictly Dirac neutrinos requires that the fields entering the FI breaking should have extremely hierarchical VEVs, forcing to call upon effective non-renormalisable couplings. Implementing a type-I seesaw mechanism via extra singlet fields whose interactions are dictated by the orbifold configuration reveals to be equally difficult. Complying with the measured mass squared differences favours VEVs for the Majorana singlets far higher than for the other fields. This again introduced the need to interpret these fields as effective non-renormalisable fields. Additionally, this mechanism fails in accommodating the current bounds on the neutrino mixing angles.

The need of additional mixing involving the Majorana singlet sector, and of an intermediate scale of about 10^{9-10} GeV motivated us to consider a third possibility. We have thus assumed that the smallness of the light neutrino masses is indeed explained by a type-I seesaw mechanism, where nor the scale, nor the mixings of the heavy singlets are predicted by the orbifold. In this case we verified that neutrino masses and mixings can be easily obtained, with a particularly interesting possibility which is that of a TeV-mass Majorana singlet.

In spite of the latter, it would be theoretically more appealing and consistent to have neutrino masses and mixings strictly from geometrical argumentations and/or from FI breaking. We pursued this challenging possibility, finding that in the simplest one-generation case, a slightly more involved FI breaking can indeed give rise to a Majorana mass term, with a scale far lower than that of FI breaking, and much higher than the electroweak scale.

Conclusions

In this Thesis we have analysed some of the main topics related to superymmetric scenarios with three Higgs families, applying the results to heterotic orbifold constructions and model building.

In Chapter 1 we have reviewed the fundamental tools for the developement of heterotic-string scenarios compactified on orbifolds, looking for explicit models with standard-like gauge group and also a realistic massless spectrum. We have explained how to obtain phenomenologically promising models through orbifolds, concentrating on the particular case of Z_3 orbifolds with two Wilson lines, since they naturally contain three generations of matter. We have also reviewed the problem of anomaly cancellation and its solution via the Fayet-Iliopoulos (FI) D-term. The effect of the FI cancellation is also crucial for reducing the gauge group down to $SU(3)\times SU(2)\times U(1)_Y$ and obtaining a particle content similar to that of the MSSM, with the existence of some extra matter and the generic appearance of three Higgs families.

In Chaper 2 we have verified that models which predict family replication in the Higgs sector offer very aesthetic and phenomenologically interesting scenarios [52]. Although the motivation for extending the Higgs sector can be justified from the theoretical point of view (in non-minimal SUSY models, GUTs or string constructions, for example), in most cases the viability of these extensions is challenged by the occurrence of potentially dangerous FCNCs at the tree-level. We have analysed the most general form of the SUSY potential with three Higgs families, studying its minimisation, and deriving the tree-level expressions for the neutral (scalar and pseudoscalar) and charged Higgses mass matrices. This analysis is also instrumental in addressing fine-tuning issues within the multi-Higgs models. Concerning this, we have found that, below an overall SUSY scale of order 1 TeV, the probability of cancellation between soft masses in order to succesfully break the electroweak symmetry ranges between 1% and 10%.

Needless to say, the huge quantity of degrees of freedom in the potential introduced by the additional μ terms and the soft masses gives us a high uncertainty in the choice of the correct pattern. This undesired ambiguity leads to the problem of finding an adequate choice of parameters for the Higgs sector. In the analysis presented here, the μ terms and the soft-breaking masses were taken as free parameters. However, this need not be so. In what concerns the μ

terms, one can build models assuming that the bilinear terms arise dynamically (as it happens in the Next-to-Minimal Supersymmetric Standard Model (NMSSM) [140] or the "μ from ν" Supersymmetric Standard Model ($\mu\nu$SSM) [141, 142]). This possibility offers very interesting scenarios that deserve further analysis.

One of the main goals in our study of the Higgs sector was to derive a model-independent evaluation of the tree-level contributions to neutral meson mass differences. We have computed the most general expression for the tree-level contributions to the mass difference of the neutral meson systems mediated by the neutral Higgses. We took into account the exchange of all Higgs states, including the effects of mixing in the Higgs sector, and made no approximation with respect to dominant/sub-dominant contributions. This analysis is completely general, and can be applied to any given model with three Higgs families, independently of its Yukawa structure. As an example, we assumed a simple ansatz for the Yukawa couplings and considered the contributions of two distinct Higgs spectra to the K^0, B_d, B_s and D^0 mass differences, finding that the strongest bound - which as expected arises from Δm_K - requires a spectrum of order 10 TeV.

It is worth remarking that the results for the Higgs masses are strongly dependent on the specific ansatz for the Yukawa couplings. Other ansätze, that account for a stronger hierarchy in the quark sector and still accommodate experimental data on quark masses and mixings, may generate quite smaller contributions to Δm_K, and thus require a lighter Higgs spectrum. On the other hand, it is also possible that while generating smaller contributions to Δm_K, the different ansätze induce larger Δm_B, or Δm_D.

In addition to the contributions to neutral meson mass differences, within the quark sector there are other processes that also deserve further investigation. For example, let us mention, at the one loop level, the very suppressed SM and MSSM B_s decays. Processes involving the lepton sector also offer an even wider field for testing the new contributions induced by the additional Higgses (neutral and charged). CP violation, given the potential tree-level contributions to ε_K, may also become a stringent bound.

In Chapter 3 we have employed the results derived in Chapter 2 in order to investigate whether it is possible to find Z_3 orbifold configurations with three Higgs families compatible with an experimentally viable low-energy scenario [53]. In particular, we have studied their ability to obtain realistic masses and mixings in the quark sector, avoiding potential problems with FCNCs.

Let us recall that orbifold models provide a beautiful geometric mechanism for the generation of the fermion mass hierarchy. The Yukawa couplings are explicitly calculable, and thus a solution to the elusive flavour problem of the SM and MSSM can be explored. The fact that additional Yukawas are present due to the existence of three families of Higgses, opens the

possibility of obtaining correct fermion masses and mixings, entirely at the renormalisable level.

Our analysis here has been a phenomenological "bottom-up" one. That is the particles were assigned to fixed points in a way that can reproduce the experimental data. In addition the scheme relies on the mixing between fields due to the FI breaking. We have not completed a full analysis of minimising the potential along D- and F- flat directions after the breaking, but we have made use of the very general features that such a minimization should have, namely mixing of the would-be MSSM fields with other singlet, doublet and triplet fields that couple to heavy fields. Under these assumptions, we have successfully reproduced the observed pattern of quark masses and mixings. Let us remark, however, that this severely constrains the orbifold parameters.

On the other hand, having six Higgs doublets (and thus six quark Yukawa couplings) poses the potential problem of having tree-level FCNCs. By assuming simple textures for the Higgs free parameters, we have verified that the experimental data on the neutral kaon mass difference, as well as on Δm_{B_d} and Δm_{B_s} can be easily accommodated for a quite light Higgs spectra, namely $m_{h_i^0} \lesssim 1$ TeV. The data from the D^0 sector proves to be a more difficult challenge, requiring a Higgs spectrum of at least 7 TeV, but we again stress that, in view of the theoretical and experimental uncertainties associated with the D^0 sector, this constraint should not be over-emphasised.

CP violation can be also embedded into the low-energy theory. Although CP is a gauge symmetry of the full theory, it can be spontaneously broken at the string scale, if the VEVs of the moduli have a non-vanishing phase. We have parameterised these effects and we have verified that one can also obtain a value for ε_K in agreement with current experimental data.

In Chapter 4 we have aimed at completing the analysis of the phenomenological viability of Z_3 orbifold compactifications, addressing in detail the implications of this class of scenarios in the lepton sector [54]. Regarding the charged leptons, we have verified that the still unconstrained orbifold parameters can easily account for the observed spectrum. Moreover, and even though one is equally likely to encounter tree-level contributions to three-body LFV decays, the typical choices of Higgs soft-breaking masses (taken as to comply with the bounds on neutral meson FCNC) ensure that the predicted BRs lie several orders of magnitude below the experimental bounds.

Regarding the neutrino sector, after having imposed the requirements of viable quark masses and mixings, as well as the correct charged lepton masses, many of the orbifold parameters have already been constrained. Nevertheless, the orbifold scenarios still offer several possibilities. Albeit promising, we verified that the hypothesis of strictly Dirac neutrinos requires that the fields entering the FI breaking should have extremely hierarchical VEVs, forcing to call upon effective non-renormalisable couplings. Implementing a type-I seesaw mechanism via extra singlet

fields whose interactions are dictated by the orbifold configuration reveals to be equally difficult. Complying with the measured mass squared differences favours VEVs for the Majorana singlets far higher than for the other fields. This again introduced the need to interpret these fields as effective non-renormalisable fields. Additionally, this mechanism fails in accommodating the current bounds on the neutrino mixing angles.

The need of additional mixing involving the Majorana singlet sector, and of an intermediate scale of about 10^{9-10} GeV motivated us to consider a third possibility. We have thus assumed that the smallness of the light neutrino masses is indeed explained by a type-I seesaw mechanism, where nor the scale, nor the mixings of the heavy singlets are predicted by the orbifold. In this case we verified that neutrino masses and mixings can be easily obtained, with a particularly interesting possibility which is that of a TeV-mass Majorana singlet. In spite of the latter, it would be theoretically more appealing and consistent to have neutrino masses and mixings strictly from geometrical argumentations and/or from FI breaking. We pursued this challenging possibility, finding that in the simplest one-generation case, a slightly more involved FI breaking can indeed give rise to a Majorana mass term, with a scale far lower than that of FI breaking, and much higher than the electroweak scale.

As a final summary, we can say that supersymmetric models with three Higgs families offer an interesting framework for studying physics beyond the Standard Model, with phenomenological properties that can be easily tested within the next generation of colliders. As an example of this class of multi-Higgs models, orbifold scenarios offer very interesting possibilities to obtain realistic values for the masses and mixings of the Standard-Model fermions. Particularly, for the case of quarks and charged leptons, the agreement between specific scenarios and experimental data turns out to be possible. For the case of the neutrino sector, it would appear that a new high-energy "seesaw" scale must be introduced in order to explain the suppression of neutrino masses. Nevertheless, the assumption of a more involved FI mixing could account for the generation of the desired scale. Regarding the Higgs sector, the commonly assumed danger coming from the tree-level FCNCs can be avoided for a fairly light Higgs mass spectrum between 100 GeV and 1 TeV. From a phenomenological point of view, all these properties make the orbifold scenarios considered in this work very attractive. Their relevance and further study as good tools for string model building will crucially depend on the confirmation of their most characteristic property, that is the existence of three Higgs generations in the low-energy spectrum. Fortunately, the certainty of this hypotesis will soon be tested. In a near future, the LHC will conduct extensive searches of the Higgs boson. If any of the experiments collects data suggesting the existence of more than one pair of SUSY Higgs doublets, this would point to a supersymmetric realization of Nature which could potentially be described by these type of Z_3 orbifold models with two Wilson lines.

Conclusiones

En esta Tesis hemos analizado algunos de los aspectos fundamentales relacionados con modelos supersimétricos con tres familias de Higgses. Los resultados obtenidos han sido aplicados a escenarios de orbifolds de la cuerda heterótica.

En el Capítulo 1 hemos repasado las herramientas principales para la construcción de escenarios de la cuerda heterótica compactificada en orbifolds, buscando modelos explícitos con el grupo gauge del Modelo Estándar y un espectro de baja energía realista. Hemos descrito las herramientas básicas para la obtención de modelos fenomenológicamente prometedores por medio del uso de orbifolds, concentrándonos en el caso concreto de orbifolds Z_3 con dos líneas de Wilson, que de forma natural contienen tres generaciones de materia. También hemos estudiado el problema de la cancelación de anomalías en estos escenarios, así como su solución mediante el término D de Fayet-Iliopoulos (FI). El efecto de la cancelación FI resulta además crucial para reducir el grupo gauge hasta $SU(3) \times SU(2) \times U(1)_Y$, obteniendo un espectro de partículas similar al del MSSM, con la existencia de materia extra y la presencia genérica de tres familias de Higgses.

En el Capítulo 2 hemos verificado que los modelos que predicen una replicación en el sector de Higgs proporcionan escenarios estética y fenomenológicamente interesantes [52]. Aunque la motivación de extender el sector de Higgs puede resultar justificada desde el punto de vista teórico (en modelos SUSY no mínimos, GUTs o construcciones de cuerdas, por ejemplo), en la mayoría de los casos la viabilidad de estas extensiones ha de enfrentarse a la existencia de FCNCs a nivel árbol potencialmente peligrosas. Hemos realizado un análisis completamente general de un potencial supersimétrico con tres familias de Higgs, estudiando su minimización y derivando las expresiones a nivel árbol de las matrices de masa de los Higgses neutros (escalares y pseudoescalares) y de los cargados. Este análisis resulta también de interés para estudiar el grado de *fine tuning* de los modelos multi-Higgs. Respecto a esto último hemos encontrado que, por debajo de una escala global de SUSY de orden 1 TeV, la probabilidad de cancelación entre masas *soft* para romper adecuadamente la simetría electrodébil se encuentra entre un 1% y un 10%.

Obviamente, la gran cantidad de grados de libertad en el potencial introducidos por los términos μ adicionales y las masas soft proporciona una considerable incertidumbre en la elección correcta de la estructura del sector de Higgs. En el estudio aquí presentado, los términos μ y las masas soft se tomaron como parámetros libres. Sin embargo, esta elección no es la única posible. En lo que respecta a los términos μ, se podría considerar otro tipo de modelos en el que los términos bilineales surgen dinámicamente (como sucede en el Next-to-Minimal Supersymmetric Standard Model (NMSSM) [140] o en el "μ from ν" Supersymmetric Standard Model ($\mu\nu$SSM) [141, 142]). Esta posibilidad ofrece escenarios interesantes que merecerían ser estudiados en detalle en el futuro.

Una de las metas principales de nuestro estudio del sector de Higgs ha sido obtener una evaluación independiente del modelo de las contribuciones a las diferencias de masa de sistemas de mesones neutros a nivel árbol. Hemos calculado la expresión más general para la contribución a dichas diferencias de masas mediadas por los Higgses, teniendo en cuenta el efecto del intercamio de todos los estados de Higgs, sin hacer aproximaciones con respecto a contribuciones dominantes/subdominantes. Este análisis es completamente general y puede ser aplicado a cualquier modelo con tres familias de Higgs, independientemente de su estructura de Yukawa. Como ejemplo, hemos tomado una textura sencilla de Yukawa y hemos calculado las contribuciones de dos espectros diferentes de Higgs a las diferencias de masas de los sitemas K^0, B_d, B_s y D^0, encontrando que la cota más restrictiva (que como cabe esperar, procede de Δm_K) requiere un espectro del orden de 10 TeV.

Es interesante destacar el hecho de que el espectro de Higgs compatible con los experimentos depende fuertemente de la textura de acoplos de Yukawa elegida. Otras elecciones compatibles con valores realistas para los quarks y sus mezclas que presenten una jerarquía mayor en sus Yukawas, podrían generar menores contribuciones a Δm_K, permitiendo por tanto un espectro de Higgs más ligero. Por otra parte, es también posible que incluso generando contribuciones menores a Δm_K, se pudiesen producir resultados mayores para Δm_B o para Δm_D.

Además de las contribuciones a las diferencias de masa en los sistemas de mesones neutros, dentro del sector de los quarks existen otros procesos que también merecen ser tenidos en cuenta en el futuro, como es por ejemplo el caso de las desintegraciones a un loop del mesón B_s, muy suprimidas en el SM y en el MSSM. Los procesos relacionados con el sector leptónico también ofrecen un marco amplio en el que probar las nuevas contribuciones inducidas por los Higgses adicionales (neutros y cargados). La violación de CP, dadas las contribuciones potenciales a ε_K a nivel árbol, pueden también ofrecer cotas restrictivas.

En el Capítulo 3 hemos empleado los resultados obtenidos previamente en el Capítulo 2 para investigar la posibilidad de encontrar configuraciones de orbifolds Z_3 con tres familias de Higgses compatibles con un escenario viable a baja energía [53]. En concreto, hemos estudiado

su capacidad para obtener masas y mezclas realistas en el sector de quarks, sin superar los límites experimentales sobre FCNCs.

Los modelos de orbifolds proporcionan un atractivo mecanismo geométrico para generar la jerarquía de masas de los fermiones. Los acoplos de Yukawa se pueden calcular explícitamente, lo que nos permite explorar una posible solución al esquivo problema del sabor del SM y el MSSM. El hecho que exista un mayor número de acoplos de Yukawa debido a la presencia de las tres familias de Higgses, abre la posibilidad de obtener masas y mezclas correctas para los fermiones exclusivamente a través de acoplos renormalizables,

Nuestro análisis ha sido de tipo "bottom-up". En él las partículas fueron asignadas a los puntos fijos de forma que se pueda reproducir los datos experimentales. Además, el esquema depende de la mezcla entre campos producida por la ruptura FI. Aunque no hemos realizado un análisis completo de la minimización del potencial a lo largo de las direcciones planas D- y F-, hemos empleado las características generales que habría de tener dicha minimización, esto es, la mezcla de los campos del MSSM iniciales con otros campos singlete, doblete o triplete que se acoplan a campos pesados. Con esta hipótesis, hemos reproducido correctamente el patrón obeservado de las masas de los quarks, así como sus mezclas. Debemos mencionar, no obstante, que este proceso restringe severamente los parámetros del orbifold.

Por otra parte, la existencia de seis dobletes de Higgs (y por tanto de seis matrices de acoplos de Yukawa) presenta el problema potencial de la aparición de FCNCs a nivel árbol. Empleando texturas sencillas para los parámetros libres del sector de Higgs, hemos verificado que las cotas experimentales sobre la diferencia de masas de kaones, así como Δm_{B_d} y Δm_{B_s} se satisfacen de forma natural para espectros de Higgses relativamente ligeros, con masas $m_{h_i^0} \lesssim 1$ TeV. En contraposición, los datos sobre el sector D^0 han resultado ser problemáticos, requiriendo un espectro de Higgses de al menos 7 TeV. No obstante, debemos recordar de nuevo que, teniendo en cuenta la incertidumbre teórica y experimental asociada al sector D^0, no deberíamos dar a este hecho una importancia excesiva.

La violación de CP también puede ser incluida en la teoría a baja energía. Aunque CP es una simetría de la teoría completa, puede ser rota de forma espontánea a la escala de la cuerda, si los VEVs de los moduli poseen una fase distinta de cero. Hemos parametrizado esta posibilidad, verificando que se puede obtener un valor de ε_K de acuerdo con su valor experimental.

En el Capítulo 4, hemos completado el análisis de la viabilidad fenomenológica de las compactificaciones de orbifolds Z_3, estudiando en detalle las implicaciones de esta clase de escenarios en el sector leptónico [54]. En lo que respecta a los leptones cargados, hemos verificado que los parámetros del orbifold no fijados por el sector de quarks pueden proporcionar fácilmente el espectro observado. Además, a pesar de la existencia de contribuciones a nivel árbol a desintegraciones a tres cuerpos, una elección típica de masas soft (compatible también con las cotas de

FCNCs en mesones) garantiza que los BRs permanezcan por debajo de los límites experimentales.

En el sector de neutrinos, después de haber impuesto que los modelos proporcionen masas y mezclas viables para los quarks, muchos de los parámetros del orbifold se encuentran ya fijados. Con todo, los escenarios de orbifolds aún ofrecen diversas posibilidades. La hipótesis de emplear neutrinos de tipo exclusivamente Dirac, a pesar de resultar prometedora en un primer momento, requiere que los campos participando en la ruptura FI posean VEVs extremadamente jerárquicos, obligándonos al uso de acoplos efectivos no renormalizables. Implementar un mecanismo de seesaw tipo I por medio de singletes cuyas interacciones estén dictadas por la configuración del orbifold ha resultado ser igualmente problemático. Satisfacer las diferencias de masas medidas experimentalmente favorece que los VEVs de los singletes de Majorana sean mucho mayores que los de los otros campos. Esto introduce de nuevo la necesidad de interpretarlos como campos no renormalizables efectivos. Además, los ángulos de mezcla obtenidos por medio de este método no son completamente satisfactorios.

La necesidad de una mayor mezcla dentro del sector de Majorana y de una escala intermedia del orden de 10^{9-10} GeV nos lleva a considerar una tercera posibilidad. Hemos asumido que la masa de los neutrinos es descrita por un mecanismo seesaw tipo I, donde ni la escala ni la mezcla de los singletes pesados son predichas por el orbifold. Para este caso verificamos que las masas de los neutrinos y sus mezclas pueden ser fácilmente obtenidas, con la interesante posibilidad de un singlete de Majorana con masas de orden 1 TeV.

A pesar de lo anterior, desde el punto de vista teórico resultaría más atractivo y consistente que las masas y las mezclas de los neutrinos procedieran de argumentos estrictamente geométricos y/o de la ruptura FI. Hemos perseguido esta interesante posibilidad, encontrando que en el caso más sencillo de una única generación un patrón de ruptura FI más complejo podría dar lugar a términos de Majorana con una escala menor que la asociada con la ruptura FI y a la vez mucho mayor que la escala electrodébil.

Como resumen final, podemos decir que los modelos supersimétricos con tres familias de Higgses ofrecen un marco interesante para el estudio de la física más allá del Modelo Estándar, con propiedades fenomenológicas que podrán ser fácilmente verificadas por la próxima generación de aceleradores. Como ejemplo esta clase de modelos multi-Higgs, los modelos de orbifolds ofrecen posibilidades satisfactorias para obtener valores realistas de las masas y mezclas de los fermiones del Modelo Estándar. En concreto, para el caso de los quarks y los leptones cargados, la coincidencia entre escenarios específicos y datos experimentales ha resultado ser posible. En el caso del sector de neutrinos da la impresión de que, si queremos explicar la gran supresión existente en sus masas, tendríamos que introducir necesariamente una escala "seesaw"

de alta energía. No obstante, la hipótesis de una mezcla más complicada durante la ruptura FI podría ser capaz de generar la escala deseada. En lo que respecta al sector de Higgs, el riesgo proveniente de las FCNCs a nivel árbol puede ser evitado para espectros de Higgs ligeros entre 100 GeV y 1 TeV. Desde un punto de vista fenomenológico, todas estos factores hacen que los modelos de orbifolds considerados resulten muy atractivos. Su relevancia y futuro estudio como buenas herramientas para la construción de modelos de cuerdas dependerá de forma crucial de la confirmación de su propiedad más característica: la existencia de tres generaciones de Higgses en el espectro de baja energía. Afortunadamente, la certeza de esta hipótesis podrá ser pronto contrastada. En un futuro ya muy cercano, el LHC realizará una búsqueda exhaustiva del bosón de Higgs. Si cualquiera de sus experimentos obtiene datos que sugieran la existencia de más de un par de dobletes de tipo up y down, ello apuntaría hacia una realización supersimétrica de la naturaleza, que podría ser potencialmente descrita por modelos de orbifolds Z_3 con dos líneas de Wilson.

Agradecimientos

En este punto final de la tesis, me gustaría dar las gracias a todas las personas que me han apoyado de una u otra forma durante estos cuatro años de ardua labor científica y profunda experiencia vital. A todos ellos les debo una parte muy importante de este trabajo.

En primer lugar, querría dar las gracias a mi director de tesis, Carlos Muñoz, por haberme guiado sabiamente por el proceloso mundo de los orbifolds, los escenarios multi-Higgs y demás "modelos del Universo". Le agradezco especialmente su voto de confianza cuando me aceptó como estudiante de doctorado, las conversaciones sobre física (de las que siempre, sin excepción, aprendo cosas útiles) y su inestimable ayuda durante la elaboración de esta Tesis. Le agradezco también que eligiera Corea como destino en 2005, lo que me permitió conocer lugares y personas que siempre recordaré con gran cariño y gratitud.

En segundo lugar, me gustaría agradecer a Ana Teixeira su enorme y fundamental apoyo durante todo el doctorado. Su generosidad, su amistad, su paciencia, su tesón, su forma de hacer física y su disposición para ayudarme siempre con cualquiera de mis dudas hacen que la admire tanto en lo científico como en lo personal. Sé que siempre compartiremos laberintos en Chartres, fideos chinos a horas intempestivas y alguna extraña fluctuación de la Fuerza los viernes, con la que milagrosamente todos los problemas se solucionan. Gracias también por darme la oportunidad de visitar el LPT en 2007.

Después, a mi madre. Por su amor, su comprensión y su ayuda en todos los momentos de mi vida, por tener la capacidad de escucharme "con el corazón" y por transmitirme los valores que hoy me forman como persona. Por ser un ejemplo para mí en tantísimas cosas. El agradecimiento que siento hacia ella necesitaría demasiadas páginas como para expresarlo aquí.

A Rebeca, por ser mi compañera en la vida. Por su amor, por compartir mis momentos de felicidad tomándolos como si fueran propios y por estar junto a mí en los momentos malos. Por su apoyo incondicional durante estos años de ciencia, y por su confianza a pesar de no entender muchos de los disparates en los que trabajo. Por haber atravesado medio mundo para ir a Corea, por huír conmigo de algún que otro Fish'n Chips, por ser mi cómplice de Karaokes y Pachinkos, porque conoce los secretos de los puentes de París y porque sabe que, en la mayoría

de las ocasiones, basta con estar junto a la persona a la que quieres para ser feliz. Por compartir canoa, palita y cubo veinticinco años atrás. Y por saber lo muchísimo que eso significa.

A mi familia, que siempre está ahí. A mi tía Mary, a mi tío Gonzalo, a mis tíos Lali y Pepe, a mi prima Mª Nieves, a mi padrino Jorge y a todos los demás. Por preguntar siempre con tanto cariño cómo va la tesis y por sus valiosos consejos. También a todos los que estuvieron y ya no están, pero que siempre nos acompañan cuando los recordamos. Va por vosotros.

A Mercedes, la mejor profesora de Física que haya tenido jamás. Por todo lo que aprendí en sus clases durante los años del Colegio Decroly, por ser tan maja, por los muchos libros que me prestó y por transmitirme la vocación por la disciplina más hermosa del mundo.

A Ernesto y a Sergio. Por compartir carrera y doctorado, por su amistad y por todas las cosas que he aprendido de ellos. Sólo por haberos conocido, esta aventura ya habría merecido la pena. Por las clases del turno de tarde en el año 2000, por los cumpleaños en Sanse, por las Noches de los Machos, por las botellas de Valdepeñas en el postre, por los extintores de Alcobendas, por las conversaciones sobre nuestras inquietudes y nuestros sueños, por nuestros enfados y desenfados. Hemos pasado juntos por tantas cosas... Estoy convencido de que nuestra amistad durará para siempre, a pesar de los azares de este bingo que es la vida.

A los demás amigos y compañeros de Departamento de la Autónoma. A María "¡Qué bien lo hemos pasado!", a Chiqui (compañera de coros, Decrolys, y primera colega de vocación), a África, a Ana Fernández, a Enrique "Guardián del Muro", a Andrés "¿Tú ere' der TAE 2004?", a Javi Menéndez, a Jose Oñorbe "¡Vamos, Jose!", a Guillermo, a Fouad, a Jorge Bellorín, a Matteo, a Luisfer "Yo soy tu padre". A Sara y a Ignacio. De los mayores, a Tomás "¡No puedo, Tomi!", por ser tan buen camarada de Rock Atlético. A Jose Delgado, Edu, Irene, Carlos Hoyos, Sergio Montañez, Alberto Ramos, Mafer, Natxo, Fermín, Juan Pedro y David Temes. A los jóvenes, Fernando, Víctor, Dani cubano, Jacobo, Adolfo, Alfonso, Antón, Ana Rodríguez, Meggy e Irene. A los compañeros del despacho 507, Pablo, Sara, David, César, Jennifer y Ki-Young. Y a la "familia Muñoz": a Dani L.-Fogliani (gran compañero de aventuras, Kimchi y cervezas en Daejeon), a Bea y a Javi, que toman ya la antorcha del relevo, a David Cerdeño y a Roberto Ruiz de Austri.

A los amigos de Decroly, que con el paso del tiempo son como mis hermanos. A Carlos Barcala, Guti, Diego, Mariano, Gabo, Rayito, Barri, Gontxa, Christian Küng, Woody, Guiomar, Foncho, Cristina Rodríguez, Cristina Linés y a todos los demás. Por supuesto, sería imposible olvidar en este apartado a los distinguidos miembros del Friki Grupo: Manuel, Juan, Rodri, Guille, Fede, Alfredo y David, por ser los mejores amigos y aliados en tantos mundos imaginarios.

A los miembros del Departamento de Física Teórica de la UAM. Gracias a los profesores, por cuidar de los estudiantes y por ser un ejemplo de vocación científica para nosotros. Agradezco especialmente a María José Herrero, Luis Labarga y Juan Terrón, por conversaciones diversas

que me ayudaron mucho en algunos momentos de duda. Y gracias a Juan Carlos, a Lola y a Jose Valenzuela, por hacernos la vida más fácil a todos cada día.

Gracias también a los miembros del Grupo de Altas Energías del KAIST en Daejeon (especialmente a Kiwoon Choi) y a los miembros del LPT en Orsay (y en especial a Asmaa Abada), por su amabilidad, por su calurosa acogida y por permitirme disfrutar de una atmósfera perfecta para aprender y trabajar durante las temporadas que pasé junto a ellos.

Al Programa FPI de la Comunidad de Madrid, por la confianza y la financiación prestadas y por haberme hecho tan feliz una tarde de septiembre mientras me encontraba en Sheffield.

Y por último, a aquellos que no he nombrado por escasez de memoria o falta de espacio-tiempo, pero que sin duda merecen estar aquí. De todo corazón, muchas gracias a todos.

Nicolás Escudero Prieto

Madrid, 15 de enero de 2008

Bibliography

[1] S.L. Glashow, "Partial symmetries of weak interactions", *Nucl. Phys.* **22** (1961) 579; M. Gell-Mann, "A schematic model of baryons and mesons", *Phys. Lett.* **8** (1964) 214: G. Zweig, "An $SU(3)$ model for strong interaction symmetry and its breaking", CERN-TH 401 (1964), unpublished; S. Weinberg, "A model of leptons", *Phys. Rev. Lett.* **19** (1967) 1264; A. Salam, "Weak and electromagnetic interactions", *Proceedings of the Eighth Nobel Symposium*, 1968, ed. N. Svartholm (Almqvist and Wiksell, Stockholm; Wiley, New York, 1978), p. 367.

[2] P. W. Higgs, "Broken symmetries, massless particles and gauge fields", Phys. Lett. **12** (1964) 132; P. W. Higgs, "Spontaneous symmetry breakdown without massless bosons", Phys. Rev. **145** (1966) 1156; F. Englert and R. Brout, "Broken symmetry and the mass of gauge vector mesons", Phys. Rev. Lett. **13** (1964) 321; G. S. Guralnik, C. R. Hagen and T. W. B. Kibble, "Global conservation laws and massless particles", Phys. Rev. Lett. **13** (1964) 585.

[3] R. Barate *et al.* [LEP Working Group for Higgs boson searches], "Search for the Standard Model Higgs boson at LEP", Phys. Lett. B **565** (2003) 61 [arXiv:hep-ex/0306033].

[4] Y.A. Golfand and E.P. Likhtman, "Extension of the algebra of Poincaré group generators and violation of P invariance", JETP Lett. **13** (1971) 323; D.V. Volkov and V.P. Akulov, "Is the neutrino a Goldstone particle", Phys. Lett. **B46** (1973) 109; J. Wess and B. Zumino, "Supergauge transformations in four-dimensions", Nucl. Phys. **B70** (1974) 39.

[5] D.Z. Freedman, P. van Nieuwenhuizen and S. Ferrara, "Progress toward a theory of supergravity", Phys. Rev. **D13** (1976) 3214; S. Deser and B. Zumino, "Consistent supergravity", Phys. Lett. **B62** (1976) 335.

[6] M. B. Green, J. H. Schwarz and E. Witten, "Superstring theory." Cambridge University Press (Cambridge Monographs On Mathematical Physics) (1987). J. Polchinski, "String theory." Cambridge University Press (1998).

[7] G. Veneziano, "Construction of a crossing - symmetric, Regge behaved amplitude for linearly rising trajectories", Nuovo Cim. A **57** (1968) 190.

[8] C. Lovelace, "Pomeron Form-Factors And Dual Regge Cuts", Phys. Lett. B **34** (1971) 500.

[9] J. H. Schwarz, "Physical states and pomeron poles in the dual pion model", Nucl. Phys. B **46** (1972) 61; P. Goddard and C. B. Thorn, "Compatibility of the dual pomeron with unitarity and the absence of ghosts in the dual resonance model", Phys. Lett. B **40** (1972) 235.

[10] T. Kaluza, "On the problem of unity in physics," Sitzungsber. Preuss. Akad. Wiss. Berlin (Math. Phys.) **1921** (1921) 966.

[11] O. Klein, "Quantum theory and five-dimensional theory of relativity," Z. Phys. **37** (1926) 895 [Surveys High Energ. Phys. **5** (1986) 241].

[12] M. B. Green and J. H. Schwarz, "Anomaly Cancellation In Supersymmetric D=10 Gauge Theory And Superstring Theory", Phys. Lett. **B 149** (1984) 117.

[13] D.J. Gross, J.A. Harvey, E. Martinec, R. Rohm, "The heterotic string", Phys. Rev. Lett. **54** (1985) 502-505. D.J. Gross, J.A. Harvey, E. Martinec, R. Rohm, "Heterotic string theory 1. The free heterotic string", Nucl. Phys. **B256** (1985) 253. D.J. Gross, J.A. Harvey, E. Martinec, R. Rohm, "Heterotic string theory 2. The interacting heterotic string", Nucl. Phys. **B267** (1986) 75.

[14] P. Candelas, G. Horowitz, A. Strominger, E. Witten, "Vacuum configurations for superstrings", Nucl. Phys. **B258** (1985) 46-74.

[15] E. Calabi, in *Algebraic Geometry and Topology: A symposium in honor of S. Lefschetz* Princeton University Press (1957).

[16] S. T. Yau, "Calabi's Conjecture and some new results in algebraic geometry", Proc. Nat. Acad. Sci. **74** (1977) 1798.

[17] L.J. Dixon, J. Harvey, C. Vafa and E. Witten, "Strings on orbifolds", Nucl. Phys. **B261** (1985) 678; L.J. Dixon, J. Harvey, C. Vafa and E. Witten, "Strings on orbifolds 2", Nucl. Phys. **B274** (1986) 285.

[18] L. E. Ibáñez, H. P. Nilles and F. Quevedo, "Orbifolds and Wilson lines", Phys. Lett. B **187** (1987) 25.

[19] L. E. Ibáñez, J. E. Kim, H. P. Nilles and F. Quevedo, "Orbifold compactifications with three families of $SU(3) \times SU(2) \times U(1)^n$", Phys. Lett. B **191** (1987) 282.

[20] L. E. Ibáñez, J. Mas, H. P. Nilles and F. Quevedo, "Heterotic strings in symmetric and asymmetric orbifold backgrounds", Nucl. Phys. B **301** (1988) 157.

[21] J. A. Casas, E. K. Katehou and C. Muñoz, "U(1) charges in orbifolds: anomaly cancellation and phenomenological consequences", Nucl. Phys. B **317** (1989) 171.

[22] E. Witten, "Some properties of $O(32)$ superstrings", Phys. Lett. **B149** (1984) 351; M. Dine, N. Seiberg and E. Witten, "Fayet-Iliopoulos terms in string theory", Nucl. Phys. **B289** (1987) 317; J.J. Atick, L.J. Dixon and A. Sen, "String calculation of Fayet-Iliopoulos D-terms in arbitrary supersymmetric compactifications", Nucl. Phys. **B292** (1987) 109; M. Dine, I. Ichinose and N. Seiberg, "F-terms and D-terms in string theory", Nucl. Phys. **B293** (1987) 253.

[23] A. Font, L. E. Ibáñez, H. P. Nilles and F. Quevedo, "Degenerate orbifolds", Nucl. Phys. B **310** (1988) 109.

[24] J. A. Casas and C. Muñoz, "Three generation SU(3) $\times$ SU(2) $\times$ U(1)$_Y$ models from orbifolds", Phys. Lett. B **214** (1988) 63.

[25] A. Font, L. E. Ibáñez, H. P. Nilles and F. Quevedo, "Yukawa couplings in degenerate orbifolds: towards a realistic $SU(3) \times SU(2) \times U(1)$ superstring", Phys. Lett. B **210** (1988) 101 [Erratum-ibid. B **213** (1988) 564].

[26] S. Hamidi and C. Vafa, "Interactions on orbifolds", Nucl. Phys. B **279** (1987) 465.

[27] L. J. Dixon, D. Friedan, E. J. Martinec and S. H. Shenker, "The conformal field theory of orbifolds", Nucl. Phys. B **282** (1987) 13.

[28] L. E. Ibáñez, "Hierarchy of quark-lepton masses in orbifold superstring compactification", Phys. Lett. B **181** (1986) 269.

[29] J. A. Casas and C. Muñoz, "Yukawa couplings in $SU(3) \times SU(2) \times U(1)_Y$ orbifold models", Phys. Lett. B **212** (1988) 343.

[30] J. A. Casas and C. Muñoz, "Fermion masses and mixing angles: a test for string vacua", Nucl. Phys. B **332** (1990) 189 [Erratum-ibid. B **340** (1990) 280].

[31] J. A. Casas, F. Gómez and C. Muñoz, "World sheet instanton contribution to Z(7) Yukawa couplings", Phys. Lett. B **251** (1990) 99.

[32] T. T. Burwick, R. K. Kaiser and H. F. Muller, "General Yukawa couplings of strings on Z(N) orbifolds", Nucl. Phys. B **355** (1991) 689.

[33] J. A. Casas, F. Gómez and C. Muñoz, "Fitting the quark and lepton masses in string theories", Phys. Lett. B **292** (1992) 42 [arXiv:hep-th/9206083].

[34] J. A. Casas, F. Gómez and C. Muñoz, "Complete structure of Z(n) Yukawa couplings," Int. J. Mod. Phys. A **8** (1993) 455 [arXiv:hep-th/9110060].

[35] T. Kobayashi and N. Ohtsubo, "Geometrical aspects of Z(N) orbifold phenomenology", Int. J. Mod. Phys. A **9** (1994) 87.

[36] R. A. Flores and M. Sher, "Higgs masses in the standard, multi - Higgs and supersymmetric models", Annals Phys. **148** (1983) 95.

[37] J. R. Ellis, D. V. Nanopoulos, S. T. Petcov and F. Zwirner, "Gauginos and Higgs particles in superstring models", Nucl. Phys. B **283** (1987) 93.

[38] M. Drees, "Supersymmetric models with extended Higgs sector," Int. J. Mod. Phys. A **4** (1989) 3635.

[39] K. Griest and M. Sher, "Phenomenology and cosmology of extra generations of Higgs bosons", Phys. Rev. Lett. **64** (1990) 135,

[40] K. Griest and M. Sher, "Phenomenology and cosmology of second and third family Higgs bosons", Phys. Rev. D **42** (1990) 3834.

[41] A. E. Nelson and L. Randall, "Naturally large tan beta", Phys. Lett. B **316** (1993) 516 [arXiv:hep-ph/9308277].

[42] M. Masip and A. Rasin, "Spontaneous CP violation in supersymmetric models with four Higgs doublets", Phys. Rev. D **52** (1995) R3768 [arXiv:hep-ph/9506471].

[43] A. Aranda and M. Sher, "Generations of Higgs bosons in supersymmetric models", Phys. Rev. D **62** (2000) 092002 [arXiv:hep-ph/0005113].

[44] S. L. Glashow and S. Weinberg, "Natural conservation laws for neutral currents", Phys. Rev. D **15** (1977) 1958.

[45] E. A. Paschos, "Diagonal neutral currents", Phys. Rev. D **15** (1977) 1966.

[46] B. McWilliams and L. F. Li, "Virtual effects of Higgs particles", Nucl. Phys. B **179** (1981) 62.

[47] O. Shanker, "Flavor violation, scalar particles and leptoquarks", Nucl. Phys. B **206** (1982) 253.

[48] H. Georgi and D. V. Nanopoulos, "Suppression of flavor changing effects from neutral spinless meson exchange in gauge theories", Phys. Lett. B **82** (1979) 95.

[49] T. P. Cheng and M. Sher, "Mass matrix ansatz and flavor nonconservation in models with multiple Higgs doublets", Phys. Rev. D **35** (1987) 3484.

[50] M. Sher and Y. Yuan, "Rare B decays, rare tau decays and grand unification", Phys. Rev. D **44** (1991) 1461.

[51] A. Font, L. E. Ibáñez, F. Quevedo and A. Sierra, "The construction of 'realistic' four dimensional strings through orbifolds", Nucl. Phys. B **331** (1990) 421.

[52] N. Escudero, C. Muñoz and A. M. Teixeira, "FCNCs in supersymmetric multi-Higgs doublet models", Phys. Rev. D **73** (2006) 055015 [arXiv:hep-ph/0512046].

[53] N. Escudero, C. Muñoz and A. M. Teixeira, "Phenomenological viability of orbifold models with three Higgs families", JHEP **0607** (2006) 041 [arXiv:hep-ph/0512301].

[54] N. Escudero, C. Munoz and A. M. Teixeira, "Lepton masses and mixings in orbifold models with three Higgs families", JHEP **0712** (2007) 080 [arXiv:0710.3672 [hep-ph]].

[55] V. Braun, Y. H. He, B. A. Ovrut and T. Pantev, "A heterotic standard model", Phys. Lett. B **618** (2005) 252 [arXiv:hep-th/0501070]; "A standard model from the E(8) x E(8) heterotic superstring", JHEP **0506** (2005) 039 [arXiv:hep-th/0502155]; "The exact MSSM spectrum from string theory", arXiv:hep-th/0512177.

[56] H. Kawai, D.C. Lewellen and S.H.H. Tye, "Construction of four-dimensional fermionic string models", Phys. Rev. Lett. **57** (1986) 1832, Erratum, ibid. **58** (1987) 429; "Construction of fermionic string models in four dimensions", Nucl. Phys. **B288** (1987) 1; I. Antoniadis, C. Bachas and C. Kounnas, "Four-dimensional superstrings", Nucl. Phys. **B289** (1987) 87.

[57] D. Gepner, "Exactly Solvable String Compactifications on Manifolds of SU(N) Holonomy," Phys. Lett. B **199** (1987) 380. D. Gepner, "Space-Time Supersymmetry in Compactified String Theory and Superconformal Models," Nucl. Phys. B **296** (1988) 757. Y. Kazama and H. Suzuki, "New N=2 Superconformal Field Theories and Superstring Compactification," Nucl. Phys. B **321** (1989) 232.

[58] See, for example, G. Aldazabal, L. E. Ibáñez, F. Quevedo and A. M. Uranga, "D-branes at singularities: a bottom-up approach to the string embedding of the standard model", JHEP **0008** (2000) 002 [arXiv:hep-th/0005067].

[59] M.J. Duff, B.E.W. Nilsson, C.N. Pope, "Kaluza-Klein supergravity", *Phys.Rept.* **130** (1986) 1-142.

[60] F. GLiozzi, J. Scherk, D. Olive, "Supersymmetry, supergravity theories and the dual spinor mode", Nucl. Phys. **B122** (1977) 253-290. A.H. Chamseddine, "Interacting supergravity in ten dimensions: The role of the six-index gauge field", Phys. Rev. **D24** (1981) 3065. G. Chapline, N.S. Manton, "Unification of Yang-Mills theory and supergravity in ten dimensions", Phys. Lett. **B120** (1983) 105-109.

[61] D. Bailin, A. Love, "Orbifold compactifications of String Theory". Phys. Rept. **315** (1999) 285-408.

[62] J. A. Casas M. Mondragón and C. Muñoz, "Reducing the number of candidates to standard model in the Z_3 orbifold", Phys. Lett. B **230** (1989) 63.

[63] W. A. Bardeen, "Anomalous Ward identities in spinor field theories," Phys. Rev. **184** (1969) 1848; D. J. Gross and R. Jackiw, "Effect of anomalies on quasirenormalizable theories," Phys. Rev. D **6** (1972) 477; L. Alvarez-Gaume and E. Witten, "Gravitational anomalies," Nucl. Phys. B **234** (1984) 269.

[64] C. Muñoz, "A kind of prediction from superstring model building", JHEP **0112** (2001) 015 [arXiv:hep-ph/0110381].

[65] J. A. Casas and C. Muñoz, "Three generation SU(3) $\times$ SU(2) $\times$ U(1)$_Y$ $\times$ U(1) orbifold models through Fayet-Iliopoulos terms", Phys. Lett. B **209** (1988) 214.

[66] S. A. Abel and C. Muñoz, "Quark and lepton masses and mixing angles from superstring constructions," JHEP **0302** (2003) 010 [arXiv:hep-ph/0212258].

[67] H. E. Haber and Y. Nir, "Multiscalar models with a high-energy scale", Nucl. Phys. B **335** (1990) 363.

[68] N. V. Krasnikov, "Electroweak model with a Higgs democracy", Phys. Lett. B **276** (1992) 127.

[69] A. Antaramian, L. J. Hall and A. Rasin, "Flavor changing interactions mediated by scalars at the weak scale", Phys. Rev. Lett. **69** (1992) 1871 [arXiv:hep-ph/9206205].

[70] M. Masip and A. Rasin, "CP violation in multi-Higgs supersymmetric models", Nucl. Phys. B **460** (1996) 449 [arXiv:hep-ph/9508365].

[71] V. S. Kaplunovsky, 'Mass scales of the string unification', *Phys. Rev. Lett.* **55**, (1985) 1036.

[72] S. Béjar, J. Guasch and J. Solà, "Production and FCNC decay of supersymmetric Higgs bosons into heavy quarks in the LHC", JHEP **0510** (2005) 113 [arXiv:hep-ph/0508043].

[73] A. M. Curiel, M. J. Herrero, W. Hollik, F. Merz and S. Peñaranda, "SUSY - electroweak one-loop contributions to flavour-changing Higgs-boson decays", Phys. Rev. D **69** (2004) 075009 [arXiv:hep-ph/0312135].

[74] J. A. Aguilar-Saavedra, "Top flavour-changing neutral interactions: Theoretical expectations and experimental detection", Acta Phys. Polon. B **35** (2004) 2695 [arXiv:hep-ph/0409342].

[75] H. Fritzsch, "Weak interaction mixing in the six - quark theory", Phys. Lett. B **73** (1978) 317.

[76] H. Fritzsch and Z. z. Xing, "Mass and flavor mixing schemes of quarks and leptons", Prog. Part. Nucl. Phys. **45** (2000) 1 [arXiv:hep-ph/9912358].

[77] W. K. Sze, "The Fritzsch ansatz revisited", arXiv:hep-ph/0511181.

[78] For a review see, A. Brignole, L. E. Ibáñez and C. Muñoz, "Soft supersymmetry-breaking terms from supergravity and superstring models", in the book "Perspectives on supersymmetry", G. L. Kane (ed.), World Scientific (1998) 125 [arXiv:hep-ph/9707209].

[79] R. Barbieri and G. F. Giudice, "Upper bounds on supersymmetric particle masses", Nucl. Phys. B **306** (1988) 63.

[80] J. A. Casas, J. R. Espinosa and I. Hidalgo, "Implications for new physics from fine-tuning arguments. I: Application to SUSY and seesaw cases", JHEP **0411** (2004) 057 [arXiv:hep-ph/0410298].

[81] Y. Sakamura, "The Higgs mass bound in the SUSY multi-Higgs-doublet model", Mod. Phys. Lett. A **14** (1999) 721 [arXiv:hep-ph/9903247].

[82] W. M. Yao *et al.* [Particle Data Group], "Review of particle physics," J. Phys. G **33** (2006) 1.

[83] M. Ciuchini *et al.*, "Delta M(K) and epsilon(K) in SUSY at the next-to-leading order", JHEP **9810**, 008 (1998) [arXiv:hep-ph/9808328].

[84] J. N. Simone *et al.* [The Fermilab Lattice, MILC and HPQCD Collaborations], "Leptonic decay constants f(D/s) and f(D) in three flavor lattice QCD", Nucl. Phys. Proc. Suppl. **140** (2005) 443 [arXiv:hep-lat/0410030].

[85] S. Aoki *et al.* [JLQCD Collaboration], "B0 anti-B0 mixing in unquenched lattice QCD", Phys. Rev. Lett. **91** (2003) 212001 [arXiv:hep-ph/0307039].

[86] G. Burdman, "Potential for discoveries in charm meson physics", arXiv:hep-ph/9508349.

[87] M. Maltoni, T. Schwetz, M. A. Tortola and J. W. F. Valle, "Status of global fits to neutrino oscillations", New J. Phys. **6** (2004) 122 [arXiv:hep-ph/0405172].

[88] A. Strumia and F. Vissani, "Implications of neutrino data circa 2005", Nucl. Phys. B **726** (2005) 294 [arXiv:hep-ph/0503246].

[89] G. L. Fogli, E. Lisi, A. Marrone and A. Palazzo, "Global analysis of three-flavor neutrino masses and mixings", arXiv:hep-ph/0506083.

[90] D. Bailin, A. Love and S. Thomas, "A three generation orbifold compactified superstring model with realistic gauge group", Phys. Lett. B **194** (1987) 385.

[91] J. E. Kim, "The strong CP problem in orbifold compactifications and an $SU(3) \times SU(2) \times U(1)^n$ model", Phys. Lett. B **207** (1988) 434.

[92] J. A. Casas and C. Muñoz, "Restrictions on realistic superstring models from renormalization group equations", Phys. Lett. B **214** (1988) 543.

[93] Y. Katsuki, Y. Kawamura, T. Kobayashi, N. Ohtsubo, Y. Ono and K. Tanioka, "Z(N) orbifold models", Nucl. Phys. B **341** (1990) 611.

[94] H. B. Kim and J. E. Kim, "An orbifold compactification with three families from twisted sectors", Phys. Lett. B **300** (1993) 343 [arXiv:hep-ph/9212311].

[95] G. Aldazabal, A. Font, L. E. Ibáñez and A. M. Uranga, "Building GUTs from strings", Nucl. Phys. B **341** (1990) 611 [arXiv:hep-th/9508033].

[96] J. Giedt, "Spectra in standard-like Z_3 orbifold models", Annals Phys. **297** (2002) 67 [arXiv:hep-th/0108244].

[97] T. Kobayashi, S. Raby, R.-J. Zhang, "Searching for realistic 4d string models with a Pati-Salam symmetry: Orbifold grand unified theories from heterotic string compactification on a Z_6 orbifold", Nucl. Phys. **B704** (2005) 3 [arXiv:hep-ph/0409098].

[98] J. Giedt, G. L. Kane, P. Langacker and B. D. Nelson, "Massive neutrinos and (heterotic) string theory," Phys. Rev. D **71** (2005) 115013 [arXiv:hep-th/0502032].

[99] T. Kobayashi and C. Muñoz, "More about soft terms and FCNC in realistic string constructions", JHEP **0601** (2006) 044 [arXiv:hep-ph/0508286].

[100] W. Buchmuller, K. Hamaguchi, O. Lebedev, M. Ratz, "Supersymmetric standard model from the heterotic string", Phys. Rev. Lett. **96** (2006) 121602 [arXiv:hep-ph/0511035]; "Supersymmetric standard model from the heterotic string (II)", Nucl. Phys. **B785** (2007) 149 [arXiv:hep-th/0606187].

[101] J.E. Kim and B. Kyae, "String MSSM through flipped SU(5) from Z_{12} orbifold", arXiv:hep-th/0608085; "Flipped SU(5) from Z_{12-I} orbifold with Wilson line", Nucl. Phys. **B770** (2007) 47 [arXiv:hep-th/0608086].

[102] O. Lebedev, H.P. Nilles, S. Raby, S. Ramos-Sánchez, M. Ratz, P.K. Vaudrevange and A. Wingerter, "A mini-landscape of exact MSSM spectra in heterotic orbifolds", Phys. Lett. **B645** (2007) 88 [arXiv:hep-th/0611095]; "Low energy supersymmetry from the heterotic landscape", Phys. Rev. Lett. **98** (2007) 181602 [arXiv:hep-th/0611203]; "The heterotic road to the MSSM with R parity", arXiv:0708.2691[hep-th].

[103] I-W. Kim, J.E. Kim and B. Kyae, "Harmless R-parity violation from Z_{12-I} compactification of $E_8 \times E_8'$ heterotic string", Phys. Lett. **B647** (2007) 275 [arXiv:hep-ph/0612365].

[104] J.E. Kim, J.-H. Kim and B. Kyae, "Superstring standard model from Z_{12-I} orbifold compactification with and without exotics, and effective R-parity", JHEP **0706** (2007) 034 [arXiv:hep-ph/0702278].

[105] W. Buchmuller, K. Hamaguchi, O. Lebedev, S. Ramos-Sánchez, M. Ratz, "Seesaw neutrinos from the heterotic string", Phys. Rev. Lett. **99** (2007) 021601 [arXiv:hep-ph/0703078].

[106] P. Candelas, G. T. Horowitz, A. Strominger and E. Witten, "Vacuum configurations for superstrings", Nucl. Phys. B **258** (1985) 46.

[107] H. Kawai, D. C. Lewellen and S. H. H. Tye, "Construction of four-dimensional fermionic string models", Phys. Rev. Lett. **57** (1986) 1832 [Erratum-ibid. **58** (1987) 429]; "Construction of fermionic string models in four-dimensions", Nucl. Phys. B **288** (1987) 1.

[108] I. Antoniadis, C. P. Bachas and C. Kounnas, "Four-dimensional superstrings", Nucl. Phys. B **289** (1987) 87.

[109] P. Horava and E. Witten, "Heterotic and type I string dynamics from eleven dimensions", Nucl. Phys. B **460** (1996) 506 [arXiv:hep-th/9510209]; "Eleven-dimensional supergravity on a manifold with boundary", Nucl. Phys. B **475** (1996) 94 [arXiv:hep-th/9603142].

[110] E. Witten, Nucl. Phys. B **471** (1996) 135 [arXiv:hep-th/9602070].

[111] B. R. Greene, K. H. Kirklin, P. J. Miron and G. G. Ross, "A superstring inspired standard model", Phys. Lett. B **180** (1986) 69; "A three generation superstring model. 1. Compactification and discrete symmetries", Nucl. Phys. B **278** (1986) 667; "A three generation superstring model. 2. Symmetry breaking and the low-energy theory", Nucl. Phys. B **292** (1987) 606.

[112] R. Donagi, Y. H. He, B. A. Ovrut and R. Reinbacher, "The spectra of heterotic standard model vacua", JHEP **0506** (2005) 070 [arXiv:hep-th/0411156].

[113] I. Antoniadis, J. R. Ellis, J. S. Hagelin and D. V. Nanopoulos, "GUT model building with fermionic four-dimensional strings", Phys. Lett. B **205** (1988) 459; "An improved SU(5) X U(1) model from four-dimensional string", Phys. Lett. B **208** (1988) 209 [Addendum-ibid. B **213** (1988) 562]; "The flipped SU(5) X U(1) string model revamped", Phys. Lett. B **231** (1989) 65.

[114] A. E. Faraggi, D. V. Nanopoulos and K. Yuan, "A standard like model in the 4-d free fermionic string formulation", Nucl. Phys. B **335** (1990) 347.

[115] G. B. Cleaver, A. E. Faraggi and D. V. Nanopoulos, "String derived MSSM and M-theory unification", Phys. Lett. B **455** (1999) 135 [arXiv:hep-ph/9811427].

[116] G. B. Cleaver, A. E. Faraggi, D. V. Nanopoulos and J. W. Walker, "Phenomenology of non-Abelian flat directions in a minimal superstring standard model", Nucl. Phys. B **620** (2002) 259 [arXiv:hep-ph/0104091].

[117] S. Chaudhuri, S. W. Chung, G. Hockney and J. D. Lykken, "String consistency for unified model building", Nucl. Phys. B **456** (1995) 89 [arXiv:hep-ph/9501361].

[118] S. Chaudhuri, G. Hockney and J. D. Lykken, "Three Generations in the Fermionic Construction", Nucl. Phys. B **469** (1996) 357 [arXiv:hep-th/9510241].

[119] R. Donagi, B. A. Ovrut, T. Pantev and D. Waldram, "Standard models from heterotic M-theory", Adv. Theor. Math. Phys. **5**, 93 (2002) [arXiv:hep-th/9912208].

[120] P. Ko, T. Kobayashi and J. h. Park, "Quark masses and mixing angles in heterotic orbifold models", Phys. Lett. B **598** (2004) 263 [arXiv:hep-ph/0406041].

[121] P. Ko, T. Kobayashi and J. h. Park, "Lepton masses and mixing angles from heterotic orbifold models", Phys. Rev. D **71** (2005) 095010 [arXiv:hep-ph/0503029].

[122] J. Giedt, "The KM phase in semi-realistic heterotic orbifold models", Nucl. Phys. B **595** (2001) 3 [Erratum-ibid. B **632** (2002) 397] [arXiv:hep-ph/0007193]; "CP violation and moduli stabilization in heterotic models", Mod. Phys. Lett. A **17** (2002) 1465 [arXiv:hep-ph/0204017].

[123] B. Acharya, D. Bailin, A. Love, W. A. Sabra and S. Thomas, "Spontaneous breaking of CP symmetry by orbifold moduli", Phys. Lett. B **357**(1995) 387 [arXiv:hep-th/9506143].

[124] D. Bailin, G. V. Kraniotis and A. Love, "CP-violating phases in the CKM matrix in orbifold compactifications", Phys. Lett. B **435** (1998) 323 [arXiv:hep-th/9805111].

[125] G. F. Giudice and A. Masiero, "A natural solution to the mu problem in supergravity theories", Phys. Lett. B **206** (1988) 480.

[126] G. Lopes Cardoso, D. Lüst and T. Mohaupt, "Moduli spaces and target space duality symmetries in (0,2) Z(N) orbifold theories with continuous Wilson lines", Nucl. Phys. B **432** (1994) 68 [arXiv:hep-th/9405002].

[127] I. Antoniadis, E. Gava, K. S. Narain and T. R. Taylor, "Effective mu term in superstring theory", Nucl. Phys. B **432** (1994) 187 [arXiv:hep-th/9405024].

[128] C. Jarlskog, "Commutator of the quark mass matrices in the standard electroweak model and a measure of maximal CP violation", Phys. Rev. Lett. **55** (1985) 1039; "A basis independent formulation of the connection between quark mass matrices, CP violation and experiment", Z. Phys. C **29** (1985) 491.

[129] M. C. González-García and M. Maltoni, "Phenomenology with Massive Neutrinos," arXiv:0704.1800 [hep-ph].

[130] Z. Maki, M. Nakagawa and S. Sakata, "Remarks on the unified model of elementary particles," Prog. Theor. Phys. **28** (1962) 870.

[131] B. Pontecorvo, "Mesonium and antimesonium," Sov. Phys. JETP **6** (1957) 429 [Zh. Eksp. Teor. Fiz. **33** (1957) 549].

[132] P. Minkowski, "$\mu \to$ e γ at a rate of one out of 1-billion muon decays?," Phys. Lett. B **67** (1977) 421; M. Gell-Mann, P. Ramond and R. Slansky, in *Complex spinors and Unified Theories* eds. P. Van. Nieuwenhuizen and D. Z. Freedman, *Supergravity* (North-Holland, Amsterdam, 1979), p.315 [Print-80-0576 (CERN)]; T. Yanagida, "Horizontal symmetry and masses of neutrinos", in *Proceedings of the Workshop on the Unified Theory and the Baryon Number in the Universe*, eds. O. Sawada and A. Sugamoto (KEK, Tsukuba, 1979), p.95; S. L. Glashow, in *Quarks and Leptons*, eds. M. Lévy et al. (Plenum Press, New York, 1980), p.687; R. N. Mohapatra and G. Senjanović, "Neutrino mass and spontaneous parity nonconservation," Phys. Rev. Lett. **44** (1980) 912.

[133] E. Arganda and M. J. Herrero, "Testing supersymmetry with lepton flavor violating tau and mu decays," Phys. Rev. D **73** (2006) 055003 [arXiv:hep-ph/0510405].

[134] S. Antusch, E. Arganda, M. J. Herrero and A. M. Teixeira, "Impact of theta(13) on lepton flavour violating processes within SUSY seesaw," JHEP **0611** (2006) 090 [arXiv:hep-ph/0607263].

[135] E. Arganda, M. J. Herrero and A. M. Teixeira, "$\mu - e$ conversion in nuclei within the CMSSM seesaw: universality versus non-universality", arXiv:0707.2955 [hep-ph].

[136] U. Bellgardt *et al.* [SINDRUM Collaboration], "Search for the decay Mu+ → E+ E+ E-", Nucl. Phys. B **299** (1988) 1.

[137] B. Aubert *et al.* [BABAR Collaboration], "Search for lepton flavor violation in the decay tau- → l- l+ l-", Phys. Rev. Lett. **92** (2004) 121801 [arXiv:hep-ex/0312027].

[138] A. G. Akeroyd *et al.* [SuperKEKB Physics Working Group], "Physics at super B factory", [arXiv:hep-ex/0406071].

[139] D. Ng and J. N. Ng, "Can μ - e conversion in nuclei be a good probe for lepton number violating Higgs couplings?", Phys. Lett. B **320** (1994) 181 [arXiv:hep-ph/9308352].

[140] P. Fayet, "Supergauge invariant extension of the Higgs mechanism and a model for the electron and its neutrino," Nucl. Phys. B **90** (1975) 104; H. P. Nilles, M. Srednicki and D. Wyler, "Weak interaction breakdown induced by supergravity," Phys. Lett. B **120** (1983) 346; J. M. Frere, D. R. T. Jones and S. Raby, "Fermion masses and induction of the weak scale by supergravity," Nucl. Phys. B **222** (1983) 11; J. P. Derendinger and C. A. Savoy, "Quantum effects and SU(2) X U(1) breaking In supergravity gauge theories," Nucl. Phys. B **237** (1984) 307; J. R. Ellis, J. F. Gunion, H. E. Haber, L. Roszkowski and F. Zwirner, "Higgs bosons in a nonminimal supersymmetric model," Phys. Rev. D **39** (1989) 844.

[141] D.E. López-Fogliani and C. Muñoz, "Proposal for a new minimal supersymmetric standard model", Phys. Rev. Lett. **97** (2006) 041801 [arXiv:hep-ph/0508297].

[142] N. Escudero, D.E. López-Fogliani, C. Muñoz and R. Ruiz de Austri, "Analysis of the parameter space and spectrum of the $\mu\nu$SSM", in preparation.